Czech Technical University In Prague

Faculty of Mechanical Engineering

Department of Automotive, Combustion Engine and Railway Engineering

Master's thesis

Optimization of a Birotary Engine by means of a Simulation Model

Supervisors:

Ing. Ondřej Bolehovský

Satrio Wicaksono ST, M.Eng., Ph.D.

2021

Bc. Daniel Piskač

MASTER'S THESIS ASSIGNMENT

I. Personal and study details

Student's name: **Piskač Daniel** Personal ID number: **459979**

Faculty / Institute: **Faculty of Mechanical Engineering**

Department / Institute: **Department of Automotive, Combustion Engine and Railway Engineering**

Study program: **Master of Automotive Engineering**

Branch of study: **Advanced Powertrains**

II. Master's thesis details

Master's thesis title in English:

Optimization of a Birotary Engine by means of a Simulation Model

Master's thesis title in Czech:

Optimalizace birotačního spalovacího motoru pomocí simulačního modelu

Guidelines:

Do a literature review of rotary combustion engines.
Learn the principle of the provided basic 1-D GT-Power model of a birotary engine.
Propose and build a sub-model of clearances between the stationary case, rotary cylinder block and their sealing.
Perform model calibration based on available experimental data.
By means of the calibrated model, optimize the manifold geometry and intake and exhaust port timing with respect to required utilization of the engine.

Bibliography / sources:

Name and workplace of master's thesis supervisor:

Ing. Ondřej Bolehovský, Department of Automotive, Combustion Engine and Railway Engineering, FME

Name and workplace of second master's thesis supervisor or consultant:

Date of master's thesis assignment: **30.10.2020** Deadline for master's thesis submission: **06.01.2021**

Assignment valid until: _____

Ing. Ondřej Bolehovský Supervisor's signature	doc. Ing. Oldřich Vítek, Ph.D. Head of department's signature	prof. Ing. Michael Valášek, DrSc. Dean's signature

III. Assignment receipt

The student acknowledges that the master's thesis is an individual work. The student must produce his thesis without the assistance of others, with the exception of provided consultations. Within the master's thesis, the author must state the names of consultants and include a list of references.

4. 1. 2021 _____

Date of assignment receipt Student's signature

Annotation

Author:	Bc. Daniel Piskač
Title in English:	Optimization of a Birotary Engine by means of a Simulation Model
Title in Czech:	Optimalizace birotačního spalovacího motoru pomocí simulačního modelu
Academic year:	2020/2021
Study program:	Master of Automotive Engineering
Major:	Advanced Powertrains
Department, faculty:	Department of Automotive, Combustion Engine and Railway Engineering, Faculty of Mechanical Engineering (CTU in Prague) Faculty of Mechanical and Aerospace Engineering (ITB)
Supervisors:	Ing. Ondřej Bolehovský Satrio Wicaksono ST, M.Eng., Ph.D.
Abstract:	This thesis consists of a review of rotary and birotary engines, update and calibration of the provided GT–Power model. It also includes proposing and creating a sub-model of clearances and optimization of the model.
Keywords:	Rotary engines, Birotary engines, Powertrain, Calibration, Clearances, Optimization, GT-Power
Number of pages:	89
Number of figures:	73

Declaration

I hereby declare that I have completed this thesis independently and that I have listed all the literature and publication used in accordance with the methodological guidelines about adhering to ethical principles in the preparation of the final thesis.

In Prague, 5th of January, 2021

Bc. Daniel Piskač

Acknowledgements

I would like to thank my supervisor Ing. Ondřej Bolehovský for guidance, support and help with the diploma thesis and KNOB ENGINES s.r.o., especially Bc. Václav Pieter for guidance, help, support and opportunity to work on this interesting topic. A big thanks belongs to my family and friends who have supported me throughout my studies.

For reason of confidentiality, just some of the data and results are shown in this thesis.

Table of contents

1. INTRODUCTION

The first goal of this thesis is to do a review of rotary and birotary engines, which were invented or built. Most of these engines were used in aircraft, but not all of them. The next chapter is about rotary engines, while the third chapter is all about birotary engines including the Knob engine, which is used for all further work.

In the fourth chapter, I am using the provided old GT–Power model and according to new parameters and specifications the model is being updated to the latest version. In this part of the thesis all these updates are described, such as change of compression ratio, blowby, intake and exhaust manifolds, intake and exhaust port timing.

After a new measurement of the engine a calibration of the GT–Power model is made, based on the new results. A simple model of clearances is proposed and calibrated, friction is also calibrated according to the measurement. After calibrating the model in motoring regime, a simulation with an ignition is made to predict the actual output of the engine.

In the sixth chapter, I propose several versions, how the sub-model of clearances could be created. The ideal option is chosen for further simulations. It is described what parameters are needed to create the sub-model in GT–Power, how they are extracted from a CAD model and what dependencies are made.

In the final chapter, I use the calibrated GT–Power model for optimization. The goal of the optimization is to get the best possible output of the engine. The parameters which are used fort the optimization are the length of the intake and exhaust manifolds and the timing and shape of the ports.

2. Rotary engines

It is a type of internal combustion engine with a radial configuration of cylinders, but in this type of engine the cylinders and combustion chambers rotate with a driven shaft and the pistons are fixed to a stationary crankshaft, which is attached to the frame. The crankshaft is not in the center of the engine and thanks to this the pistons are moving in the cylinder. These types of engines were air cooled and mostly used in aircraft. A propeller is mounted to the front of the rotating crankcase. Rotary engines have usually odd number of cylinders, so every other piston is firing, which results in smooth running and the crankcase acts as a flywheel. Rotary engines have a good cooling, because of the rotating movement and the walls of the case can be thinner, resulting in better power-to-weight ratio. [1] [2] [3]

2.1. Millet motorcycle

At the end of the 18th century Félix Théodore Millet put a five-cylinder rotary engine into a front wheel of his tricycle (Figure 1). A few years later he put the same engine in the rear wheel of a bicycle. The crankshaft is fixed to the frame of the bicycle and the cylinders are rotating with the wheel. The rear fender is also a fuel tank and a surface carburetor and air filter are placed between the wheels. It is an air-cooled engine with a displacement of 1925 cm^3 and 1,2 HP. It has a clutch with rotary handle, controlled valves and a suspension. [4] [5]

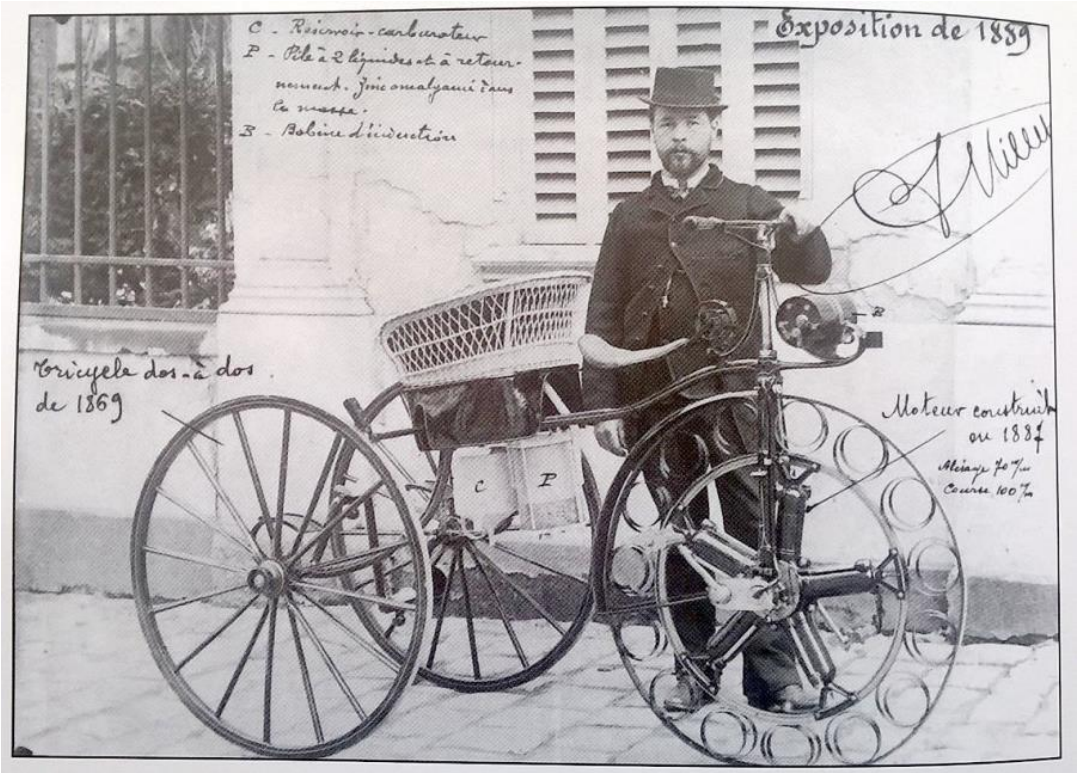

Figure 1 Millet's tricycle with rotary engine [5]

2.2. Hargrave's engine

In 1889 Lawrence Hargrave created a radial rotary engine with 3 cylinders (Figure 2). The cylinders rotate around its central axis while the crankshaft remains stationary. This engine is small, light, smooth running with good air cooling and has a great power-to-weight ratio. [6] [7]

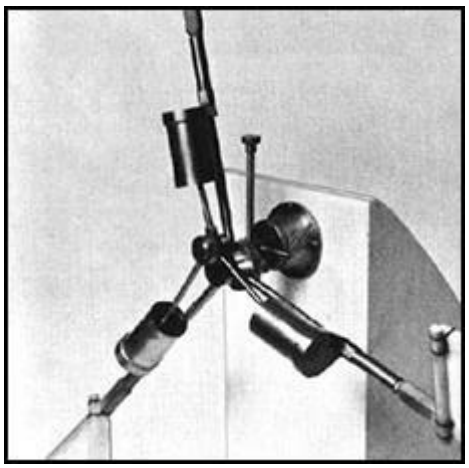

Figure 2 Lawrance Hargrave's engine [6]

2.3. Balzer's rotary engine

Stephen M. Balzer created a vehicle in 1894 (Figure 3). It has an air-cooled rotary engine with 3 cylinders which are placed under the seat in a quadricycle. The crankshaft is stationary while the crankcase is rotating. It is equipped with a 3-speed transmission. This engine was lately modified by Charles M. Manly to a 5-cylinder radial engine, which has the best specifications in terms of power-to-weight ratio. [8] [9] [10] [11]

Figure 3 1894 Balzer's Cyclecar [12]

2.4. Adams-Farwell engine

Fay Oliver Farwell designed a rotary engine with 3 cylinders. This engine was redesigned to a 5-cylinder engine (Figure 4), which was also air-cooled and piston-driven. This engine was mounted horizontally with a vertical stationary crankshaft attached to a frame in a car. Each cylinder has its own exhaust pipe. Which are connected to the side of the cylinder. The engine speed is controlled by a variable control valve, when you operate the time opening of the valve during the compression. The cylinders are between two discs, the top disc is for the intake pipe and the bottom disc is used for a beveled gear which transfer the power to the transmission. This type of engine is well lubricated, but at higher speeds the consumption of oil increases, because of the centrifugal force.

This engine was also used for experiments in a helicopter for its light weight. In 1909 a helicopter with these two engines successfully took off the ground with a person in it. [13] [14] [15]

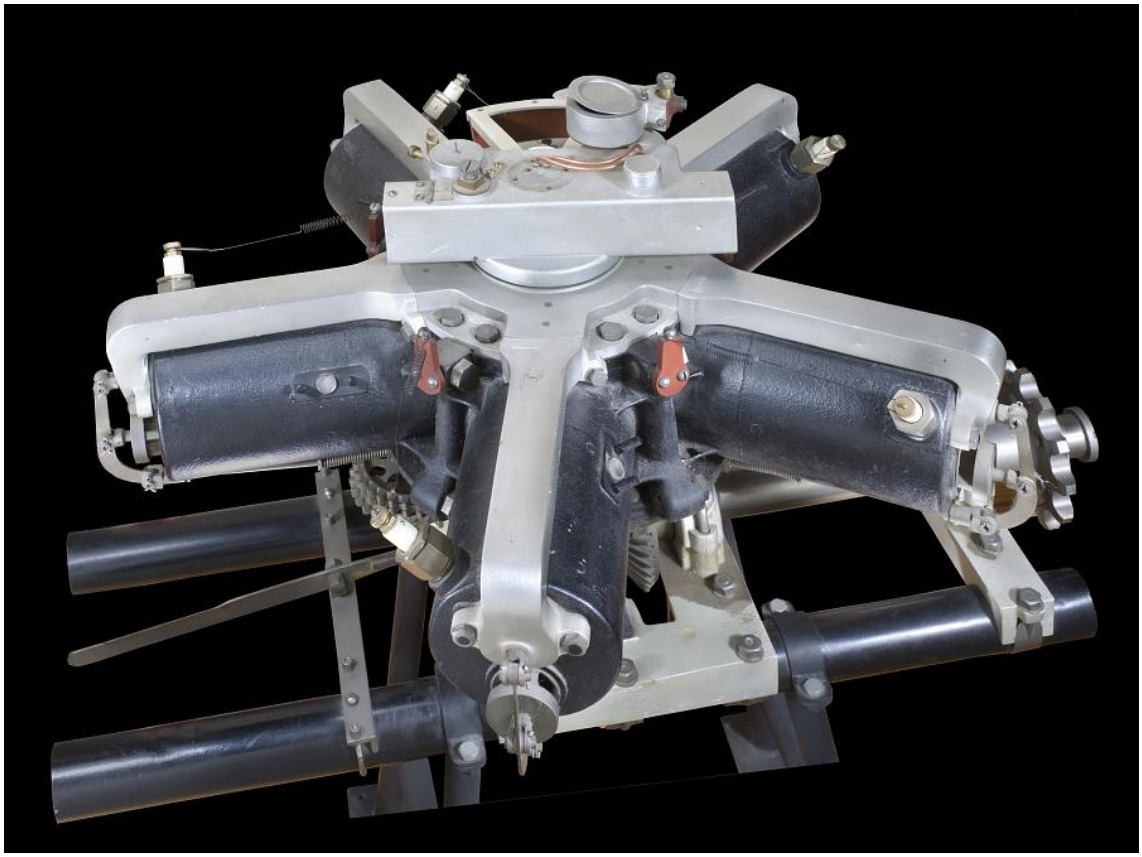

Figure 4 Adams-Farwell engine [13]

2.5. Gnome engine

The Seguin brothers developed the Gnome engine at the beginning of the 20th century. The first Gnome engine had two valves. The exhaust valve was placed in the cylinder head and the intake valve was placed in the piston crown. During the intake stroke the pressure in the cylinder drops and the intake valve opens, after the fresh charge with the fuel is drawn into the cylinder and after the pressure rises again the intake valve closes. Based on this principle the volumetric efficiency is lower because the intake valve opens later and closes sooner than in the ideal case.

In 1913 a new type of the Gnome engine was introduced, the Monosoupape engine (Figure 7). The inlet valve was removed from the piston crown. It has only one valve on the top of the cylinder, which is used for intake and exhaust. The fuel-air mixture is mixed and delivered through the hollow crankshaft and then through the small ports (Figure 5 and 6) to the combustion chamber. These ports are similar as in the two-stroke engine and they are placed on the bottom of the cylinder. During the power stroke the exhaust valve is opened before the piston uncovers the ports, which reduces the pressure inside the cylinder so when the ports are opened, the pressure inside the combustion chamber and in the crankcase is the same so no mixture is drawn into the cylinder. During the intake stroke the inlet valve closes before the piston reaches the ports, which results in a pressure decrease, so after the ports are opened the rich mixture is drawn into the combustion chamber.

The Gnome engine was light and reliable with good power output. On the other hand, the engine was consuming a lot of fuel and oil. Because of the gyroscopic effect the airplanes were hard to control, while turning left was easy, turning right was difficult.

There were a few variants of this engine, but mostly with 9 cylinders and some other companies used this principle of mixture delivery, but they used more conventional pushrod operated valves. Manufacturers such as Le Rhone, Clerget, Oberursel and Bentley. [16] [17] [18] [19] [20]

Figure 5 Ports in cylinder [19]

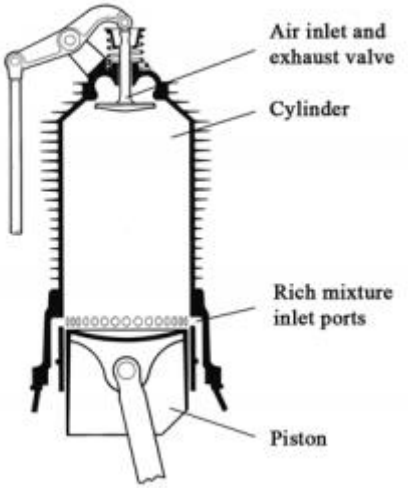

Figure 6 Gnome Monosoupape cylinder [16]

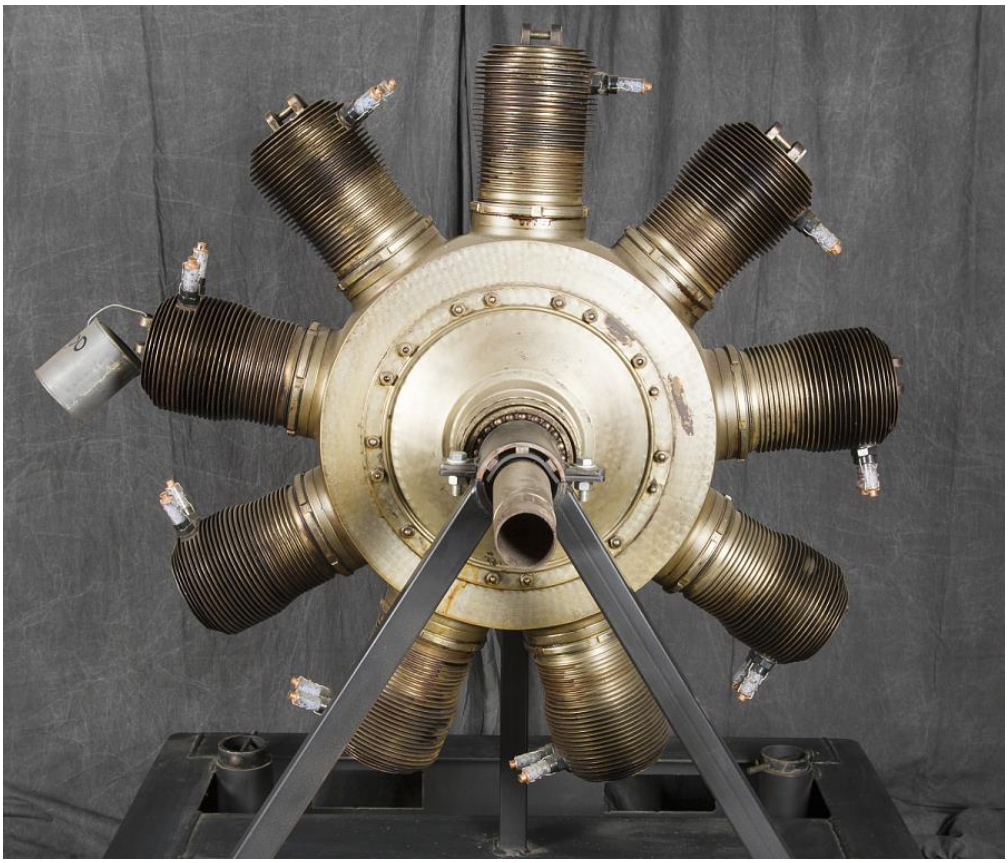

Figure 7 Gnome Monosoupape Type N engine [17]

2.6. Barry engine

In 1904 the Barry engine was introduced in the Barry motorcycle. It was a 2-cylinder supercharged opposed-piston rotary engine. The engine was placed between the knees of the driver. The mixture is getting into the crankcase through the hollow crankshaft and when the pistons are moving down, they act as a pump and the mixture is compressed and pushed into the storage chamber. This chamber is connected by pipes to the intake valve. [21] [22] [23]

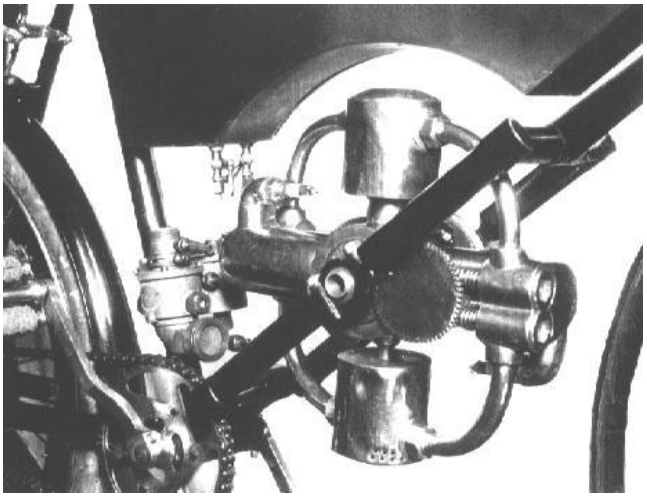

Figure 8 Barry engine [24]

2.7. Wankel engine

Felix Wankel created his first rotary engine in 1954 and was tested for the first time in 1957. The Wankel engine does not have usual pistons and cylinders like any other engine. It has an almost triangular rotor which rotates in an almost elliptical housing. The engine is equipped with 2 main gears. One small gear is mounted to the housing, while the second one is the inner gear inside the rotor. Thanks to this the rotor can turn on an eccentric shaft, which serves as an output shaft. The gear ratio is 1:3 which means that for one revolution of the rotor the eccentric shaft turns 3 times.

The three tips of the triangular rotor are in continuous contact with the closed housing. The rotor divides the closed chamber into 3 spaces. The three apexes of the rotor are fitted with seals to prevent leaking from one space to another. The volume of each chamber depends on the rotor position (Figure 9).

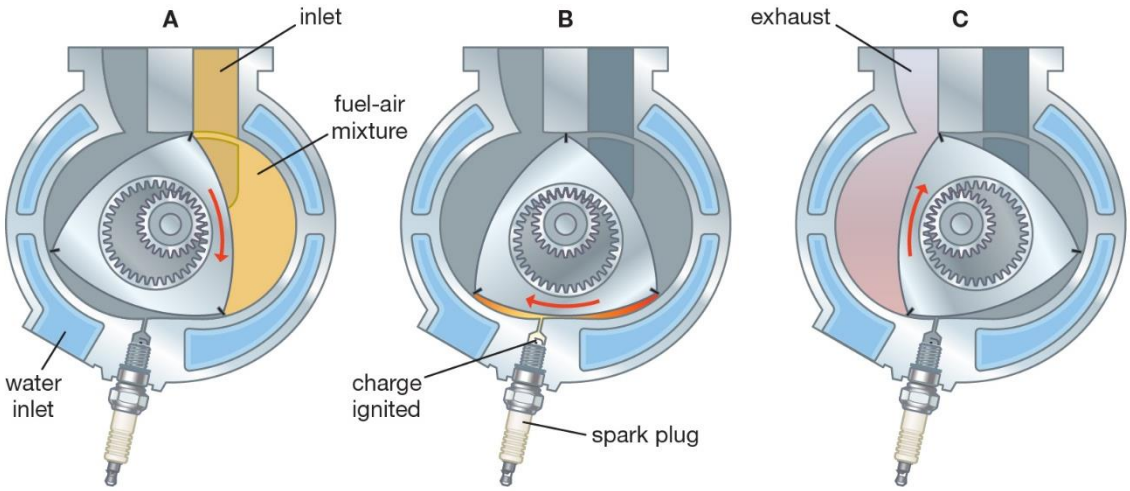

Figure 9 Wankel engine principle [26]

To produce power in a classic engine only one fourth of the crankshaft rotation is used, but in the Wankel engine it is more. There are 3 firing pulses per revolution of the rotor and the output shaft is three times faster, which results in one firing stroke per revolution of the output shaft.

The fuel is drawn into the engine through the intake port with a fresh charge. Not having valves results in lower weight of the engine and less moving components. The timing can be change by the shape of the intake and exhaust ports.

The lubrication and cooling of the rotor and its gears are done by oil circulation through the hollow rotor. Also, water is circulating through cooling jackets in the casing. A small amount of oil is added to the fuel to lubricate the three tips of the rotor. The sealing and wear are the major problem of the Wankel engine. Mazda modified the apex seal's shape to a cross-hollow seal with a cross-shaped hole near the apex of the seal, which brought improvements.

The Wankel engine is compact, smooth, without a big vibration, quite light, has a good power and lower costs for manufacturing. Also, it can operate at higher speeds than usual engines. [25] [26] [27] [28]

2.8. Bricklin-Turner Rotary Vee engine

This two-stroke engine was tested in the late 1970s. Inside the V-shaped case the V-shaped pistons are revolving. All the pistons are the same length, but because they are placed in the case with 135 degree, the distance from the top of the cylinder is different in each phase of the cycle (Figure 10). As the engine rotates and the piston is going down and making power, the exhaust gases are expelled through the port place at the bottom of the cylinder. Also, the fresh charge with the fuel is taken into the cylinder through another port operated by piston movement. The 2 output crankshafts are fixed to the rotating housing. It has 6 cylinders on each side, which results in 12 cylinders in total. This engine is light for its power and smooth running, because at every moment there are 6 cylinders out of 12 in a power stroke. [29] [30]

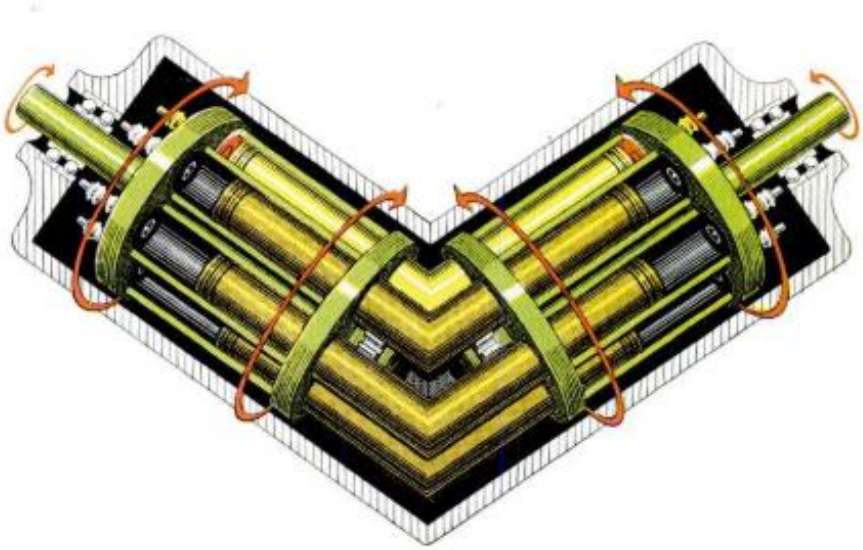

Figure 10 Rotary Vee engine [29]

3. Birotary engines

A birotary engine is a new type of rotary engine. The cylinder block with the cylinder row rotate in the opposite directions than a crankshaft and at different speeds. The inlet and exhaust ports are placed in the casing. The pistons are connected to the crankshaft and the relative movement of the crankshaft and the block provides the reciprocating movement of the pistons. [31] [32]

3.1. Sklenar engine

Sklenar patented a birotary engine which has an annular ported valve member and in this member the cylinder bank is placed. The cylinders are arranged radially, and they have a rotary movement. Through the port the gases are taken into the cylinder or out of the cylinder thanks to the rotary movement. Either the cylinder bank or the valve member is rotationally stationary, or they can both have a rotational movement. [31]

3.2. Mawen birotary engine

Mawen was one of many concerns that used Sklenar's engine patent. He refines the design believing that the engine has a big potential in aircraft and in automotive applications.

They developed two engines. One with seven cylinders with 75 HP and one with nine cylinders with 175 HP. And they were developing an engine with 1000 HP.

After Andre J. Meyer started collaboration with Mawen, he made some improvements in the construction, lubrication, design, and durability of the engine with his team.

The cylinder bank rotates as the crankshaft, but in the opposite direction. The exhaust and intake ports are stationary. The engine is constructed out of several parts. There is a front and a rear case which are connected with an annular ported valve

member with 4 ports for gases to be admitted or exhausted. These parts are stationary. In this case a cylinder bank is rotatably mounted and formed of a radially arranged cylinders. The pistons in the cylinders are connected via the connecting rods to the crank pin of the crankshaft. The last main part is the power output shaft, which is mounted in alignment with the axis of ration of the crankshaft. [31] [33]

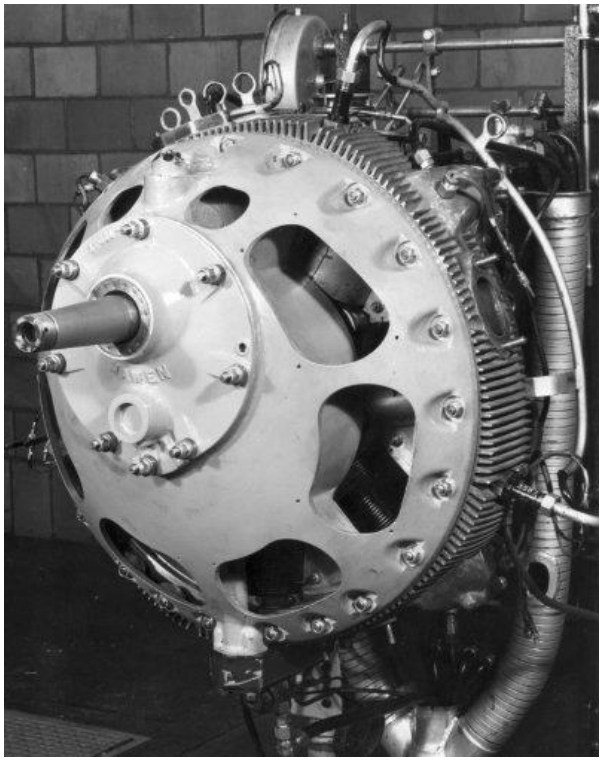

Figure 11 Mawen engine [31]

3.3. Siemens-Halske engine

The Siemens-Halske engine has 11 cylinders in a radial order. The crankcase with the mounted propeller rotates in one direction and the crankshaft rotates in the opposite direction. The rotation in the opposite direction is managed by a type of differential gear. One bevel gear is mounted to the crankcase and one to the crankshaft. These two bevel gears are meshed with two floating bevel wheels, which are fixed to the stationary member. Because of this system, the speed of the propeller is reduced without reducing the power output. When the engine operates at 1800 RPM

the rotational speed of the propeller is 900 RPM. There is a reduction in a gyroscopic effect thanks to the lower speed of the cylinders and this results in a better maneuverability, because of the counter rotating crankcase and crankshaft.

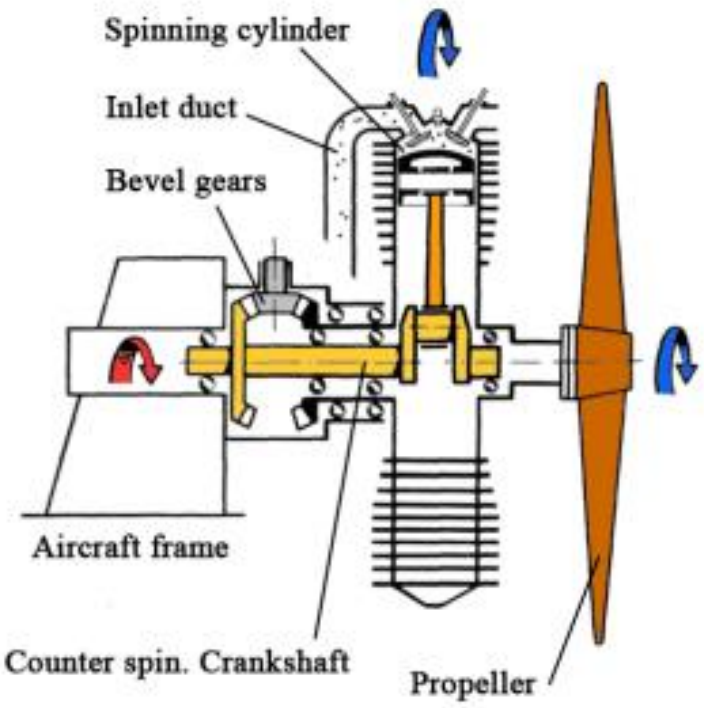

Figure 12 Siemens & Halske Sh.IIIa system [16]

The intake and the exhaust valves at the top of each cylinder are controlled by rocker arms operated by pairs of pushrods. The air goes first through a carburetor and then through the hollow crankshaft to the annular chamber and finally the air/fuel mixture is drawn into the cylinder through the copper pipes at the back of the engine. The exhaust gases are expelled from the combustion chamber directly into the atmosphere because it is not possible to fit the exhaust pipes to the spinning engine. [16] [34] [35]

Figure 13 Siemens & Halske Sh.IIIa [34]

3.4. Radial Bi-rotary (RBR)

This type of engine is designed by Franky Devaere and as the other birotary engines the crankcase with the cylinders rotates in one direction while the crankshaft rotates in the opposite direction. Two of four cylinders are connected via connecting rods to the crankshaft and the other two pistons are connected to these two pistons (Figure 14).

Figure 14 Connection of pistons [38]

The rotating cylinder block is mounted in the stationary cylinder head, where are placed three intake ports and three exhaust ports. As the block rotates, it passes the first intake port, and the mixture is drawn into the cylinder and after the combustion it is expelled to the exhaust port and then the block passes the second intake port, and the process is repeated. In one cylinder the combustion occurs three times per one revolution of the cylinder block. By modifying the size and place of the ports it is possible to create a small overlap of the ports. By elongating the intake port, the compression stroke is shortened so the power stroke is longer than the compression stroke.

It is a very smooth-running engine, and the gyroscopic forces are decreased thanks to the counter rotation. The relative counter rotation depends on a planetary gearing selection. The valve train is eliminated because of the system of intake and exhaust ports. [36] [37] [38]

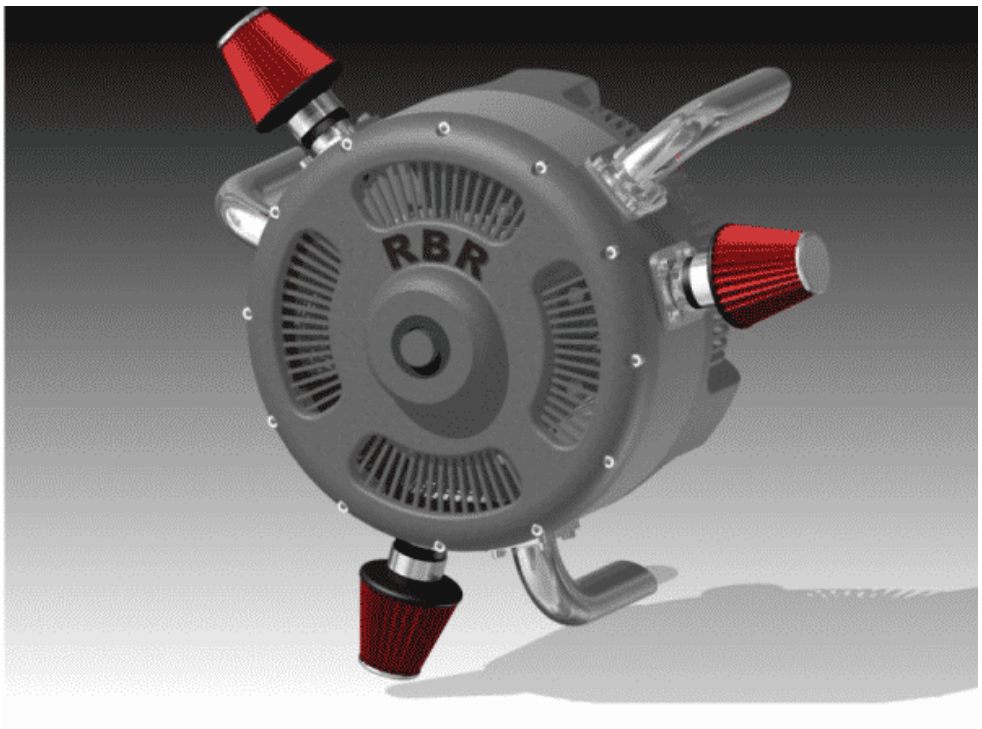

Figure 15 radial birotary engine [36]

3.5. Knob engine

Knob engine is a new type of birotary engine where the crankshaft rotates three times faster than the cylinder block and in the opposite direction. This is provided by a planetary gear set with the gear ratio of three. There are three cylinders in the cylinder block and the combustion occurs two times per one revolution of the cylinder block in each cylinder. This requires two intake ports, two exhaust ports and at least two spark plugs, because it is a spark ignition engine.

The intake and exhaust ports are placed in the stationary case in which the cylinder block rotates (Figure 17). This means that the valves and the valve train are eliminated. In a conventional engine the valves are placed in a cylinder head and their size is limited by the bore area. In the birotary Knob engine the ports are not limited by the size of the bore area, which allows to have bigger cross-sections areas of the exhaust and intake ports. The opening and closing of the ports are faster with good port shape and it also has a better flow character.

Knob engine is equipped with a new system of sealing. The major parts of the sealing assembly are side seals and transverse sealing strips (Figure 18). There are three transverse sealing strips between each port and the spark plug, and they are placed in the stationary case, which provides a stable force on the sealing strips, which does not depend on the engine rpm. [39]

Figure 16 Knob engine [39]

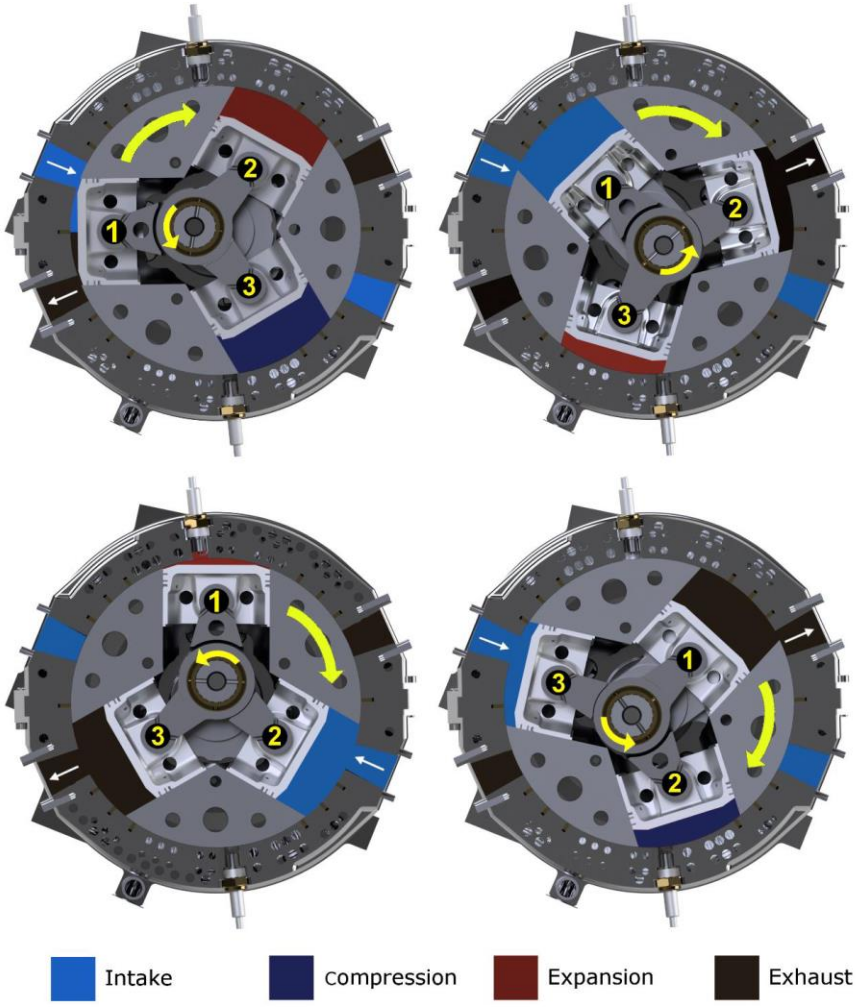

Figure 17 Principle of function of Knob engine [39]

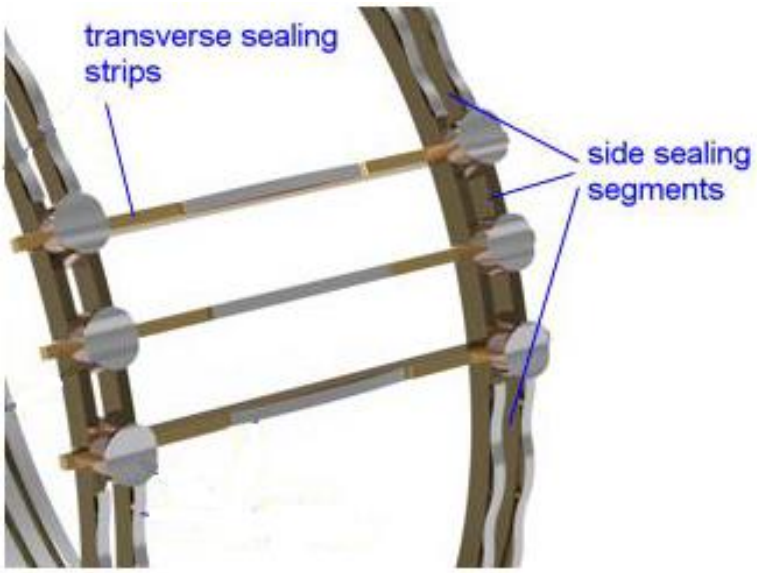

Figure 18 Sealing assembly [39]

4. Update of 1-D GT–Power model

4.1. Original model of Knob engine

The provided basic 1-D GT-Power model of a birotary engine was made by Ing. Ondřej Bolehovský in 2015. The company KNOB ENGINES s.r.o used this model and its results in their presentations and as a prediction of its potential. Based on this data they built an actual engine. After testing this engine there were a lot of differences between the measured data and the simulated model. After that, several modifications were made, and these changes were not included in the provided model. Further improvements in the model relate to a different compression ratio, blowby in the model, exhaust and intake pipes, exhaust and intake port timing and clearances between the stationary case, rotary cylinder block and their sealing.

The results of these updates are shown in the tables, which include maximum cylinder pressure, brake torque, brake power, etc. Sometimes the maximum cylinder pressure is used for a comparison of the results, although there are other factors that affect the maximum cylinder pressure such as burn rate. Burn rate has a big influence on the cylinder pressure curve, therefore comparing the maximum cylinder pressure is not ideal, when the burn rate is not properly calibrated. But because we do not have a lot of data from measurements, the maximum cylinder pressure is still used for the comparison, assuming the “Combustion object” in the GT-Power is set optimally.

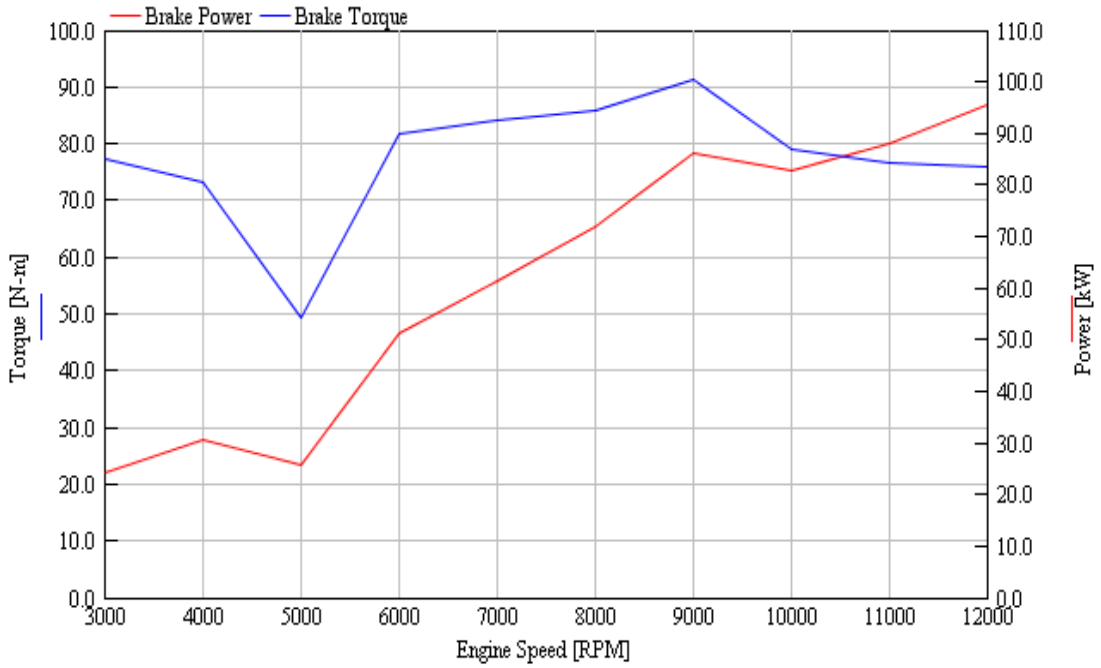

Figure 19 Power and torque characteristics of the original model simulated in GT-Power

Table 1 Parameters of the original model simulated in GT-Power [39]

Geometrical parameters		
Bore	92	mm
Stroke	37	mm
Connecting rod length	69.3	mm
Number of cylinders	3	-
Swept volume	738	cm^3
CR - effective	10	-
CR - dynamic	9.7	-
Rotating cylinder block diameter	250	mm
Valve timing data		
Intake port closes		20° after BDC
Exhaust port opens		20° before BDC
Intake port opens		16° before TDC
Exhaust port closes		16° after TDC
Manifold lengths		
Intake manifold	200	mm
Exhaust manifold	750	mm
Operating parameters		
Crankshaft max. RPM	7500	1/min.
Cylinder block max. RPM	2500	1/min.
Relative max. RPM	10000	1/min.
Max. power	115	HP
Max. mean piston speed	12.3	m/s
Max. speed on the seal elements	32.7	m/s

Table 2: Results of the original model for 3000 RPM

	Max cylinder pressure [bar]	Brake torque [Nm]	Brake power [kW]	Vol. efficiency [%]	Blowby [l/min]	Air flow rate [l/min]
Given model	70.57	77.47	24.34	118.64	0	1552

4.2. Change of compression ratio and influence of blowby

4.2.1. Compression ratio

The calibration of the model is based on the cylinder pressure, while the estimated pressure from the model is much higher than the measured pressure from the experiment. In order to reduce the cylinder pressure curve in the provided model, the idea of decreasing the compression ratio is made. The idea is based on the volume of clearances, which lowers the real compression ratio. The original CR is 10 and the engine is simulated with CR = 8.8, CR = 8 and CR = 6.6. For further calculations, we decide to use CR = 8 as the best option and most realistic option. It is because after simple estimation of the volume of clearances and this volume together with the volume at TDC makes the CR of 8. When we compare the Table 2 for CR = 10 and the Table 3 for CR = 8, we can see that the change of CR has a major impact on the maximum cylinder pressure but not such a big impact on the other parameters.

Table 3: Results for CR = 8 for 3000 RPM

	Max cylinder pressure [bar]	Brake torque [Nm]	Brake power [kW]	Vol. efficiency [%]	Blowby [l/min]	Air flow rate [l/min]
CR = 8	58.01	74.91	23.53	116	0	1517

4.2.2. Blowby

Another thing, how to make the model more accurate is taking blowby into account, which was not included in the previous model. The pressure curve of the simulated model is still quite different from the pressure curve from the measurement. This is the main reason why the blowby is created in the GT-Power model. From a measurement, we have data of the blowby and of the leaking flow through the sealing in the cylinder head. Because the leaking through the sealing is a little bit more complicated, we combine it with the blowby for now, to simplify the simulation. Five cases are made from the measurement (Table 4), from the best values to the worst values of the leaking. The blowby into the crankcase is measured and remains constant, while the leaking flow through the sealing is also measured, but it is changing with the wear of the sealing. When the sealing is new and in the best condition the leaking is minimal, but when it starts to wear the leaking rises. The worst value of the leaking in the Table 4 is for the critical wear of sealing strips. As we can see in Figure 20 the blowby with the leaking has quite a big influence on the cylinder pressure peak. With higher leaking and blowby the cylinder pressure decreases.

Table 4: Simulated cases of blowby with leaking for 3000 RPM

Case	Blowby [l/min]	Leaking through sealings [l/min]	Combined [l/min]
1.	0	0	0
2.	20	0	20
3.	20	80	100
4.	20	180	200
5.	20	300	320

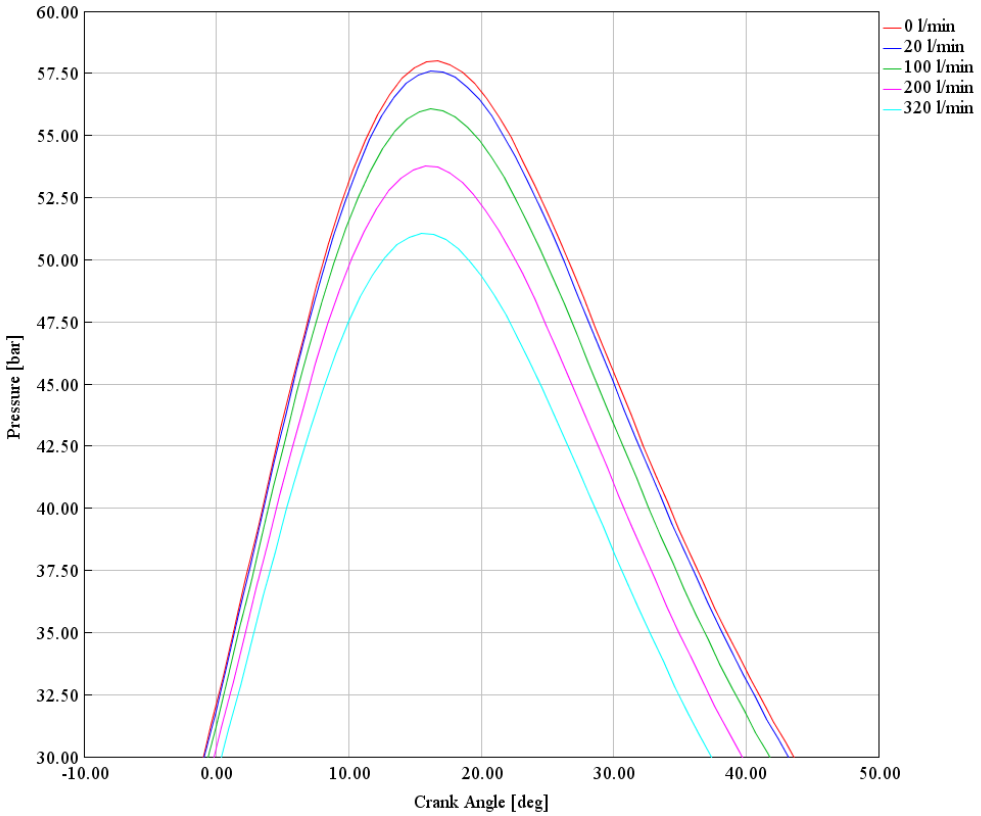

Figure 20 Influence of blowby on cylinder pressure peak (3000 RPM)

4.3. Exhaust system

4.3.1. Influence of exhaust systems

An exhaust system has an influence on the engine's performance. According to what we want to achieve the exhaust system must be designed. The properties of the pipes such as length, a diameter and overall design have a major influence on the performance.

The diameter of the pipe has a big impact on a gas velocity, the smaller the diameter the higher velocity and better throttle response. On the other side with a small diameter of the pipe, the backpressure will increase and therefore the pumping losses increase, and the blowdown is reduced.

The length of the pipe is also important, while the short pipes have the same effect as the large diameter and the long pipe has similar effect as the small diameter. When the exhaust port is opened, the pressure wave travels through the pipe until it

hits the end of the pipe and then travels back. The ideal timing for the wave to reach the exhaust port is during the overlap or during the closing of the exhaust port, so the pressure in the exhaust pipe is reduced, which helps the scavenging. The pressure waves can help the scavenging only over a narrow rpm range. Short pipes help the scavenging in high rpm and long pipes in low rpm. [40] [41]

4.3.2. Creating exhaust manifolds in GT - Power

From each cylinder goes an exhaust tube with a length of 30 mm which ends in a fake flow split, which does not exist in reality, but it is created in the model as the best solution how to connect these tubes into one final exhaust pipe for one port. Then there is one straight pipe with a length of 750 mm (Table 1) which opens into the atmosphere. That is how the exhaust system is created in the GT model. To make the model more accurate and see how big the influence of the exhaust manifolds is, the new exhaust system had to be done according to the reality (Figure 21).

After extracting all dimensions from a CAD model, I created the exhaust pipes in the GT-Power from a “PipeRound” elements with a different thickness, length, diameter and bending. To see how big impact the exhaust pipe has on the cylinder pressure and the engine performance I made a few options of the exhaust manifolds.

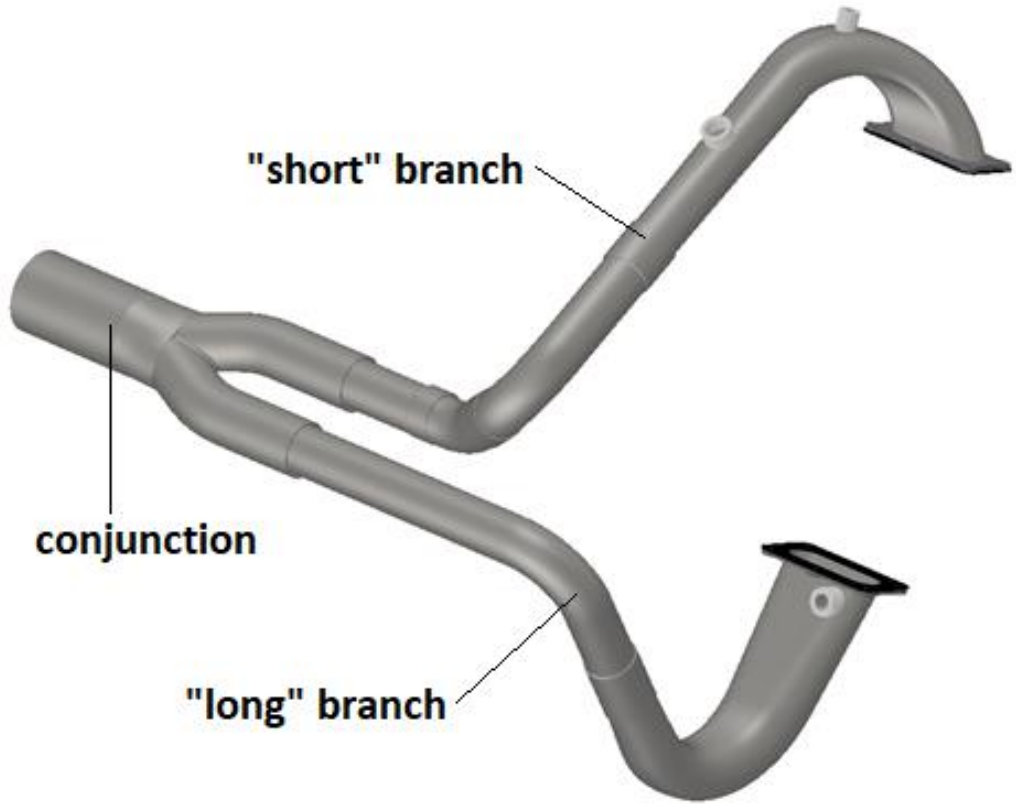

Figure 21 Exhaust manifolds [44]

At first, I used only the “short” branch for both ports and both open to the atmosphere. For a next simulation I used a conjunction to connect these two branches into one, which opens into the free space. The same approach I used for the “long” branch. Then I combined the “short” and the “long” branch and both of them open into the atmosphere on their own. As the final and more accurate model I put the conjunction on the combined branches with only one opening into the free space.

The results of all these options are shown in the Table 5. As we can see the influence of the exhaust manifolds is not particularly big and the best results while using the new exhaust manifolds are with the “short” branch without the conjunction, while the worst results are with the “long” branch with the conjunction. The most accurate option according to the reality, which is the combined version with the conjunction is not used for further simulation, because the system cannot reach a steady state (Figure 23), therefore the “long” branch with the conjunction is used as the most pessimistic version. Because it is unconventional engine and each cylinder alternates between two different exhaust pipes, the GT-Power has a numerical problem with reaching the steady state for the combined version.

Table 5 Cases of exhaust manifolds for 3000 RPM

	Max cylinder pressure [bar]	Brake torque [Nm]	Brake power [kW]	Vol. efficiency [%]	Blowby [l/min]	Air flow rate [l/min]
Old exhaust	51.92	58.54	18.39	120.03	308	1591
"short" branch	50.30	56.53	17.76	113.01	302	1497
"short" branch + conjunction	48.33	53.62	16.85	105.05	290	1392
"long" branch	47.37	52.33	16.44	101.83	285	1349
"long" branch + conjunction	46.30	50.50	15.87	97.70	279	1294
combined	50.52	53.73	16.88	105.65	291	1396
Combined + conjunction	49.63	50.84	15.97	99.13	282	1298

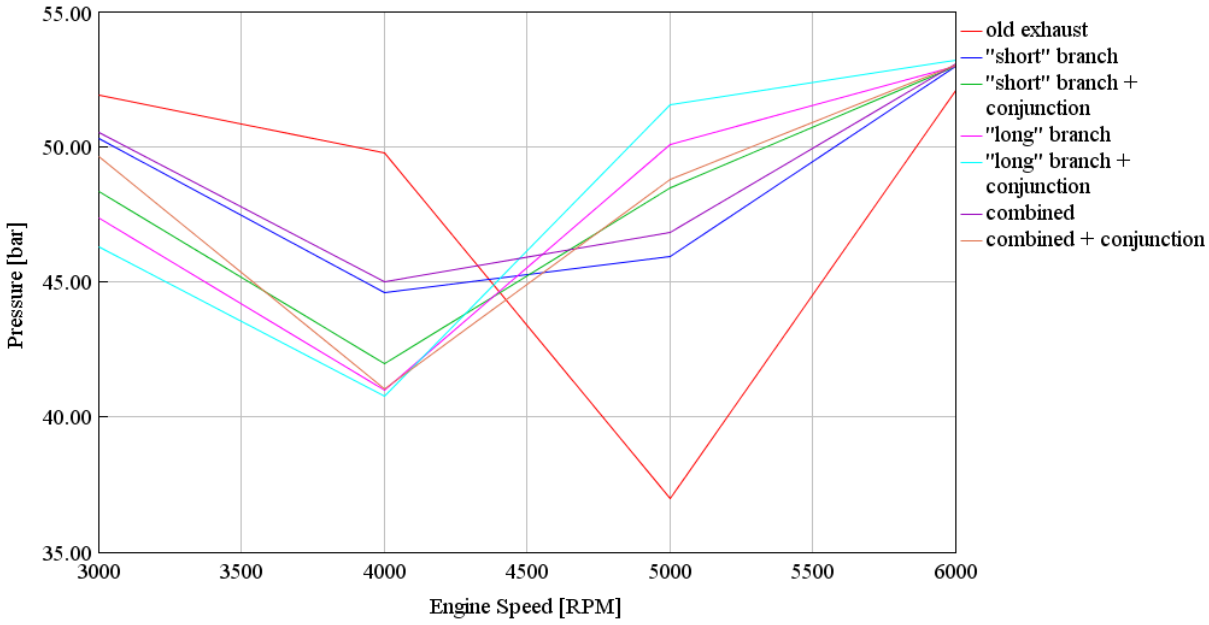

Figure 22 Comparison of maximum pressure with different exhaust manifolds

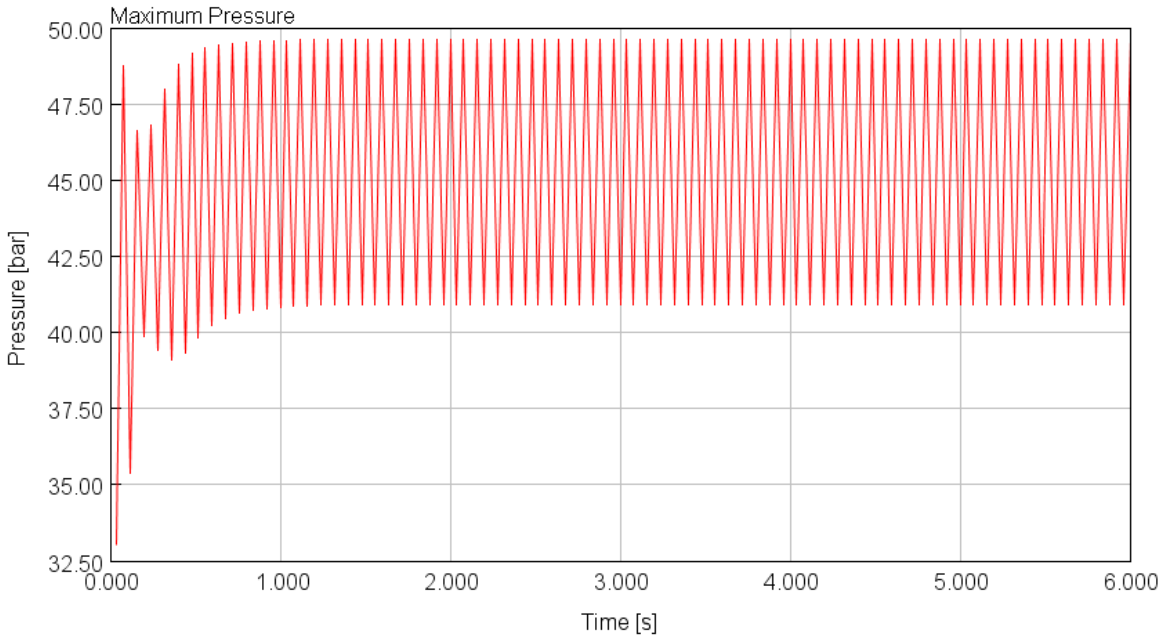

Figure 23 Time RLT of maximum pressure in the cylinder

4.4. Intake system

4.4.1. Influence of intake systems

The intake system has a big influence on a volumetric efficiency and output power. It must be designed in a specific way, according to what we want to achieve. The length of the manifold has a major effect on the engine performance. Not only the length of the pipes, but also a diameter and an overall design.

The length of the intake pipe is important for the volumetric efficiency. The volumetric efficiency is increased, while using long manifolds at low RPM, but at high RPM the volumetric efficiency is decreased. With the shorter intake pipes the effect is exactly the opposite, as the volumetric efficiency is good at high RPM and worse at low RPM.

With the diameter it is similar as in the exhaust system, with smaller diameter the gas velocity is higher and the better intake air charge, but at high engine speed the pressure drop is higher thus worse volumetric efficiency. For high RPM, the large diameter produces the best volumetric efficiency, and for the lower RPM it produces the lowest volumetric efficiency. [42]

4.4.2. Creating intake manifolds in GT-Power

The intake manifolds in the model are two separated pipes, one for each intake port. Each pipe is straight and 200 mm long (Table 1.) and then it is divided by a fake flow split (same as in the exhaust system) into three 30 mm long tubes, which connect to the cylinder with valves.

The actual intake system for measurement is made of several different components. It starts with a big barrel, which is connected by a straight pipe to a box of a specific shape. From this box two branches are coming out and each branch has a throttle and an injector. Each branch leads to one intake port. This quite complex intake system could not be done in the GT–Power with only straight and bend pipes, but also a few flow slits had to be used to create the intake system as accurately as possible.

As we can see in Table 6 after the update of the intake system, there are not any significant changes in the engine performance and properties at low engine speed.

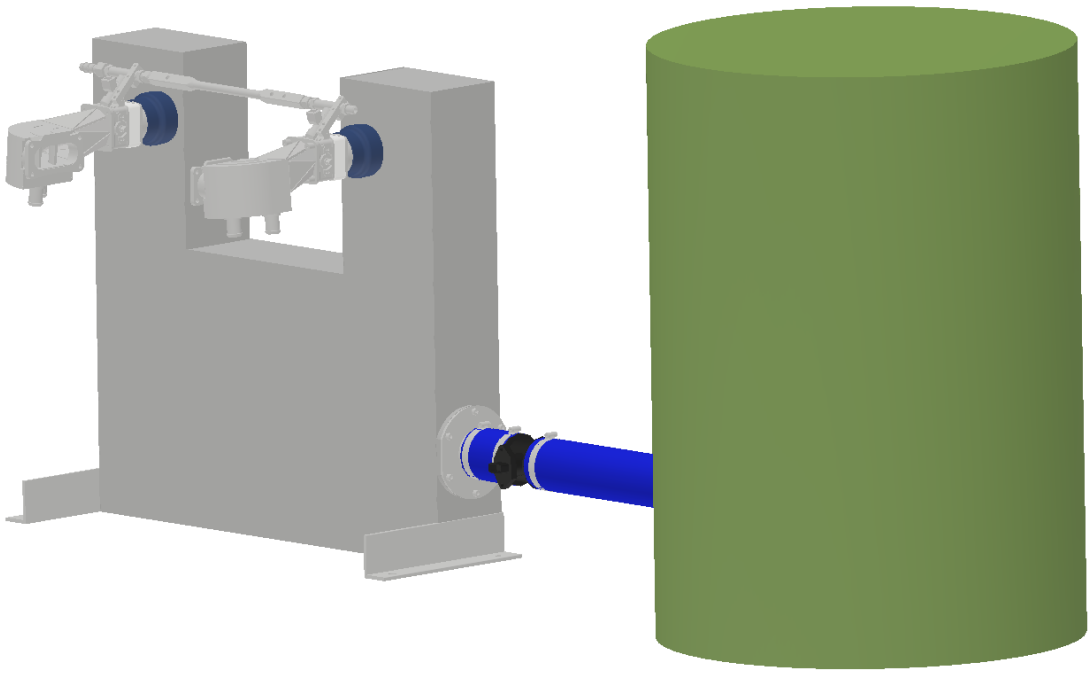

Figure 24 Intake system [45]

Table 6: Results of intake manifolds for 3000 RPM

	Max cylinder pressure [bar]	Brake torque [Nm]	Brake power [kW]	Vol. efficiency [%]	Blowby [l/min]	Air flow rate [l/min]
Old intake	46.30	50.50	15.87	97.70	279	1294
New intake	46.13	49.78	15.64	96.84	279	1267

4.5. Intake and exhaust port timing

The shape of the intake and exhaust ports was modified, and the overlap was canceled. The reasons for this modification was the difference in the measured and calculated air flow. Because this engine has an indirect injection, there was a possibility that something around 30 % of the mixture could go straight to the exhaust manifolds, which could result in a bad filling of the cylinder and lower cylinder pressure.

Table 7 New valve timing data

Intake port closes	24° after BDC
Exhaust port opens	24° before BDC
Intake port opens	0° before TDC
Exhaust port closes	0° after TDC

In the model the ports cannot be used because they are only for two-stroke engines, therefore they are replaced by valves, with a specific control system. In the valve settings the flow coefficients of the old intake and exhaust port shape are set from a measurement. A new measurement is planned, but for now the old flow coefficients are used for the new shaped ports. The overlap is canceled with decreasing the peak of the lift and narrowing the crank angle of the lift.

For 3000 RPM there is not a significant difference in the results, but the results for 4000 RPM are better. For the maximum cylinder pressure, brake torque, brake power, etc. there was a drop at 4000 RPM and with canceling the overlap the drop disappeared. But for the higher RPM range, the results are significantly worse than with the overlap. (Figure 25, Figure 26, Figure 27)

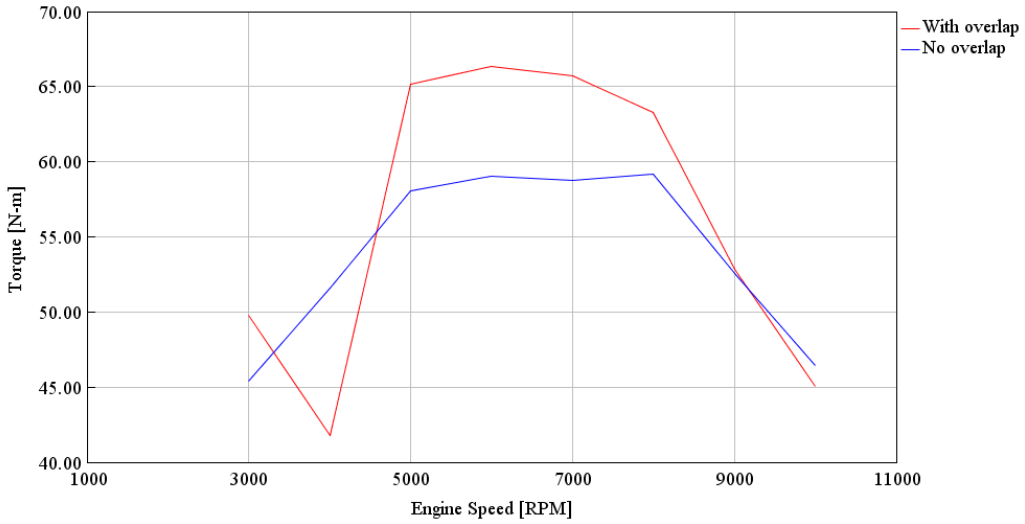

Figure 25 Brake torque

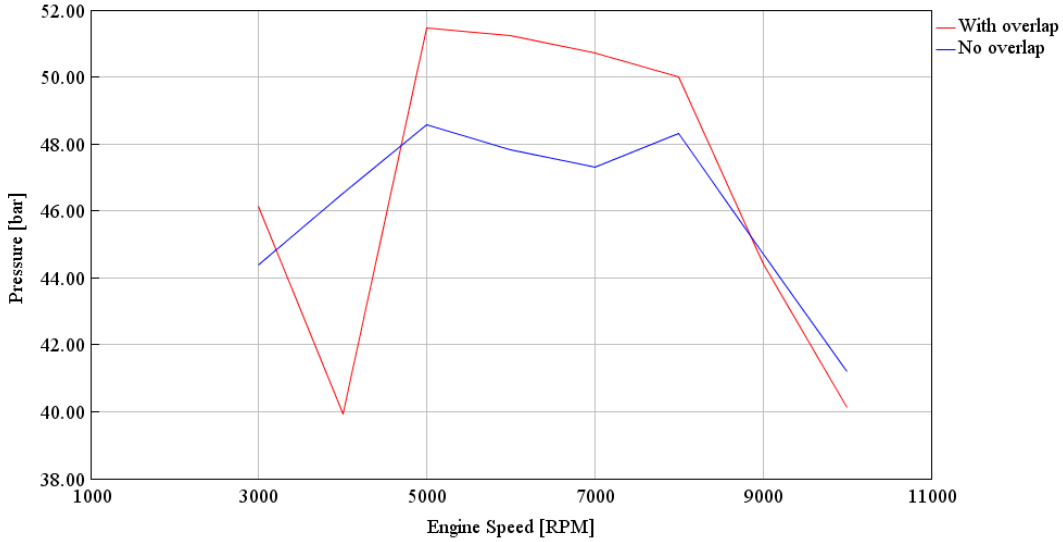

Figure 26 Maximum cylinder pressure

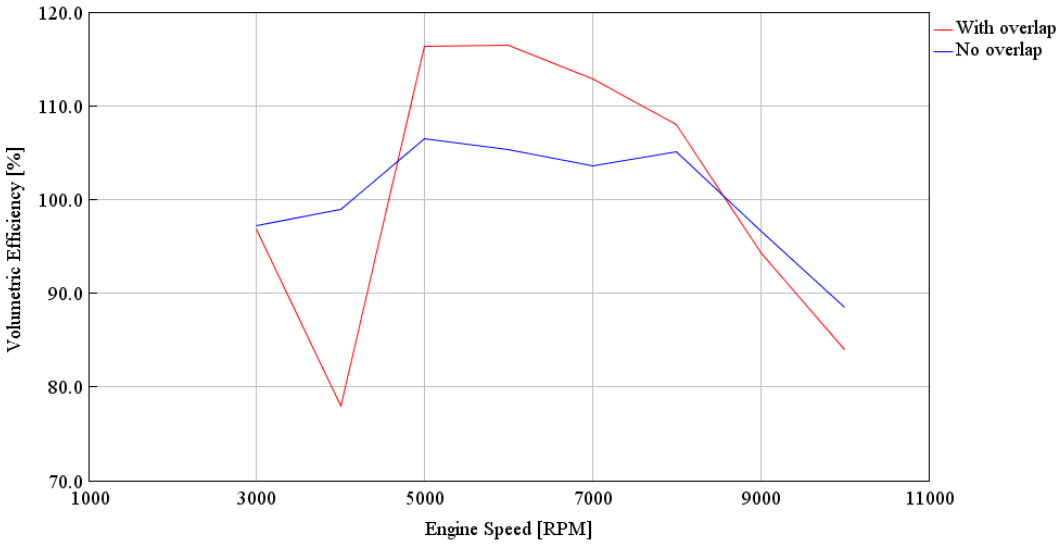

Figure 27 Volumetric efficiency

4.6. Summary of update

Several changes were made in the GT-Power model to make it as accurate as possible. In the Figure 29 we can see all the modifications and their influence on the cylinder pressure curve. With all these updates the original pressure curve is now closer to the measured data, but there is still a difference, which must be eliminated. It must still be considered that the burn rate has a major impact on the pressure curve, therefore the influence of these changes is not 100% accurate.

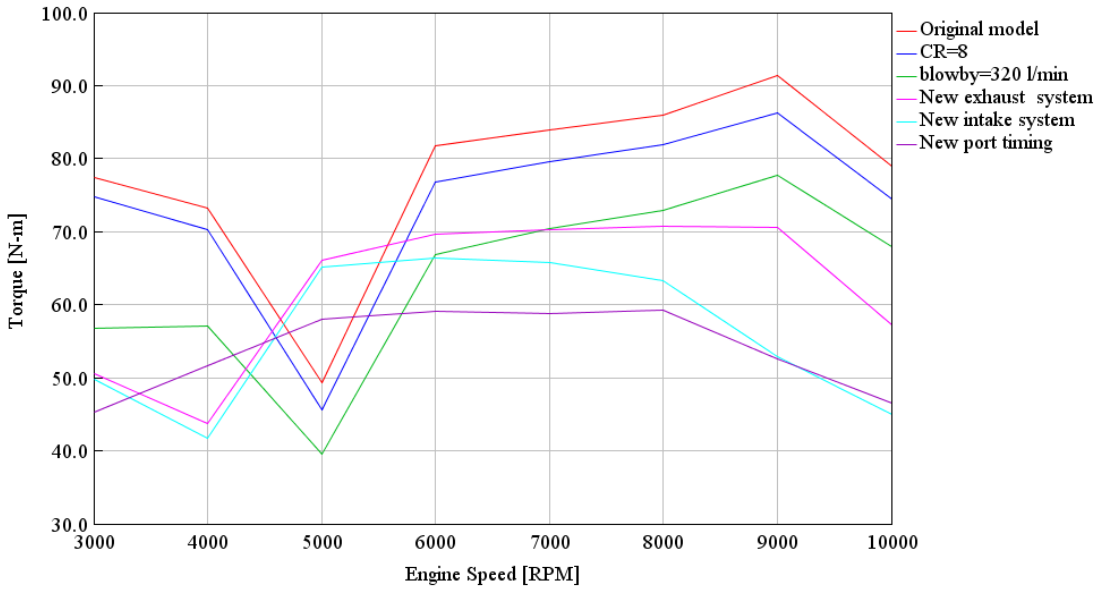

Figure 28 Influence of updates on brake torque

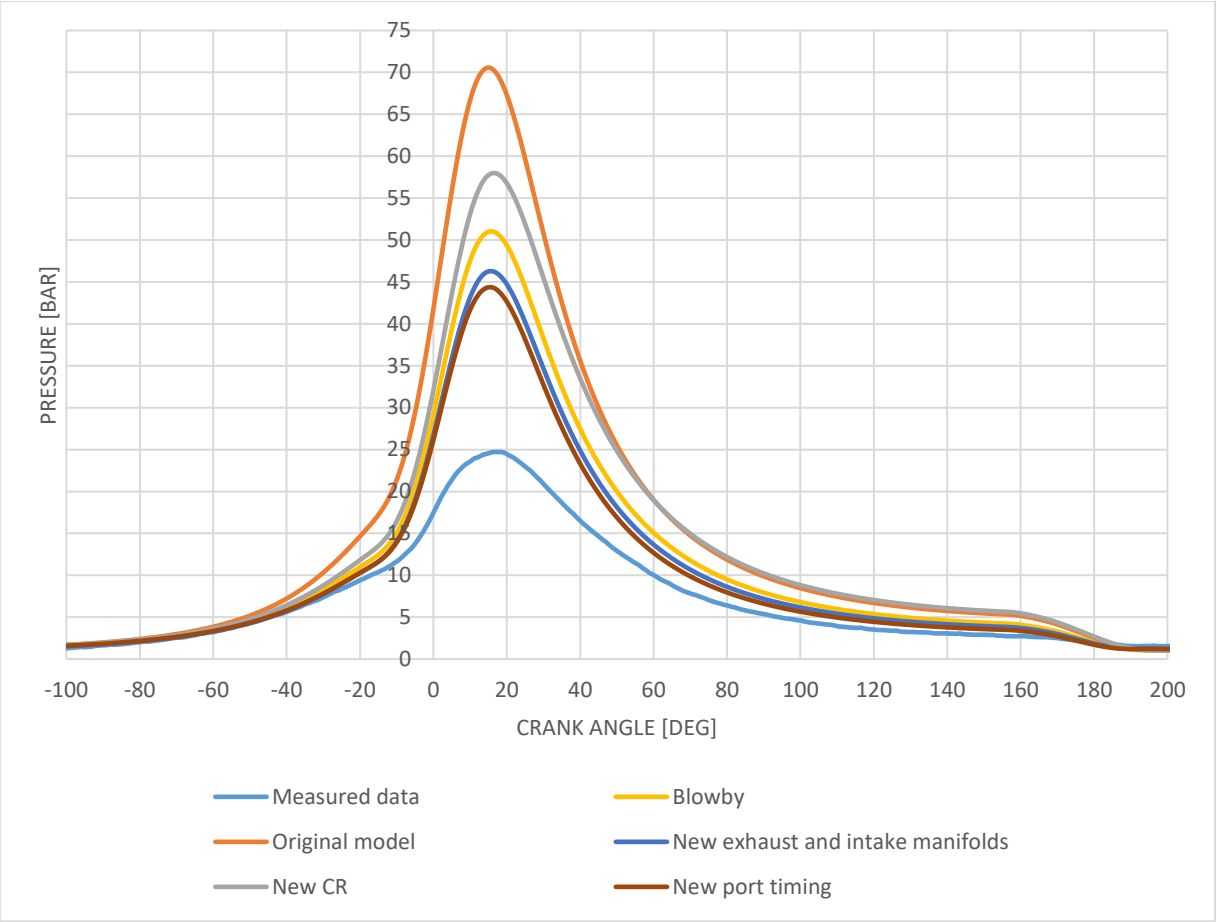

Figure 29 Influence of changes on the pressure curve for 3000 RPM

5. Calibration of 1-D GT–Power model

5.1. Simple model of clearances

To make the model more accurate for a next measurement a simple model of clearances is proposed. The clearances in the engine are located between the stationary case, rotary cylinder block and their sealing (Figure 30). All these small volumes are estimated, summed, and created in the GT-Power model as a one single volume. This volume is made as a one small straight pipe with a diameter of 8 mm and a length of 191.7 mm which equals the final volume of 9636 mm^3. This pipe is connected directly to the cylinder with an orifice connection and on the other end of the pipe an end flow cap is added to prevent escaping the mixture into the atmosphere.

By taking clearances into account the compression ratio must be changed, because an extra volume is added to the cylinder, therefore the CR must be higher to maintain the same properties. The clearance volume at TDC is taken from a CAD model without the estimated clearances, which means that with the new clearance volume at TDC the compression ratio is changed to 10.1.

This simple model of clearances has a really big impact on the engine output. Blowby was calibrated again for the value of 321 l/min. In Table 8 we can see the huge decrease of the maximum cylinder pressure, brake torque and brake power. The most interesting thing is the added column “Burned fuel”. In all the previous simulations the burned fuel was equal to 99,8 % and now it is only two thirds of it. This decrease is exactly proportional to the volume of the clearances, which is one third of the clearance volume at TDC. This means there is a problem with burning in these clearances and the flame propagation extinguish in the entrance to the sub-volume, therefore the burning occurs only in the cylinder.

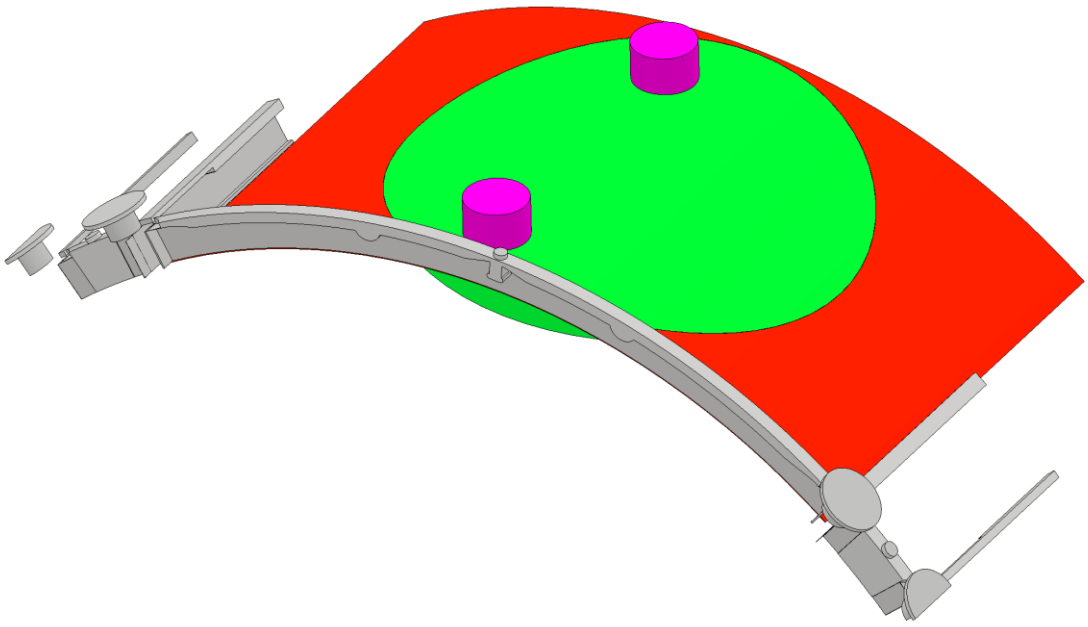

Figure 30 CAD model of clearances (green – combustion chamber; purple - clearance of the spark plug; red – clearance between the cylinder block and the cylinder head; grey – clearance of the sealing strips) [47]

Table 8: Results for the model of clearances for 3000 RPM

	Max cylinder pressure [bar]	Brake torque [Nm]	Brake power [kW]	Vol. efficiency [%]	Blowby [l/min]	Air flow rate [l/min]	Burned fuel [%]
A model of clearances	31.15	33.32	10.47	96.43	323.44	1261.59	66.65

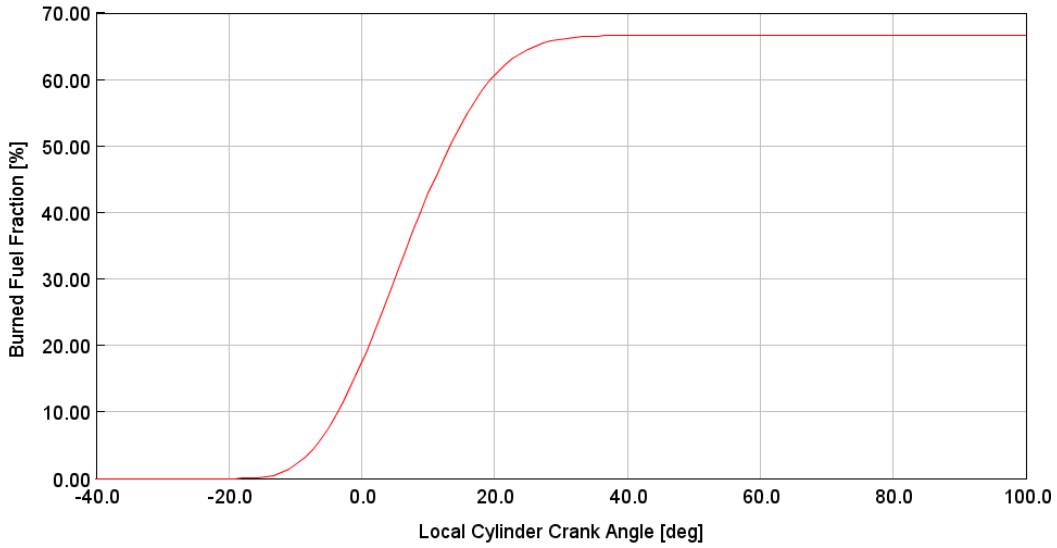

Figure 31 Burned fuel

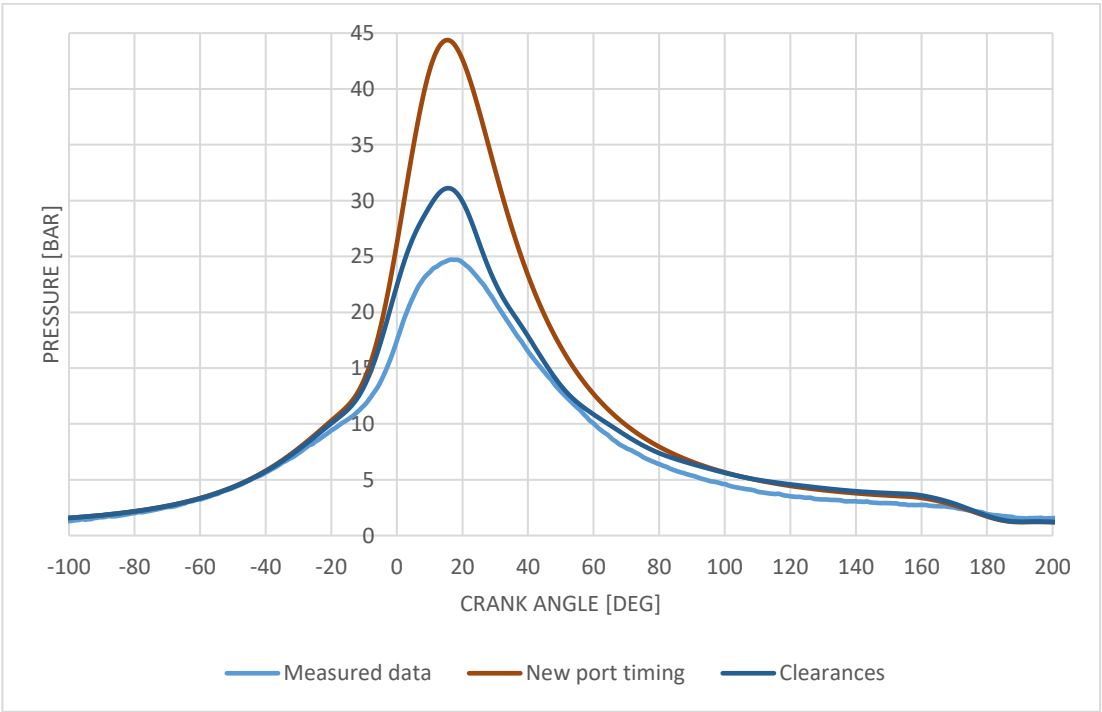

Figure 32 Influence of simple model of clearances on pressure curve for 3000 RPM

5.2. Calibration based on new experimental data

A new measurement of the engine was made for further calibration of the model. The engine was tested primarily without ignition, which means that further calibration is made in a motoring regime. The results from the simulated model are not still equal to the results from the measurement, therefore new changes are made in the model.

The first modification is with the clearance object, which is made from a small pipe with and end flow cap. The pipe is replaced with a flow split sphere object with the same volume. The end flow cap is removed and replaced with a small straight pipe, which opens into the atmosphere, as the gas in the engine is also leaking from the clearances into the free space. With this modification the blowby can be separated into the blowby into the crankcase and the leaking from the clearances. The straight output pipe is designed so the leaking into the atmosphere is the same as the measured data.

The second modification is the temperature of the head, the piston, and the cylinder. All the temperatures are reduced. This change has just a small impact on the cylinder pressure, brake torque, brake power, heat transfer etc.

With no significant change on the pressure curve with previous updates, the total volume of the clearances is re-evaluated. The space of the spark plug is now included in the combustion chamber. The object of the clearances is connected to the combustion chamber by a specific area. This area is simulated by an orifice with a constant diameter. Also, the gas is leaking from the clearances into the atmosphere through a small area, which is also simulated in the model by an orifice with a constant diameter (Figure 33). With previous 9636 mm^3 the new volume is set to 14000 mm^3 and compression ratio to 9.31.

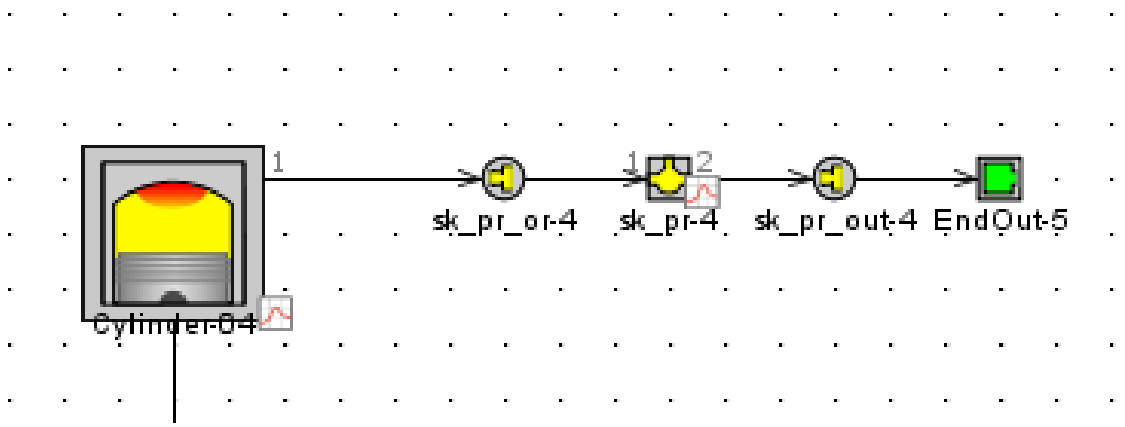

Figure 33 New settings of clearances

The change of volume has a major impact on the pressure curve and lowers its peak (Figure 34). The simulated data are quite close to the measured data in the lower RPM range. In the higher RPM range the simulated maximum cylinder pressure is smaller than the measured one (Figure 35), which might be caused because the air flow rate in the higher RPM range differs. The difference of the air flow can be caused by old flow coefficients of the valves. The used flow coefficients are measured with the old intake manifolds, therefore the results can be slightly different. The comparison of the maximum cylinder pressure can be seen in Figure 36 for a wide range of RPM. For 5600 RPM the measured data were not reliable, thus they are not shown in the graph.

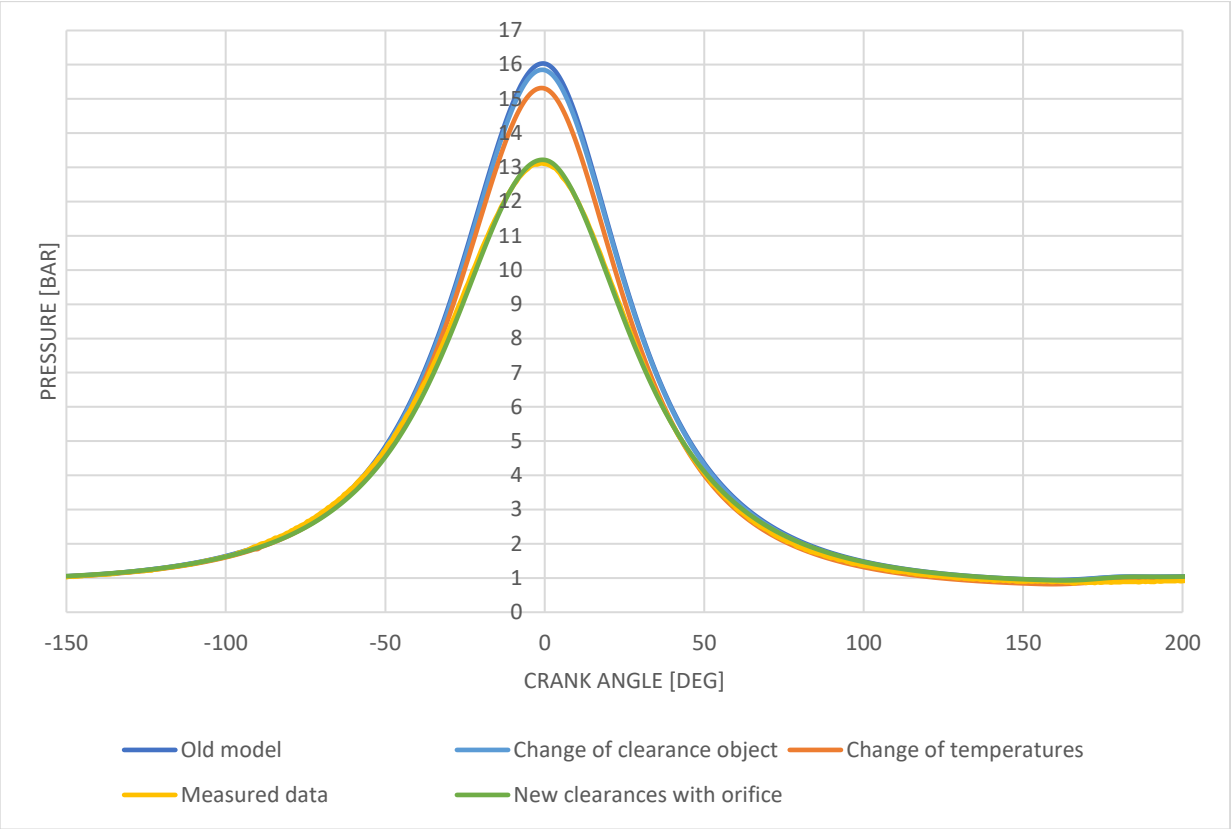

Figure 34 Effect of changes on pressure curve for 2400 RPM

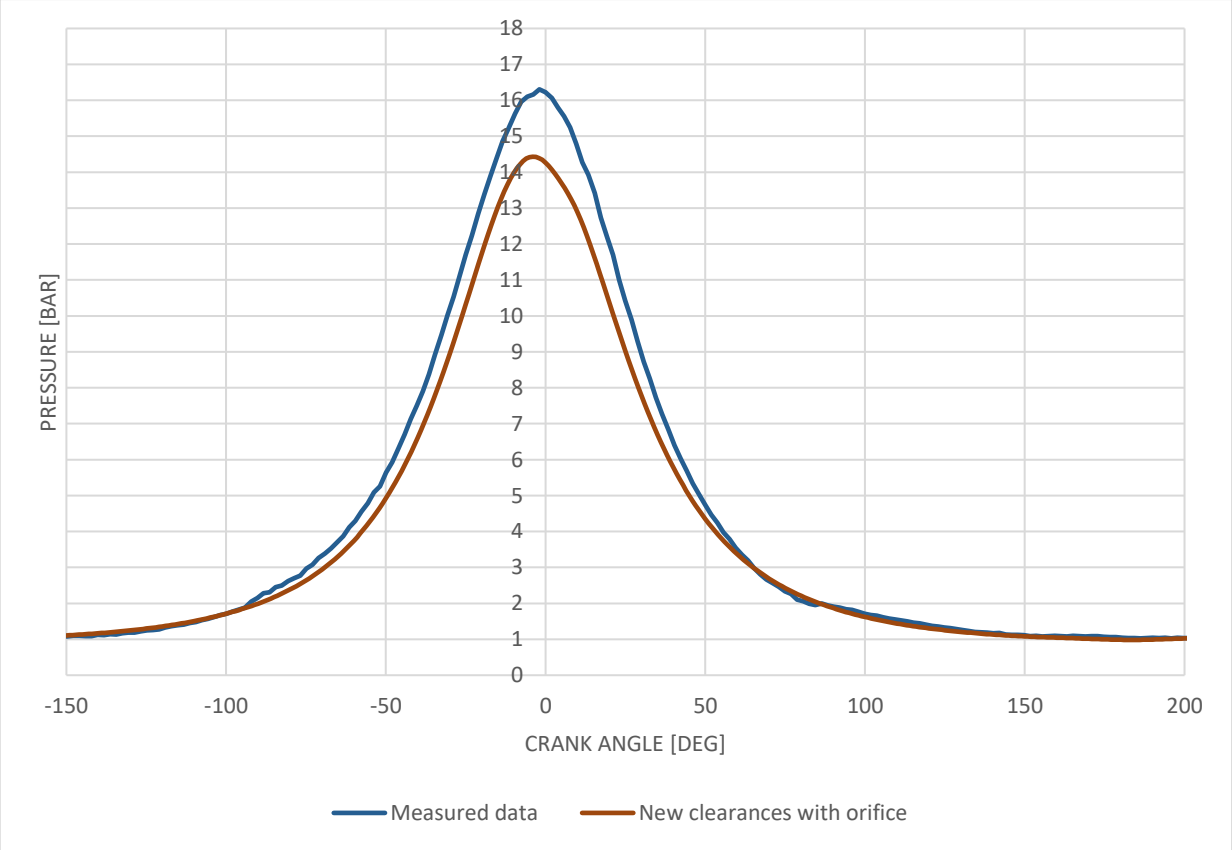

Figure 35 Comparison of measured and simulated data for 6400 RPM

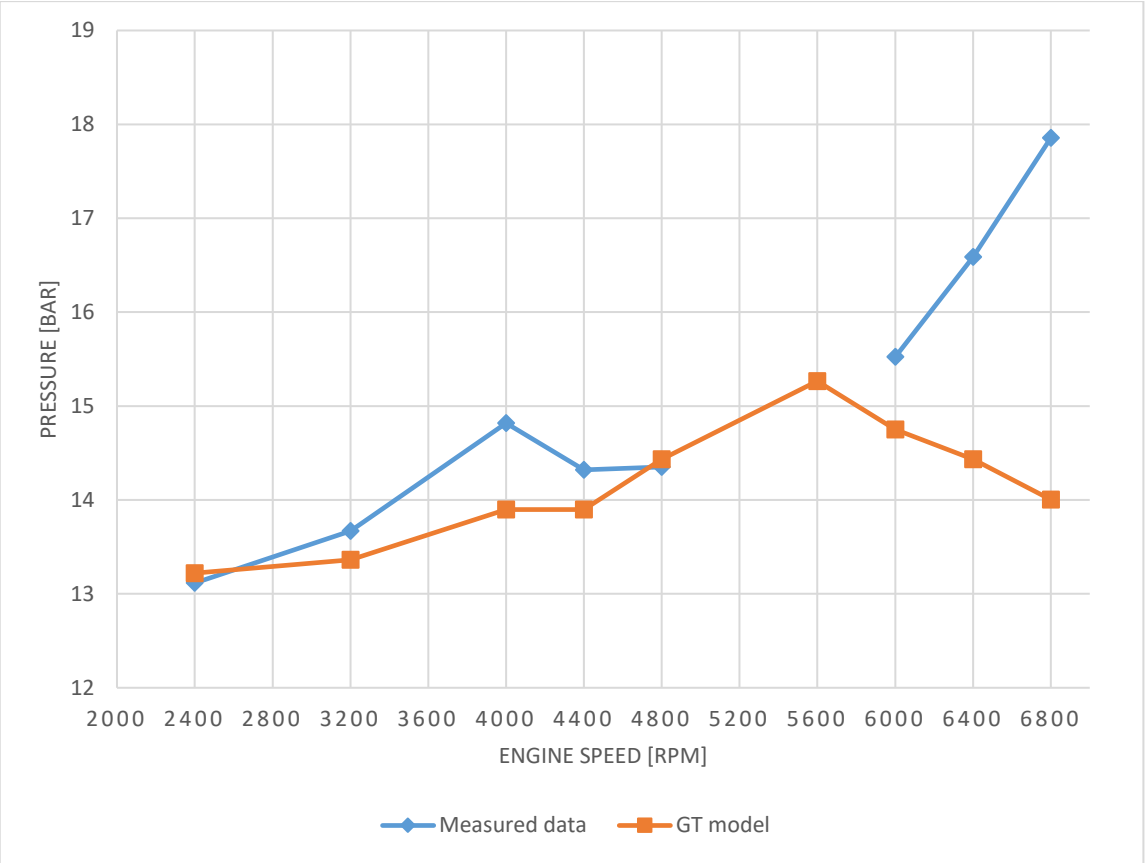

Figure 36 Comparison of measured and simulated data

5.3. Pressure sensitivity of volume change of clearances

To see how big impact the volume of clearances on the cylinder pressure has, a volume sensitivity is made. The compression ratio remains the same and the volume of the flow split sphere object, which simulates the clearances, is changing. The original volume is 14000 mm^3 and it is decreased by 1000 mm^3 till the volume is 8000 mm^3. For every step of lowering the volume the data are stored (Figure 37). The difference in the pressure for every 1000 mm^3 difference is about 2 – 3 %.

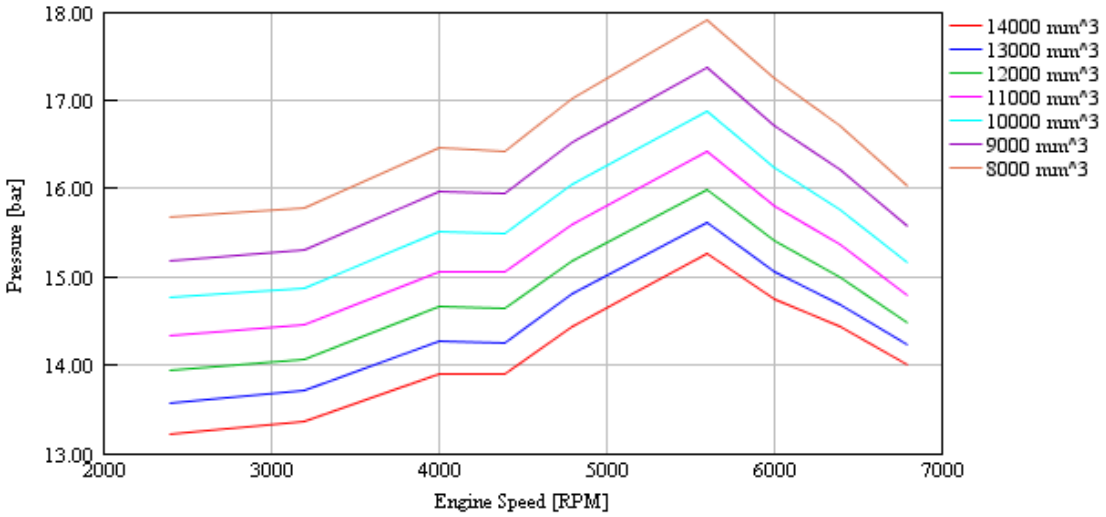

Figure 37 Pressure sensitivity of volume change of clearances

5.4. Calibration of friction

While the engine was running and tested in motoring regime the brake power and brake torque were measured. From the measurement of the brake power or the brake torque it is possible to calculate BMEP. To calculate FMEP, which is needed for further calibration in the GT model the IMEP is also needed. The pressure in the cylinder during the cycle was also measured, but because the sensor was placed between the two spark plugs, we have results only for the high-pressure part of the cycle. This means that IMEP cannot be calculated from the measurement.

$$FMEP = IMEP - BMEP \quad \text{[Pa]} \quad (1)$$

$$BMEP = \frac{W_e}{V_s} \quad \text{[Pa]} \quad (2)$$

$$W_e = \frac{P_e}{\frac{n}{2}} \quad \text{[J]} \quad (3)$$

$$P_e = T_e * \omega \quad \text{[W]} \quad (4)$$

$$\omega = \frac{\pi * n}{30} \quad \text{[rad*s}^{-1}\text{]} \quad (5)$$

As the GT model is calibrated for the max cylinder pressure, the cylinder high-pressure part from the measurement is compared with the pressure curve from the GT model. For some engine speed the curves are similar and for some they are not, therefore a compression ratio is changed for those speeds to make the pressure curves also similar (Figure 38). When these two curves are almost the same, we can assume that also the low-pressure part is the same, therefore we can take the IMEP from the GT model.

After calculating BMEP for all the measured engine speeds and extracting IMEP from the GT model, the FMEP can be calculated for each engine speed. In the GT-Power the Chen-Flynn model is used to calculate engine friction according to the equation number 6. I used dependency of the previously calculated FMEP on the engine speed and in the same graph I put a FMEP calculated from the equation number 6. Where I was changing coefficients $FMEP_{const}$, A, B and C (Table 9) to get these two curves as similar as possible. The higher the coefficients, the higher the friction losses are. Then I used these coefficients in the "Engine Friction Object or FMEP" in the GT-Power. It is only calibrated in the motoring regime for the measured engine speeds. [46]

$$FMEP = FMEP_{const} + A * p_{cyl,max} + B * c_{p,m} + C * c_{p,m}^2 \qquad \text{[bar]} \quad (6)$$

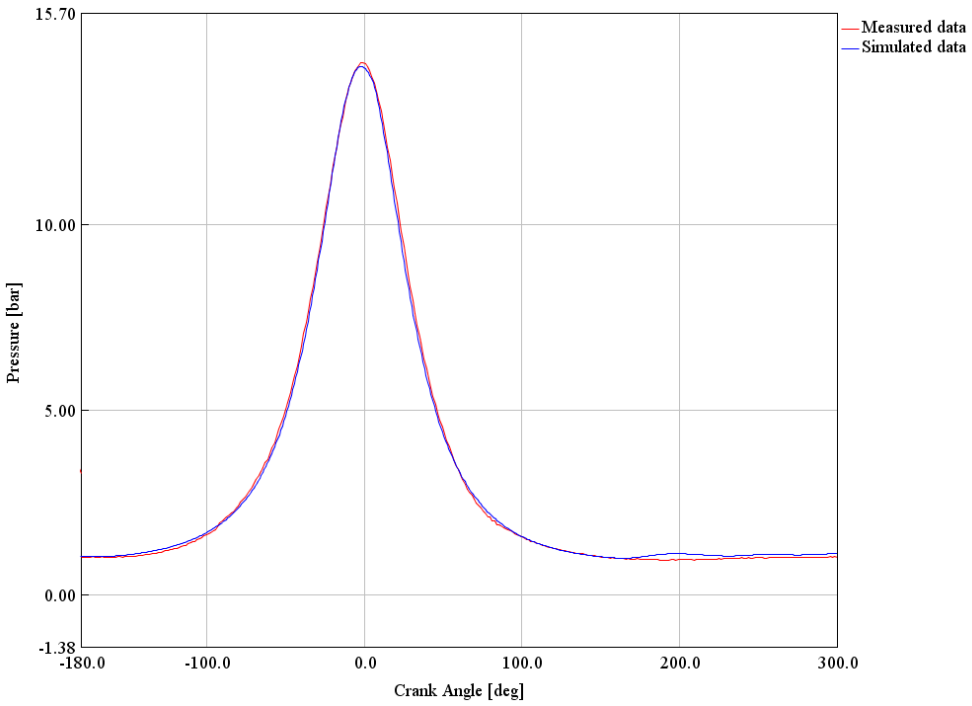

Figure 38 Comparison of measured and simulated data for 4800 RPM

Table 9 Coefficients for Chen-Flynn model

	Recommended values	Used values
$FMEP_{const}$ [bar]	0.3 - 0.5	1.5
A - Peak cylinder pressure factor [-]	0.004 - 0.006	0.009
B - Mean piston speed factor [bar*s/m]	0.08 - 0.10	0.17
C - Mean piston speed squared factor [bar*s^2/m^2]	0.0006 - 0.0012	0.003

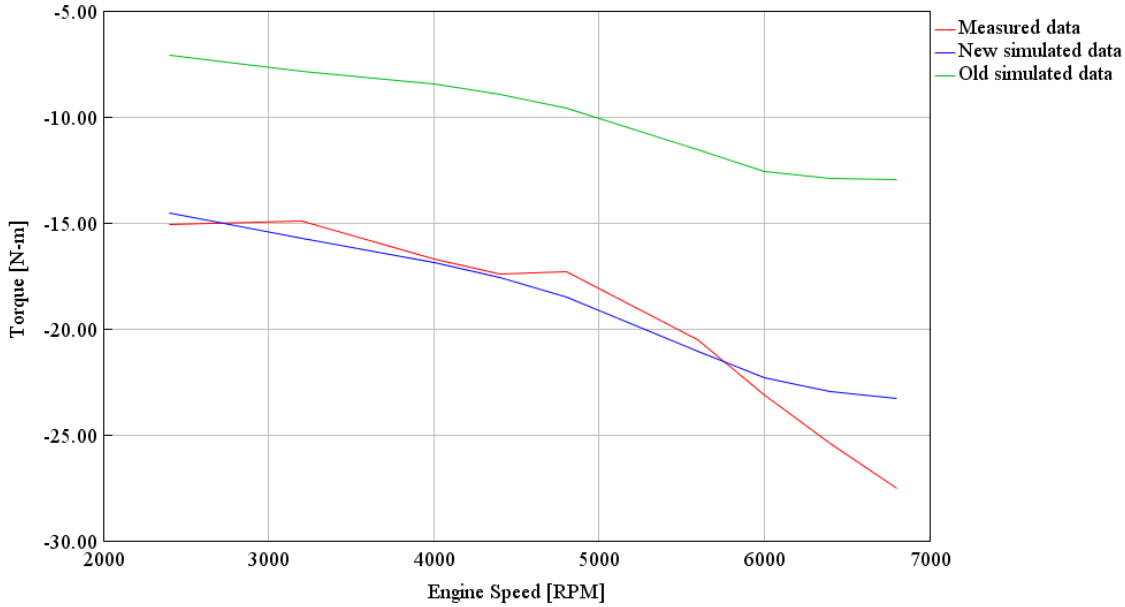

Figure 39 Comparison of friction torque

5.5. Simulation of the calibrated model with an ignition

When the engine was tested in the motoring regime a problem occurred. When the block of the engine reached 1800 RPM, suddenly the torque and the leaking flow through sealing strips rapidly raised (Figure 40). This happened because the engine's sealing strips got seized a bit. The exhaust manifolds were removed and through exhaust manifolds we checked if there are not any broken parts in the cylinder. There were not any broken parts, therefore another motoring regime was tested. In Figure 41 we can see that the torque and the leaking flow through sealing strips vary at a constant speed of the block. Knowing that the engine is not in a good condition, a measurement with an ignition was still performed. But because the engine was seized the results cannot be considered reliable (Figure 42).

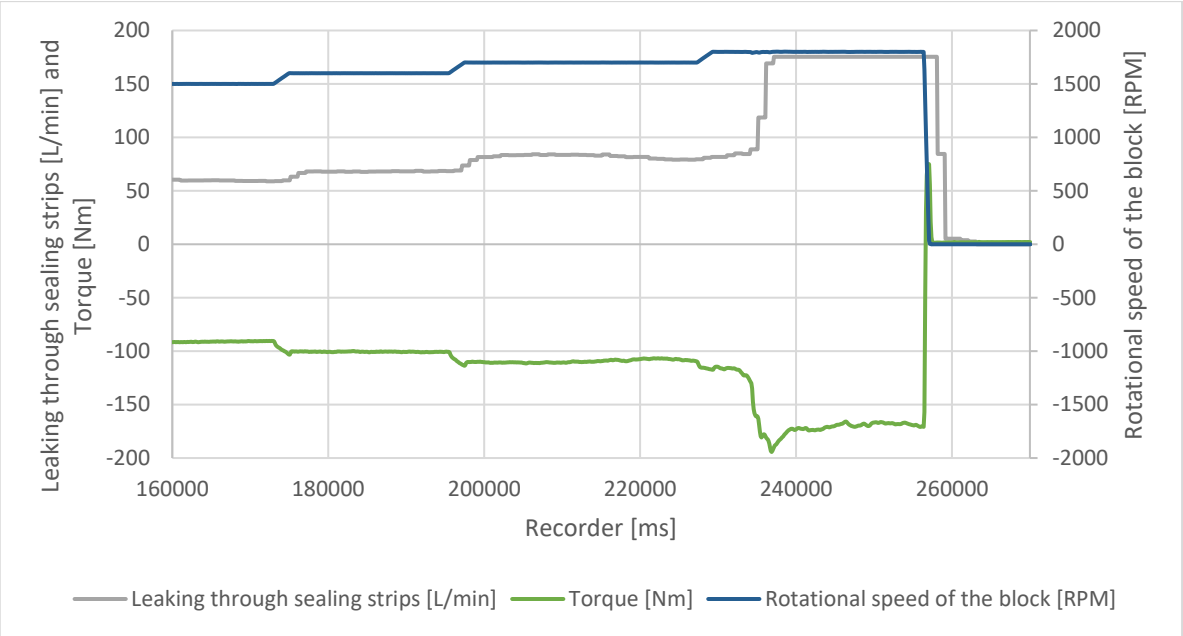

Figure 40 Motoring regime with sudden seizing

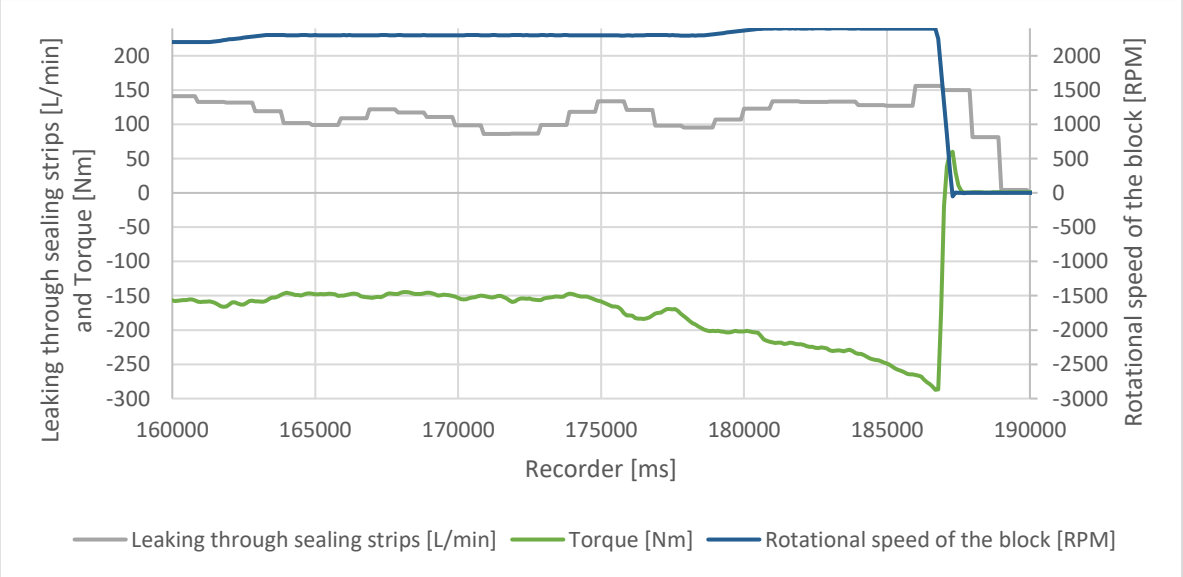

Figure 41 Motoring regime with seized engine

Table 10 Results for new simulated model with ignition for 3000 RPM

	Max cylinder pressure [bar]	Brake torque [Nm]	Brake power [kW]	Vol. efficiency [%]	Blowby [l/min]	Air flow rate [l/min]	Burned fuel [%]
Ignition	30.45	37.43	11.76	98.57	18.03	1289.21	59.99

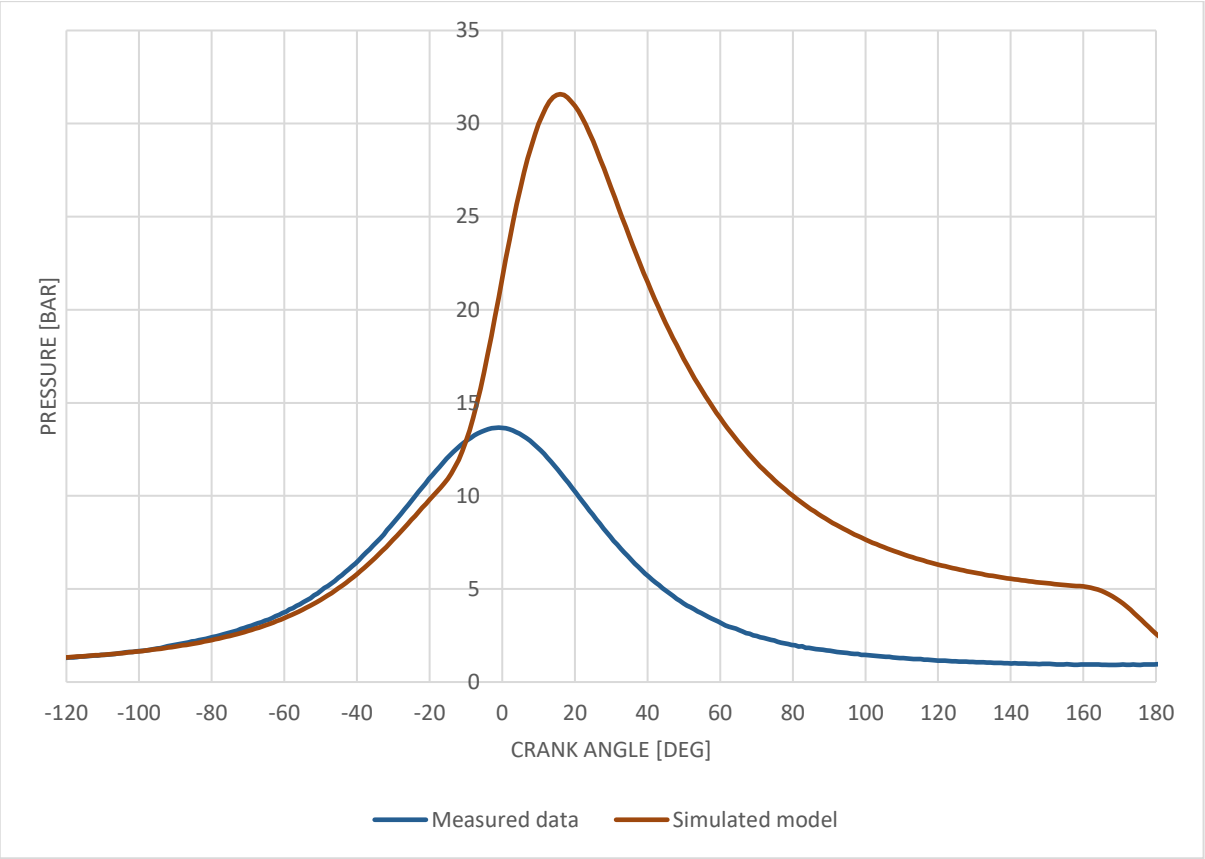

Figure 42 Comparison of measured data with seized engine and simulated model for 5600 RPM

5.6. Flow split

As it was mentioned, for the intake and exhaust pipes a fake flow split was created. This flop split connects manifolds from each cylinder into one manifold as in reality. A flow split general is used with a volume of 100000 mm^3 and specific angle configuration. It acts as a part of the pipe with properties and the flow can be in every direction. But because there is not anything like the flow split in real manifolds, therefore a better solution is desired. This flow split general is replaced with a new object, which is a slave flow state. The three short pipes from the cylinders are set as the “slave” ports and the one long manifold is set as the “master” port. This object allows the flow only between a “master” port and a “slave” port, therefore there cannot be a flow between the three short pipes, which is desired. As we can see in the Figure 44 the influence of the slave flow state object is mainly in the higher RPM range. [43]

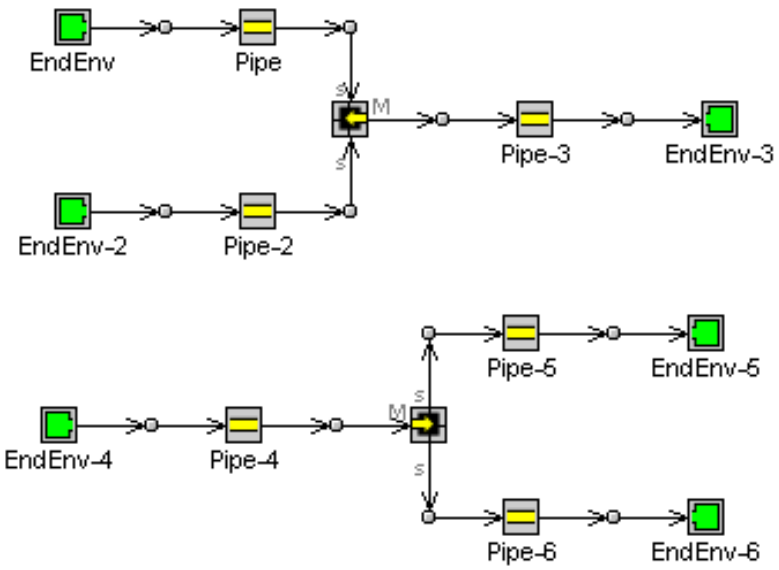

Figure 43 Use of slave flow state object [43]

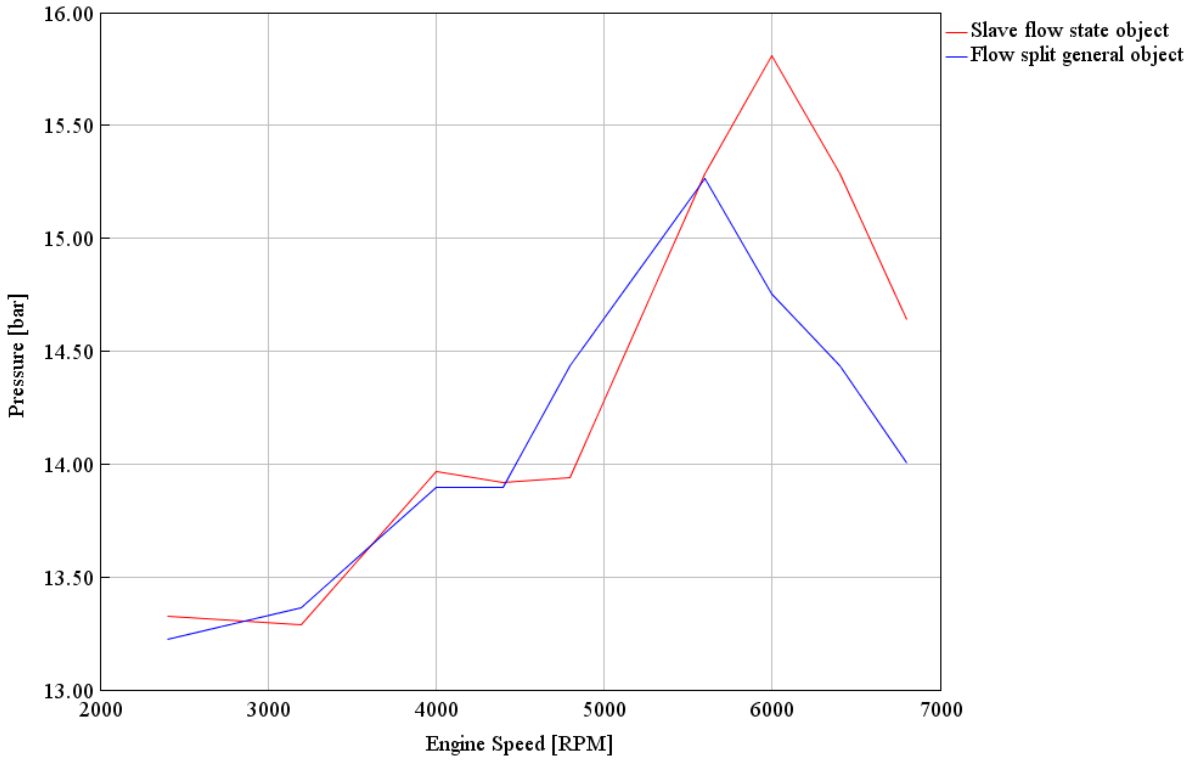

Figure 44 Influence of flow objects on maximum cylinder pressure

6. Sub-model of clearances

6.1. Sub-model proposal

The simple model of clearances, which is used in previous simulations has a major influence on the pressure curve and other properties of the engine. Therefore, a more accurate and complex model of clearances is desired. The company KNOB ENGINES s.r.o. provides a CAD model of clearances (Figure 45) with a total volume of 20495 mm^3, so the sub-model can be created in the GT model. Based on this model several options for creating the sub-model are proposed. The model is divided into several objects with corresponding volumes.

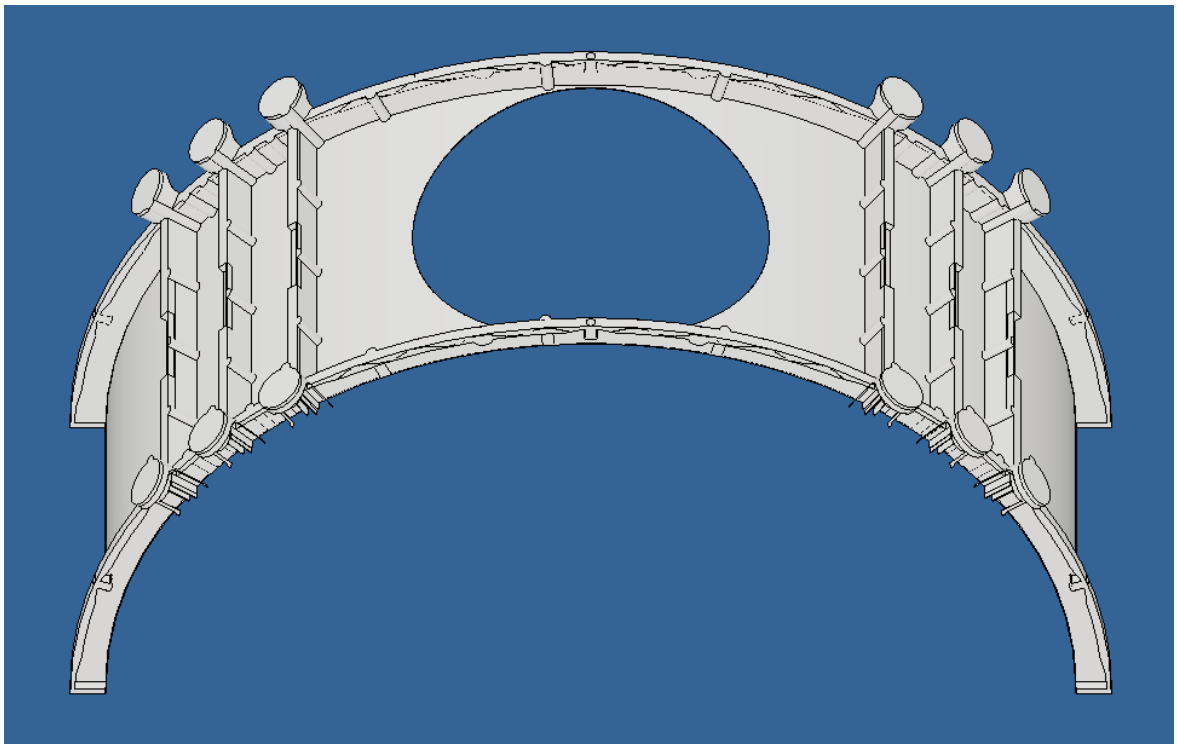

Figure 45 CAD model of clearances [47]

6.1.1. Version 1

In the first proposed option, the clearances of the sealing strips remain as a one single object. The space between the cylinder block and cylinder head is split into 5 segments, which are marked with a color in the Figure 46. Four of these segments are equal and the one in the middle is the biggest one. Small half cylinders of small volumes are included in these segments. The total volume has almost remained the same as in the simple model (Table 11).

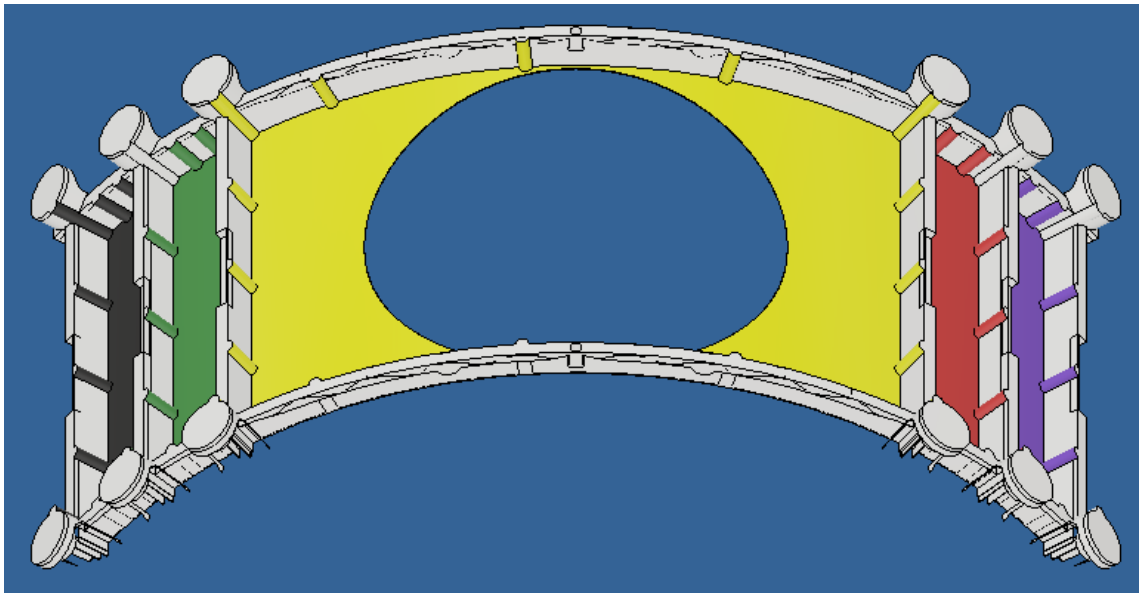

Figure 46 Version 1 of the sub-model

Table 11 Volume of clearances; version 1

	Total	Sealing strips	Yellow segment	1 of 4 equal segments
Volume [mm^3]	14637	9897	2000	685

6.1.2. Version 2

The second point of view of creating the sub-model is the same as the first one, but the small half cylinders are included in the volume of the sealing strips (Figure 47). These small half cylinders are made in the cylinder head and in order to reduce the total volume, they might not be created in the cylinder head in the future. But because the data are measured with this half cylinders, they are considered in all versions.

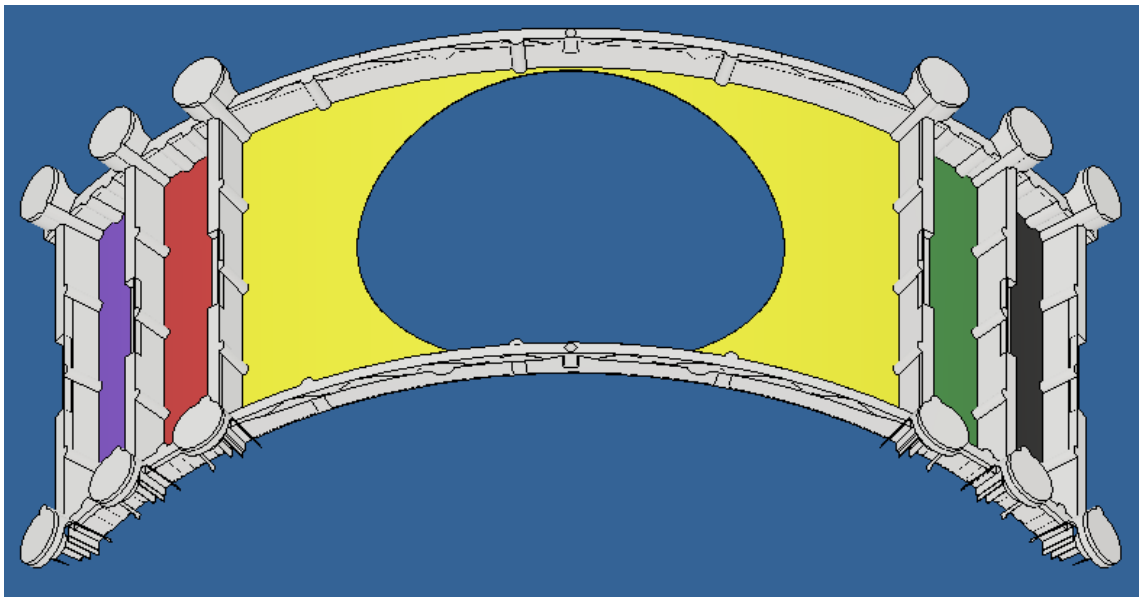

Figure 47 Version 2 of the sub-model

Table 12 Volume of clearances; version 2

	Total	Sealing strips	Yellow segment	1 of 4 equal segments
Volume [mm^3]	14637	11500	1485	410

6.1.3. Version 3

Another proposal is connecting the space of sealing strips to the space between the cylinder block and cylinder head. Then dividing the whole volume into 5 smaller volumes, where 4 of them are the same and the fifth volume is the biggest (Figure 48).

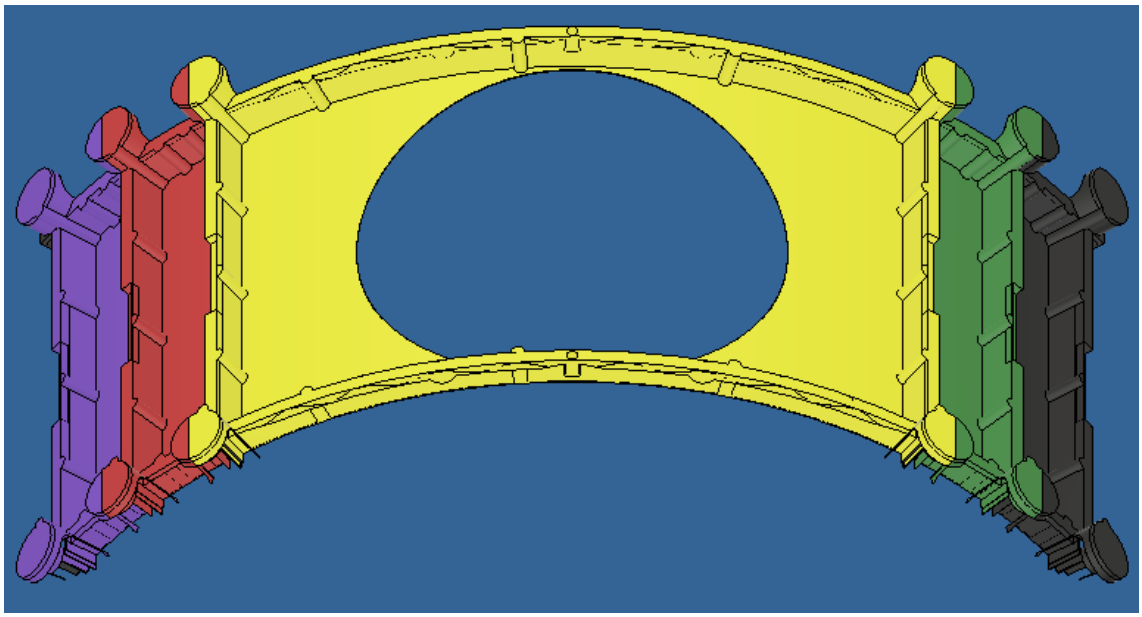

Figure 48 Version 3 of the sub-model

Table 13 Volume of clearances; version 3

	Total	Yellow segment	1 of 4 equal segments
Volume [mm^3]	14637	6585	2013

6.1.4. Version 4

The next version of dividing the volume of clearances is taking the version 3 and separate the volume of the sealing strips and the space between the cylinder block and cylinder head (Figure 49). This is the most complex and probably the most accurate option of the sub-model.

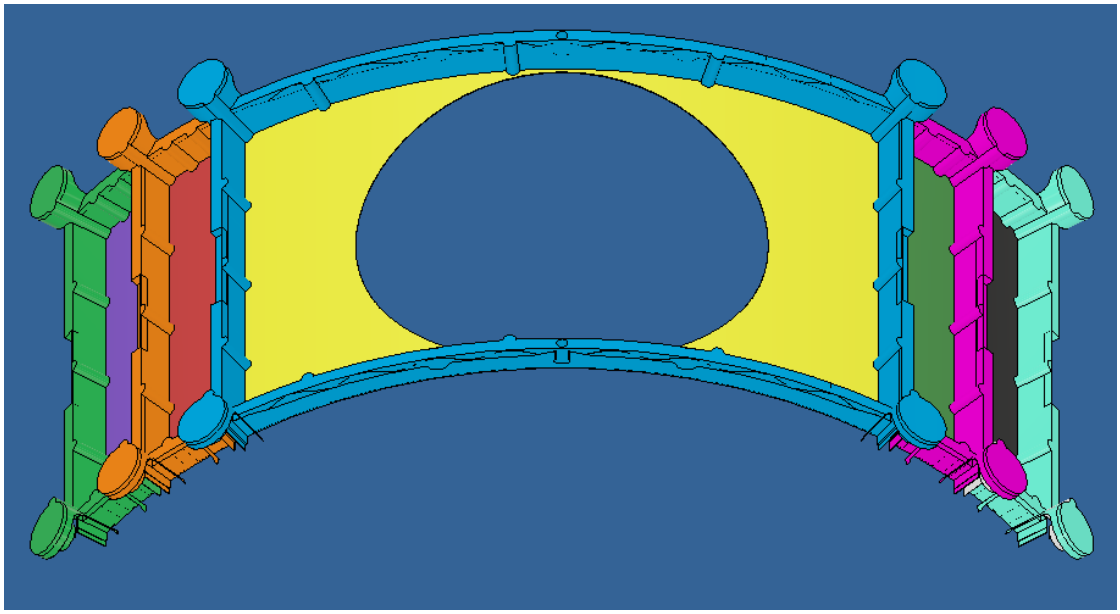

Figure 49 Version 4 of the sub-model

Table 14 Volume of clearances; version 4

	Total	Blue sealing strips	1 of 4 equal sealing strips	Yellow segment	1 of 4 equal segments
Volume [mm^3]	14637	5100	1600	1485	413

6.1.5. Version 5

In the Figure 45 we can see that the space of sealing strips and the space between the cylinder head and the cylinder block is even more on the side than in previous versions. All these clearances are divided as in the Figure 50. This option is not considered for further use, because in the space between the cylinder block and the cylinder head the intake and exhaust manifolds are placed, therefore these two spaces are not considered as clearances. These two spaces of sealing strips on these two sides are permanently connected to the spaces where the intake and exhaust manifolds are, therefore, there are not also considered as clearances.

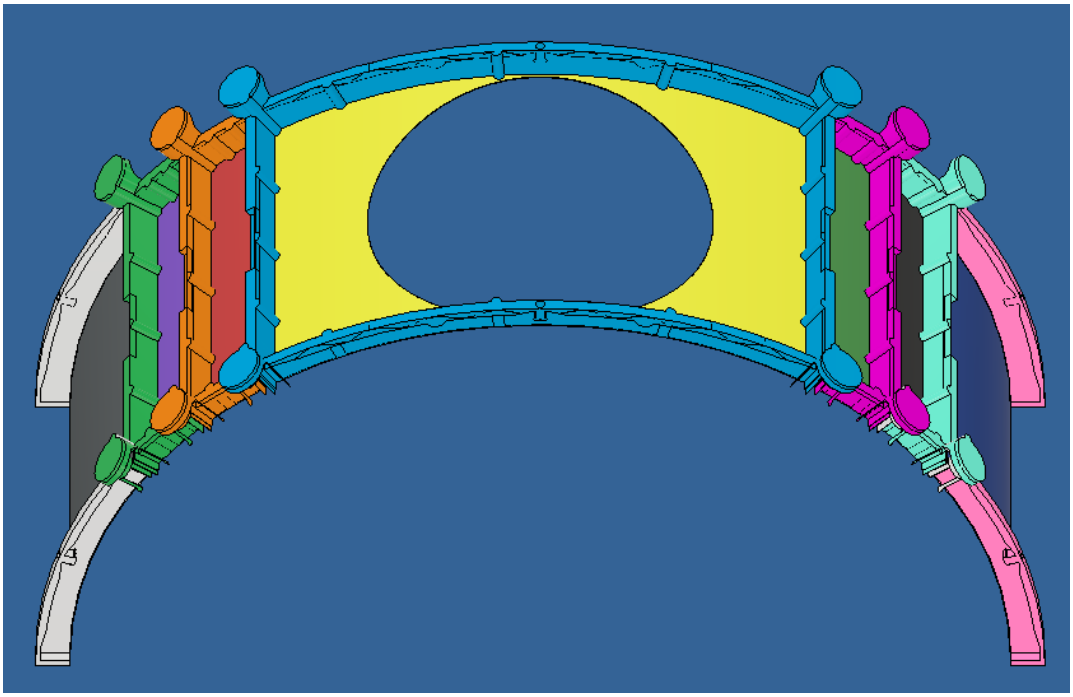

Figure 50 Version 5 of the sub-model

6.2. Choosing a version

As the best and the most accurate proposal of the sub-model the Version 4 is chosen. To create this complex model in GT-Power a lot of parameters had to be taken from the CAD model, as the volumes of every segment and the connections between these segments.

6.2.1. Volume of spaces between cylinder block and cylinder head

Starting with the spaces between the cylinder block and cylinder head. Their volume depends on the crank angle. As the cylinder block rotates, the cylinder is passing every segment and connects it with the combustion chamber (Figure 51). In the CAD model the extrusion of the cylinder is rotated and the volume of all the segments is written down for every single degree. Then the dependency of the volume on the crank angle is created for every part (Figure 52).

Figure 51 Change of volume with change of cylinder position

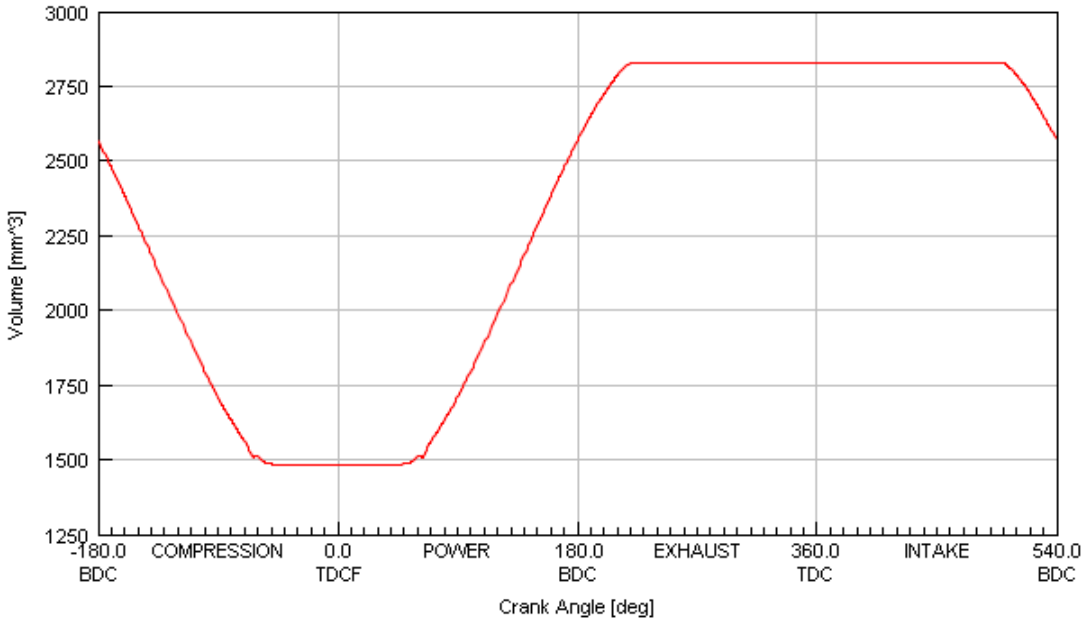

Figure 52 Dependency of volume on crank angle of the yellow segment

6.2.2. Connection of clearances and combustion chamber

The connection between these spaces and the combustion chamber is also changing with the rotating cylinder block (Figure 53), therefore the dependency of the connection area on the crank angle is created the same way as the volume dependency. In the GT model this connection area is created by an orifice with a changing hole diameter. The effective area of this changing diameter corresponds to the area of the connection.

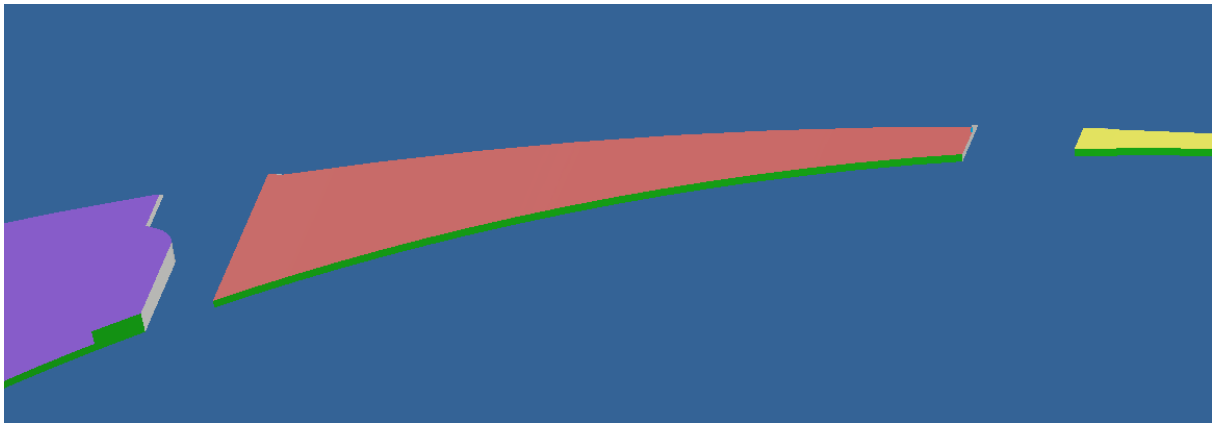

Figure 53 Green surface –connections area of clearances and combustion chamber

6.2.3. Clearances of sealing strips

The volume of clearances of the sealing strips remains constant with the rotating cylinder block, therefore no dependency is needed for the volume. But the connection (Figure 54) between these clearances and the space between the cylinder block and the cylinder head is changing with the rotating cylinder block, therefore the dependency for the connection is desired and created by an orifice the same way as before. The connection between the sealing strips (Figure 55) is constant for the whole time and is made by an orifice with a constant hole diameter.

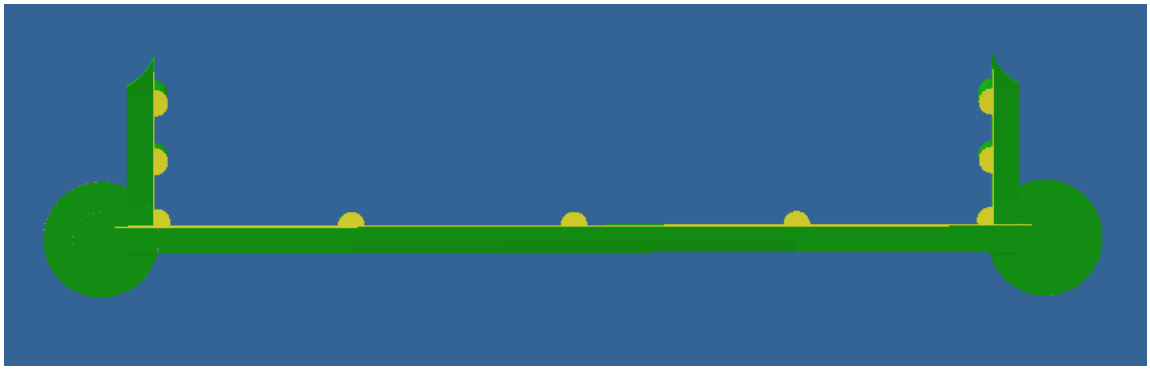

Figure 54 Yellow area – connection of clearances of sealing strips and space between cylinder block and cylinder head

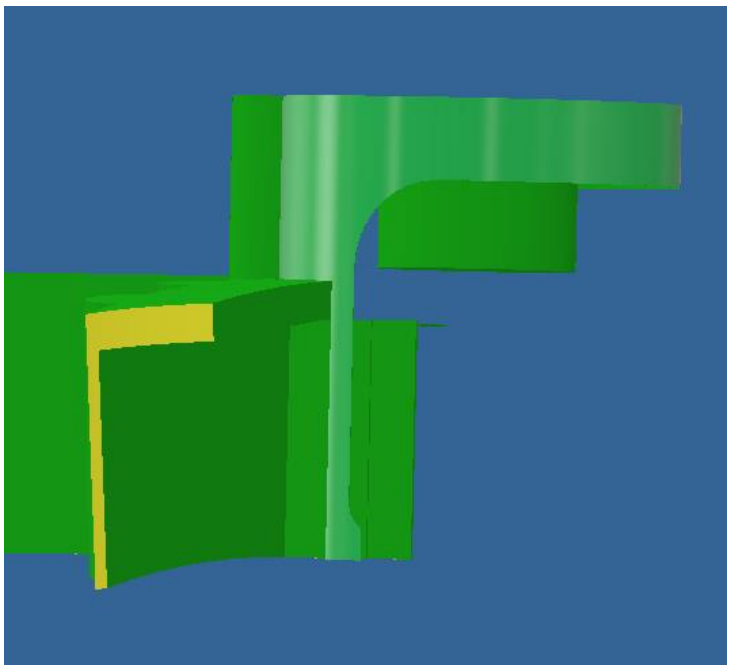

Figure 55 Yellow area – connection of clearances of sealing strips

Table 15 Example of properties of the yellow segment

Angle of rotation of the block [°]	Relative angle of rotation [°]	Volume [mm^3]	Connection with the combustion chamber [mm^2]	Diameter of connection with the combustion chamber [mm]	Connection with the sealing strip [mm^2]	Diameter of connection with the sealing strip [mm]
-56	-224	2829.77	0	0	169	14.67
-55	-220	2829.77	0	0	159.58	14.25
-54	-216	2815.61	5.779	2.71	157.09	14.14
-53	-212	2797.37	8.283	3.25	155.27	14.06
-52	-208	2775.94	10.212	3.61	150.91	13.86
-51	-204	2751.87	11.852	3.88	145.48	13.61
-50	-200	2725.64	13.311	4.12	144.41	13.56

6.2.4. Leaking into the atmosphere

When the gas gets through the clearances into the space of sealing strips it can leak into the atmosphere through a small area (Figure 56). This leaking area is created by an orifice with a constant hole diameter.

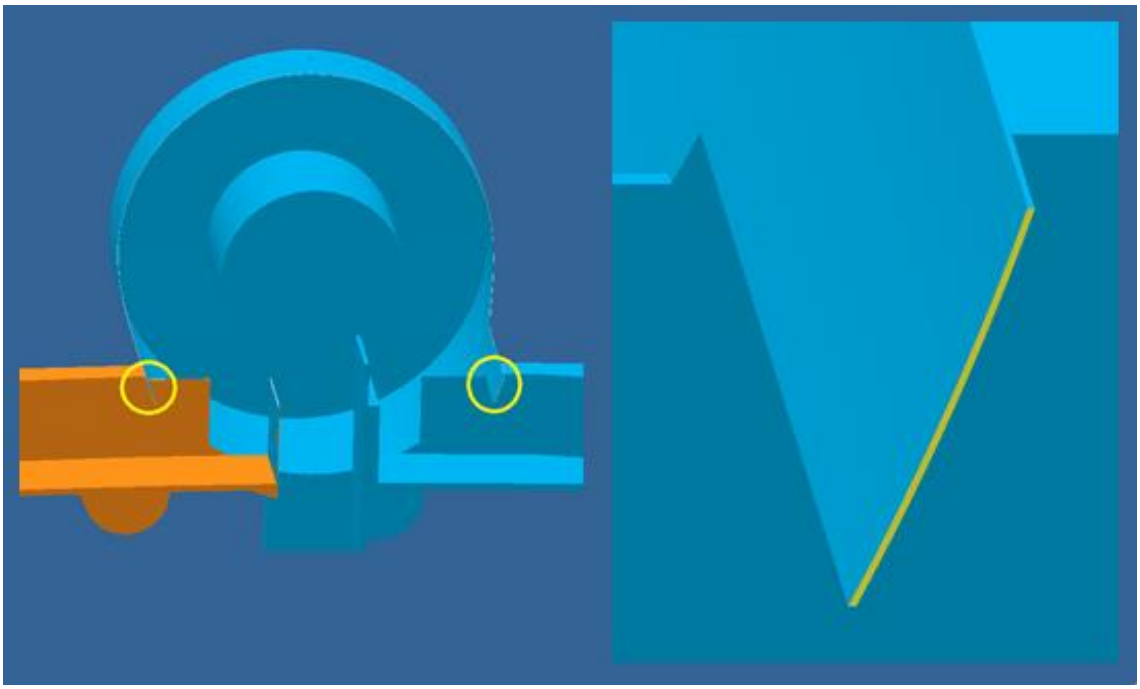

Figure 56 Yellow area – leaking area

6.3. Creating sub-model in GT-Power

As the best option of creating the sub-model in GT–Power the flow split sphere object is used for every part of clearances. These spheres are connected through the orifices as it is described earlier. After finishing this model and running the simulation several warnings occurred. For the flow split spheres, creating the clearances between the cylinder block and the cylinder head, the warning says that the total area of flow split holes is too large. This means that the surface area of the created sphere is smaller than the effective area of the orifices. Even that the program simulates the model, the results cannot be considered valid, thus a different approach needs to be applied.

For the free space of the sealing strips the flow split sphere is used, because it does not report any warnings. For the clearances between the block and the head the flow split general object is used instead. By using this object, the simulation runs well and does not report any warnings according to the hole area.

After running this model, the results were not still accurate and similar as the measured data. It is caused because the effective area of the orifices is the same as the connection area between the clearances, but the actual shape of the connection is different. This difference is resolved by changing and calibrating the discharge coefficients in the orifices.

Every single cylinder has its own sub-model of clearances, which means they are not connected together. In reality, there are only two sub-models and every cylinder alternates these two sub-models. But because the dependencies are created for the volumes of the clearances and for the diameters of the orifices, the sub-models cannot be connected. The dependencies are on the crank angle, which is only 720°, therefore it is not possible to get involved all 3 cylinders in one dependency. For example, the dependency of the volume for 1 cylinder takes place for about 400°, therefore only one cylinder can be included (Figure 52).

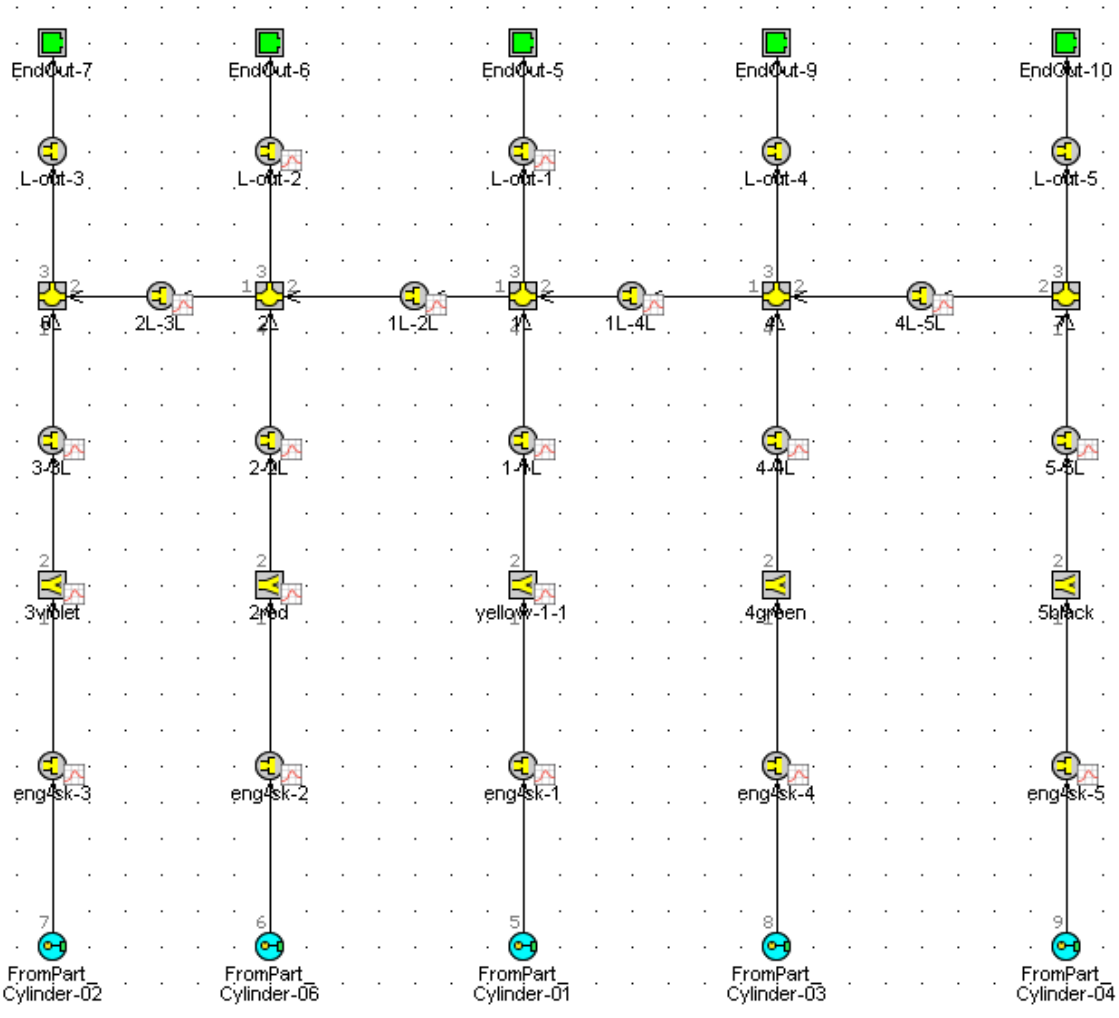

Figure 57 Scheme of clearances created in GT-Power

In the Figure 58 we can see the comparison of the measured data, the old model, and the new created sub-model of clearances. In the low RPM range the new model is more accurate and the results are almost the same. In the high RPM range the results are still not as much accurate as we would like it to be, but they are more promising than the in the old model.

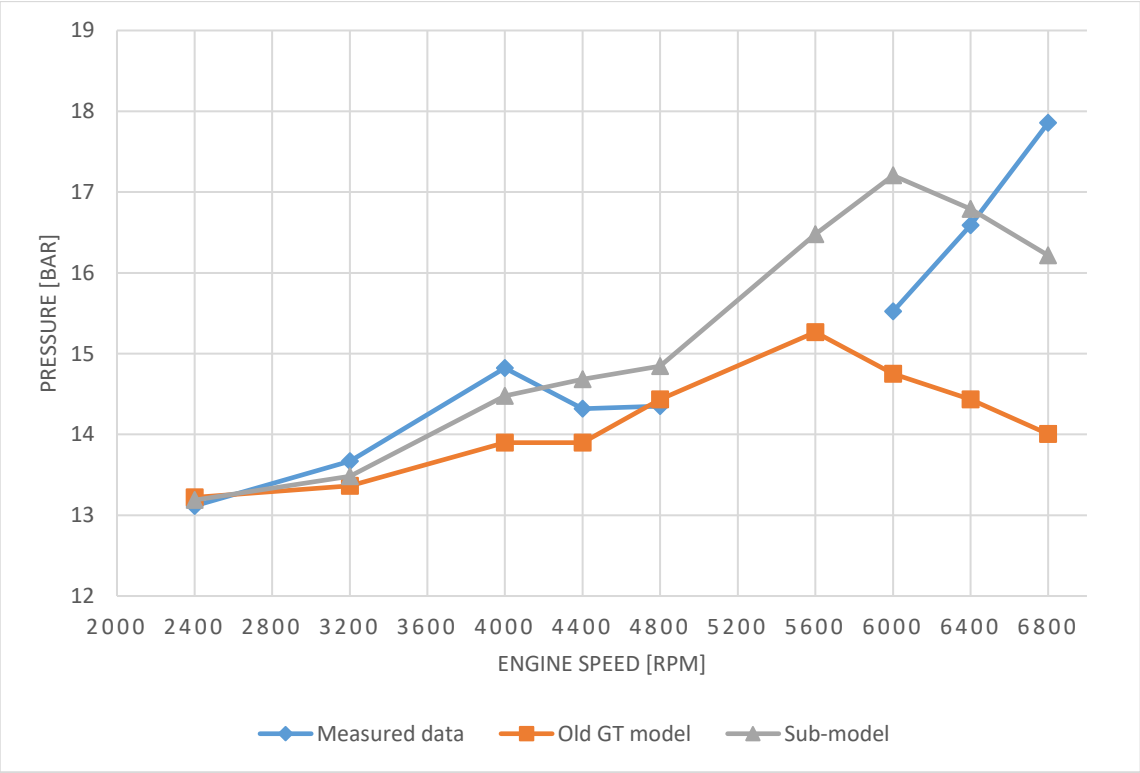

Figure 58 Comparison of measured data, old GT model, and new sub-model

As another possibility the half cylinders (Figure 59) are removed from the volume of the sealing strips clearances. This half cylinders are made in the cylinder head for better placing the sealing strips, but without them, the volume of clearances reduces, and the performance of the engine could be better. This is simulated in the same sub-model, but with the new reduced volume. The influence on the maximum cylinder pressure is shown in the Figure 60. And we can see that the maximum cylinder pressure is higher for the whole RPM range.

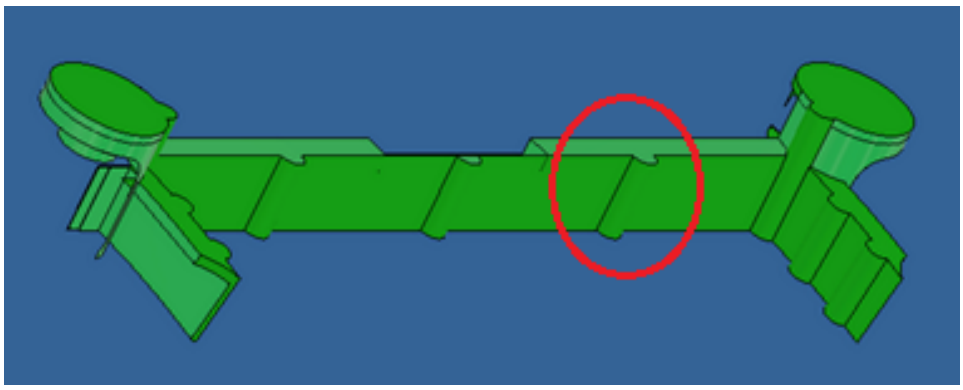

Figure 59 Half cylinders in sealing strips clearances

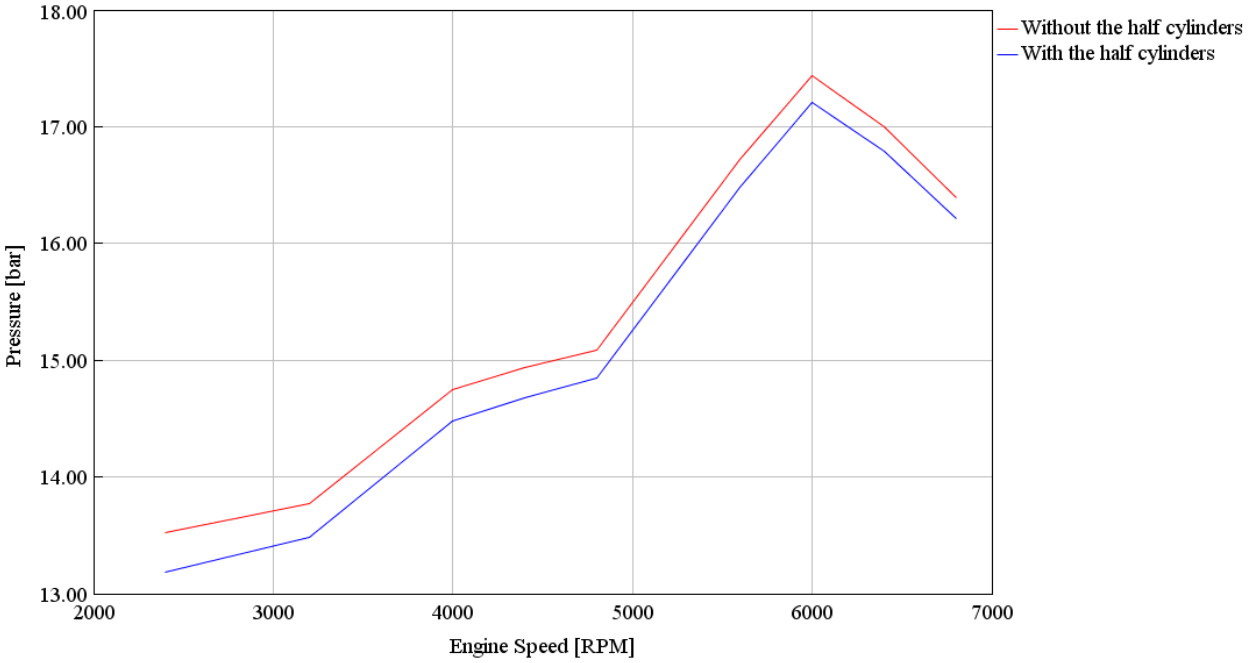

Figure 60 Comparison of maximum cylinder pressure with and without half cylinders

7. Optimization

For optimization is used the GT–Power model with the simple model of clearances. The latest model with the sub-model of clearances is not used due to its complexity and long simulation time. The simple version works well for all the prediction with quite accurate results.

7.1. Optimization of intake manifold geometry

In the Figure 61 we can see the chosen part of intake manifolds for the optimization. In the GT–Power model this part is made of 4 objects with different length and thickness. The length of one of these objects is created as a parameter and is defined in the case setup. The actual and initial length of this object is 17 mm, while the lower limit in the “Design Optimizer” is set to 10 mm and the upper limit is set to 150 mm.

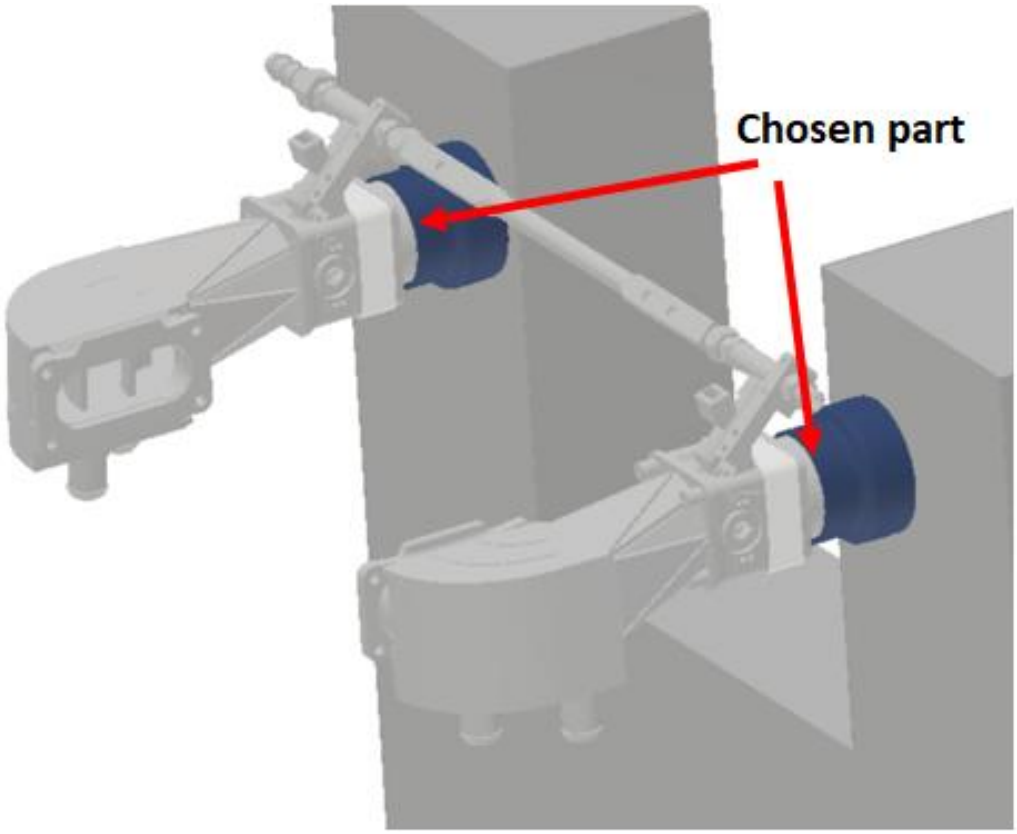

Figure 61 Chosen part for intake optimization [45]

7.2. Optimization of exhaust manifold geometry

The chosen part for the optimization can be seen in the Figure 62. It is the long tube after the bending and before the conjunction. This section of the exhaust manifold is chosen as the best part for optimization, to see what effect has the length of this section. Its length is set as a parameter, which is specified in the case setup as for the intake. The initial length of this pipe is 205 mm, while the lower limit in the “Design Optimizer” is set to 10 mm and the upper limit is set to 300 mm.

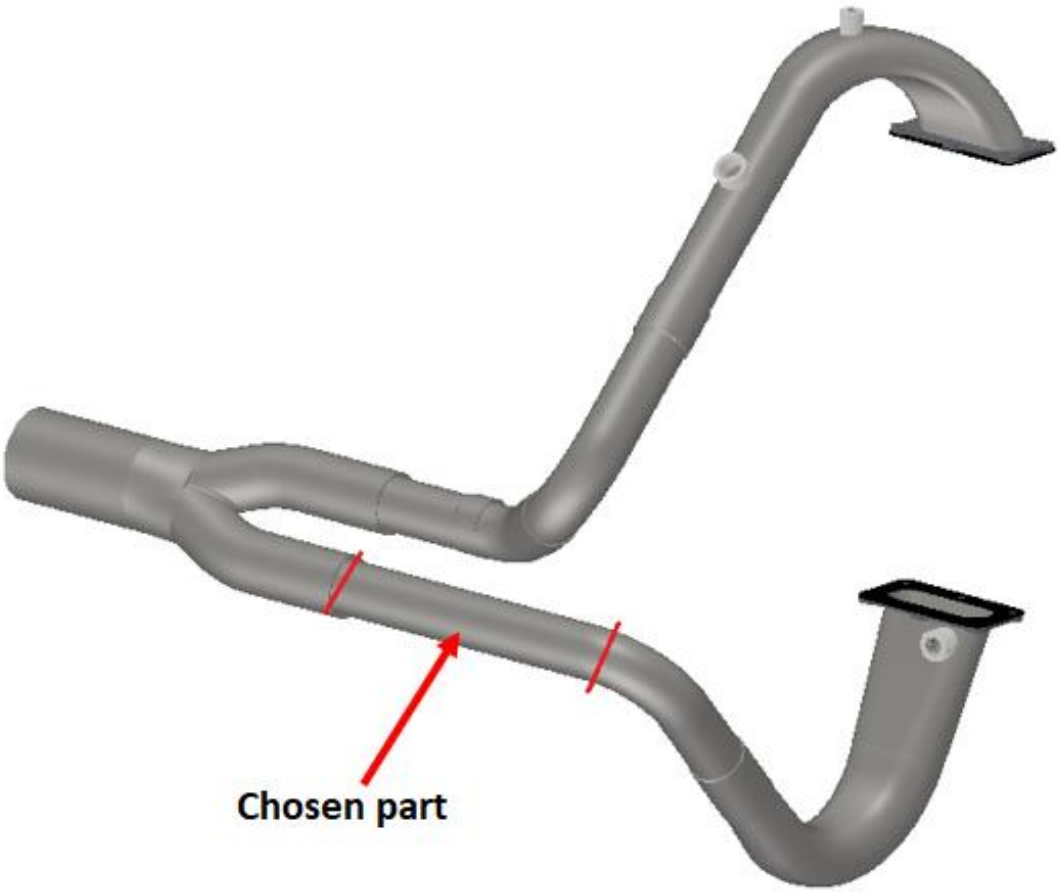

Figure 62 Chosen part for exhaust optimization [44]

7.3. Optimization of intake and exhaust port timing and their shape

In the GT–Power model the intake and exhaust ports are replaced by valves. The lift depends on the crank angle and its flow coefficients are set from a measurement to simulate these ports. The flow coefficients of the old shape of the intake and exhaust ports are used, because a new measurement could not be done, because of the COVID–19 situation. Although the old coefficients are still used, the optimization of the intake and exhaust port timing and their shape is still performed. Two parameters are created for both intake and exhaust.

The first parameter is for the timing of the ports. A “Cam Timing Angle” is set as a parameter, which basically says when the valve lift in the GT–Power model starts for the intake and when it ends for the exhaust. In the case setup the initial and until now used value is 0, which means that the timing starts (ends) at TDC between the exhaust and intake stroke. The lower limit in the “Design Optimizer” for the “Cam Timing Angle” is set to -20 and the upper limit is set to 20.

The second parameter is about the shape of the ports, more correctly about the crank angle array for the lift. The parameter is “Angle Multiplier”, which multiplies the whole crank angle range for the valve lift and can make the range wider or narrower. The initial value of this parameter is 1 in the case setup and in the “Design Optimizer” the lower limit is 0.75 and the upper limit is set to 1.25.

7.4. Optimization number 1

For the first optimization the brake torque is selected as the RLT response, which is set to be maximized for the average case RLT. That means the goal of this optimization is to reach the maximum brake torque in the middle cases. It is set for 6 cases of the engine speed in the range of 2400 – 5600 RPM. This is the range of the engine speed that the last measurement of the engine was performed. The results of this optimization are shown in Table 16. For the exhaust part there is not a big difference, but for the intake part the length of the chosen section is bigger. In Table 17 we can see the comparison of the old and new settings of the valves. The time when the exhaust valves are open is a little bit longer and for the intake valves it is a little bit shorter, but still there is not an overlap.

Table 16 Optimization number 1

	Initial value	Optimized value
Length of the exhaust manifold part [mm]	205	231.58
Length of the intake manifold part [mm]	17	73.93
Cam Timing Angle – intake [°CA]	0	1.251
Angle Multiplier – intake [-]	1	0.93
Cam Timing Angle – exhaust [°CA]	0	0.099
Angle Multiplier – exhaust [-]	1	1.01

Table 17 Intake and exhaust valves settings of the first optimization

Exhaust valves	Initial	Optimized	Intake valves	Initial	Optimized
Open [°CA]	-204	-207.25	Open [°CA]	0	1.25
Close [°CA]	0	0.099	Close [°CA]	204	191.25

The original brake torque is compared with the new one in the Figure 63. With the optimized values the brake torque is higher in the middle section of the engine speed as it was desired. The biggest difference in the brake torque is approximately about 10 %, which means that there is a small space for an improvement with this setting. The Figure 65 shows the optimized value of the angle multiplier for intake versus the new design. In Figure 65 we can see the designs versus the angle multiplier for intake and how the values for the multiplier are between 0.9 and 1.

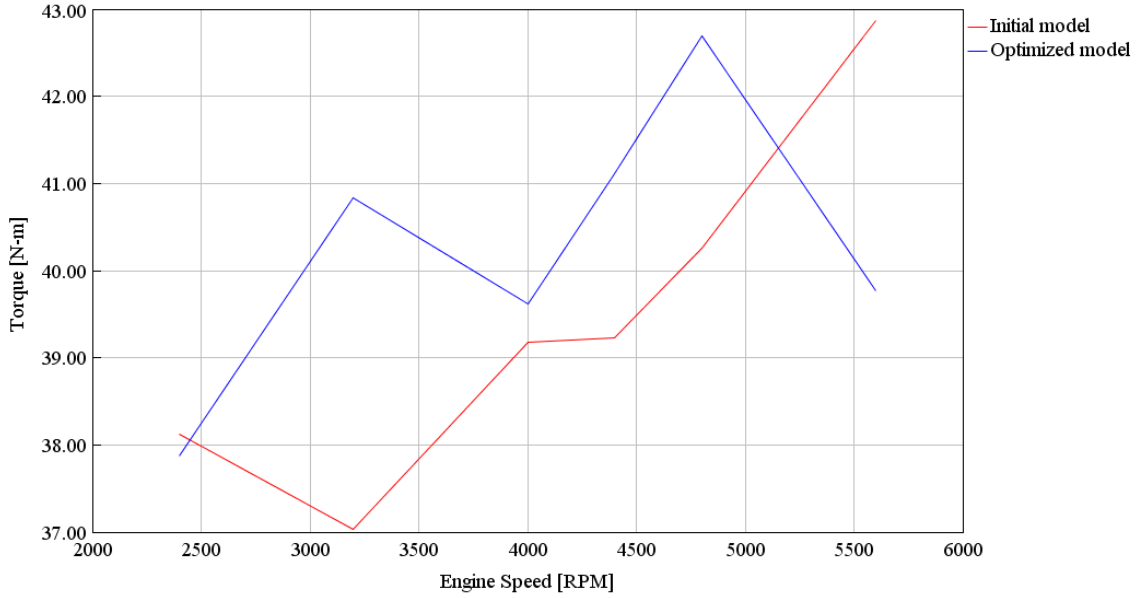

Figure 63 Comparison of brake torque of initial model and the first optimized model

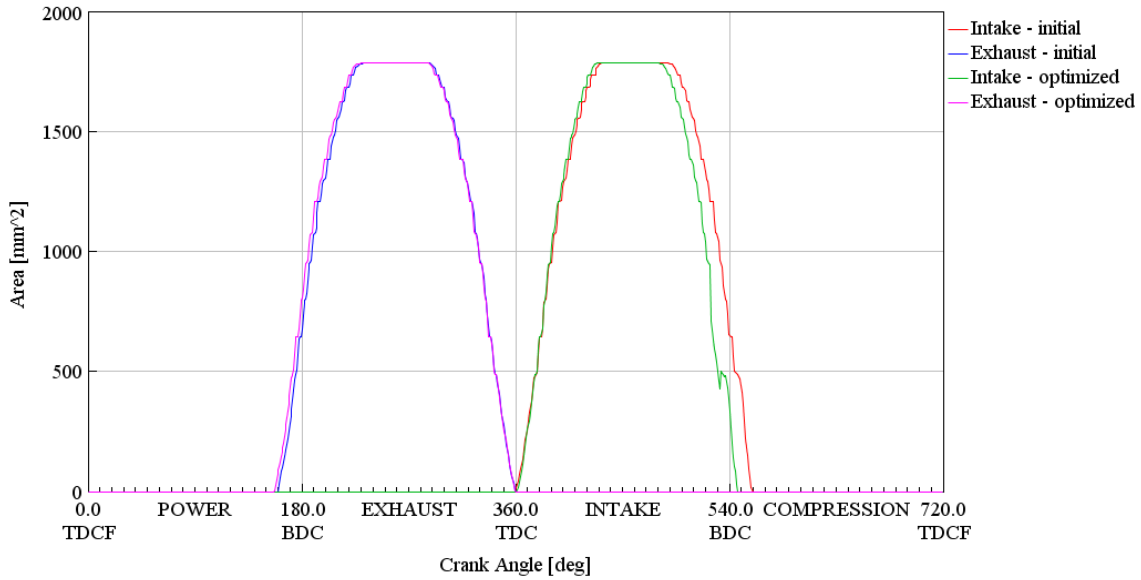

Figure 64 Comparison of intake and exhaust effective´s areas for optimization number 1

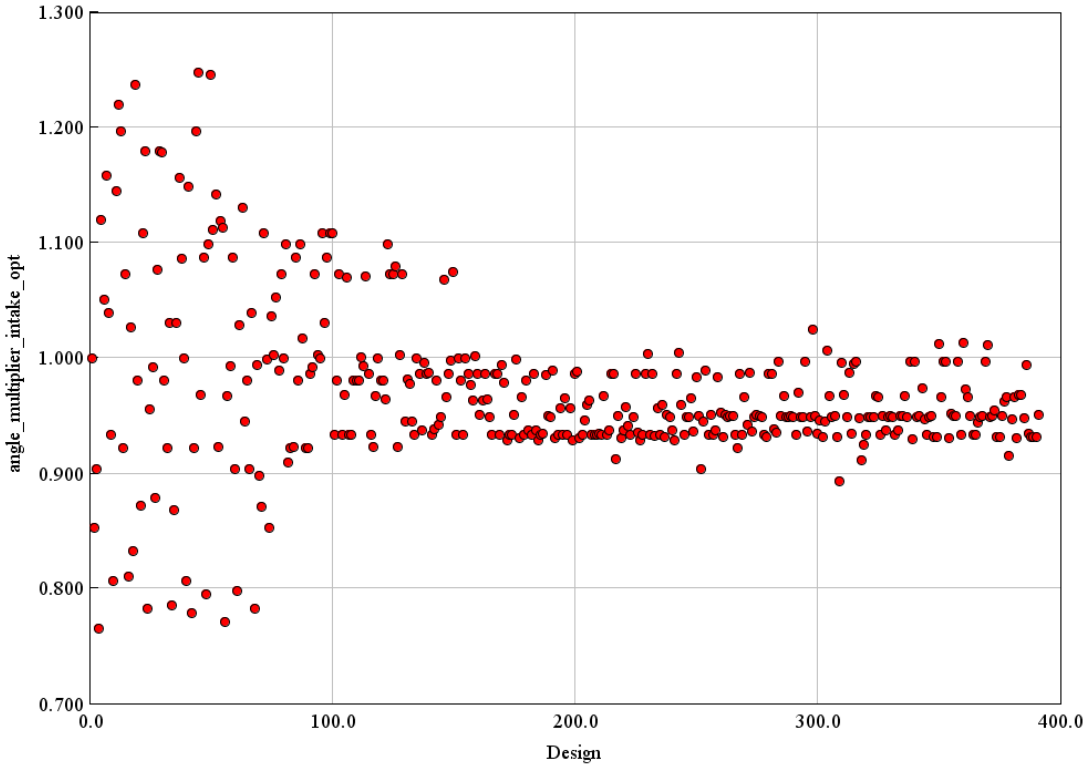

Figure 65 Optimized angle multiplier – intake vs design

7.5. Optimization number 2

For the second optimization the brake power is selected as the RLT response. The brake power is also set to be maximized, but this time instead of setting it on the average case RLT it is set to maximum case RLT. This means that instead of maximizing the brake power in the middle cases, it is maximizing the brake power in the upper cases. It is set again for the 6 measured cases of the engine speed in the range of 2400 – 5600 RPM. This optimization is also done without any clearances objects to optimize the parameters while using a more ideal model of the engine. Using the model without clearances does not have a big influence on the shape of the curves, the shape is basically the same, only the values are higher. Also, the CR is set to 8.

In Table 18 we can see the results of the second optimization. The length of the intake and exhaust manifold parts is basically unchanged. The significant changes occurred for the intake and exhaust valve settings. Table 19 shows the initial and the new optimized values of the timing of the valves. It can be seen that the exhaust valve

opens and closes later than the original one. For the intake valve it is the other way, it opens and closes earlier than the original settings. This means that with this optimization an overlap is created again. In this case the overlap is approximately for 47 °CA.

Table 18 Optimization number 2

	Initial value	Optimized value
Length of the exhaust manifold part [mm]	205	198.29
Length of the intake manifold part [mm]	17	19.72
Cam Timing Angle – intake [°CA]	0	-11.32
Angle Multiplier – intake [-]	1	0.97
Cam Timing Angle – exhaust [°CA]	0	36.61
Angle Multiplier – exhaust [-]	1	1.11

Table 19 Intake and exhaust valve settings of the second optimization

Exhaust valves	Initial	Optimized	Intake valves	Initial	Optimized
Open [°CA]	-204	-190.50	Open [°CA]	0	-11.32
Close [°CA]	0	36.61	Close [°CA]	204	186.92

In the Figure 66 and the Figure 67 we can see the results of this optimization comparing with the original model. The brake power and the brake torque are just slightly higher in the higher engine speeds at the expense of a bigger reduction in the middle engine speeds. For the 4000 RPM the drop for the brake torque is approximately 40 % and for the brake power it is also approximately 40 %. This is a big drop, which is not worthy just because in the 5600 RPM the gain of the brake torque is approximately 4 % and for the brake power it is also almost 4 %. This drop is caused by the burned mass at the combustion start. A much higher percentage of the residual gases remains in the cylinder after the exhaust stroke (Figure 68), which results in lower cylinder pressure, brake torque, brake power etc.

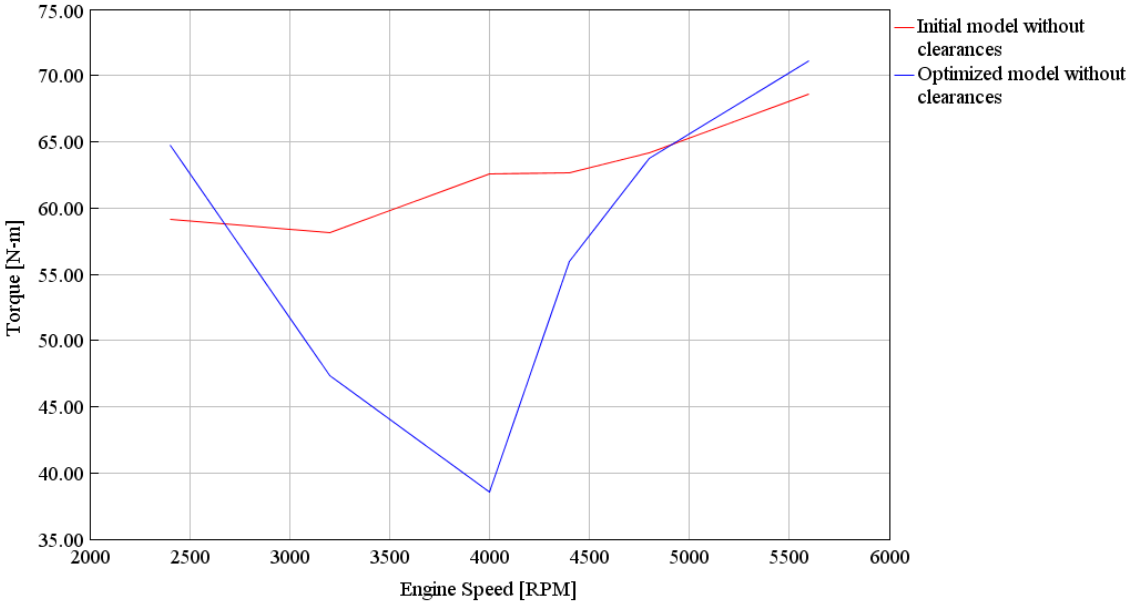

Figure 66 Comparison of brake torque of initial model and the second optimized model

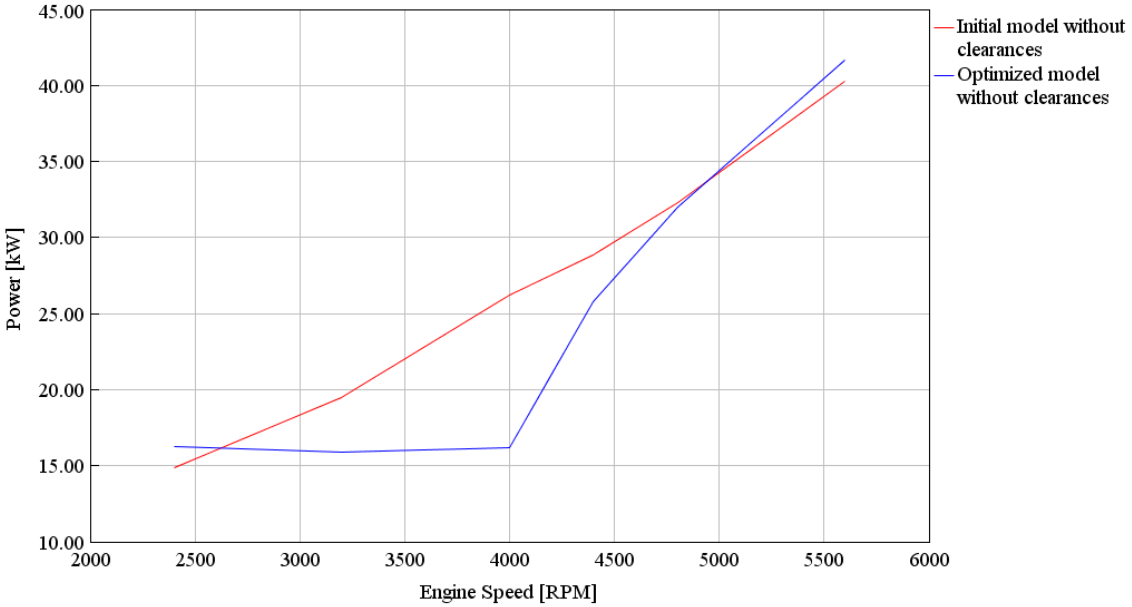

Figure 67 Comparison of brake power of initial model and the second optimized model

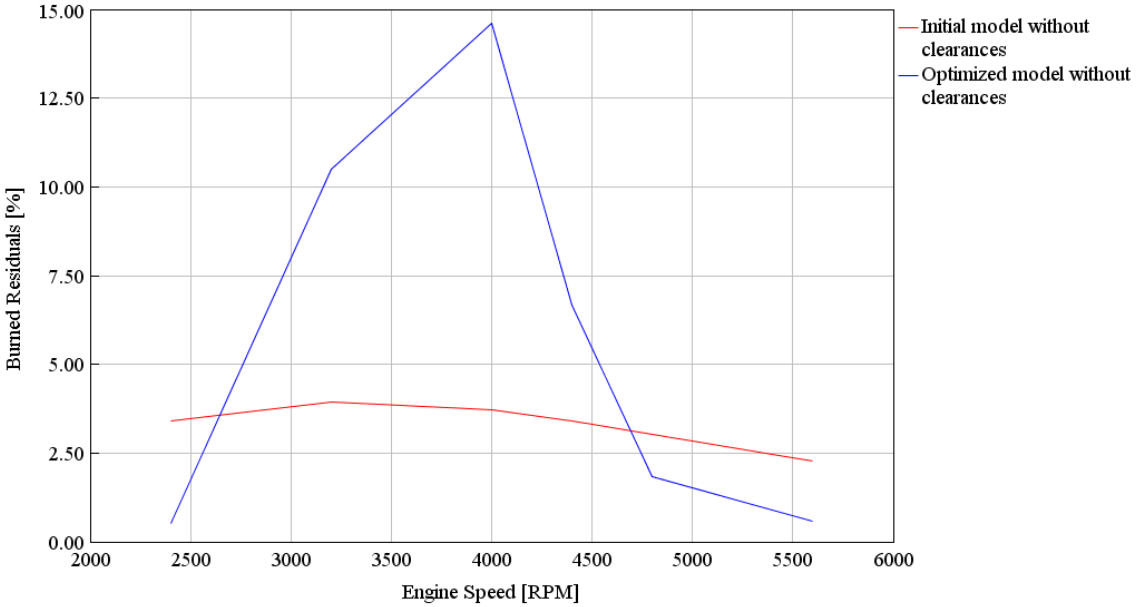

Figure 68 Burned mass percent at combustion start

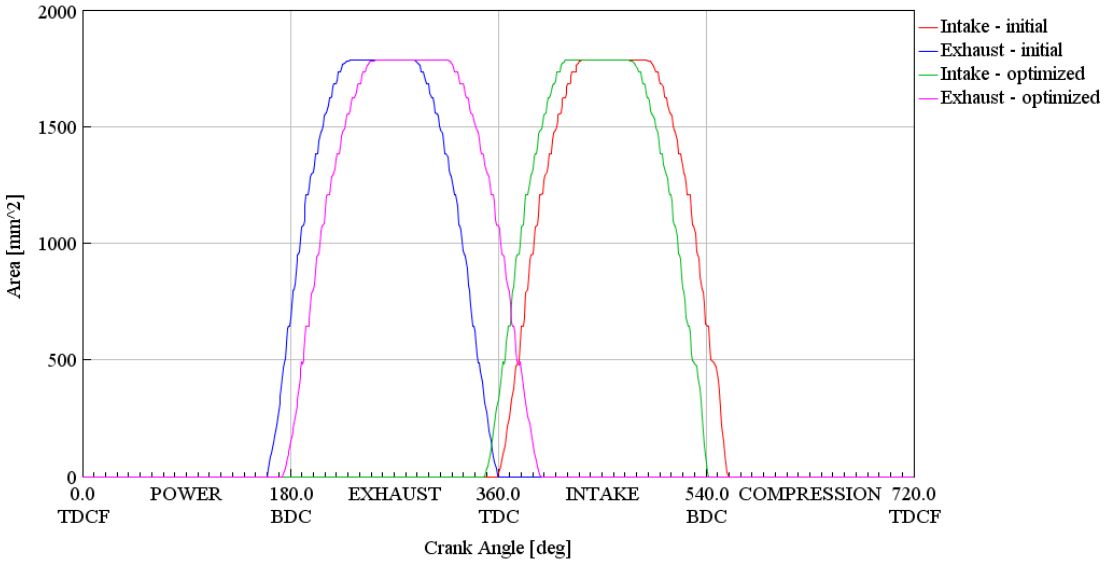

Figure 69 Comparison of intake and exhaust effective´s areas for optimization number 2

7.6. Optimization number 3

The brake torque is used as the RLT response for the third optimization. In this optimization the brake torque is also set to be maximized for the average case RLT as in the first one. Therefore, the optimization is trying to get the maximum brake torque in the middle cases. Eleven cases are turned on starting with 6000 RPM and ending with 10000 RPM. It is set for the higher RPM range, which are the engine speeds where this engine should be ideally used, even though we still have not done any measurement in this RPM range.

Table 20 shows the results of this optimization and it can be seen that the length of the intake manifold part is almost the same as the initial value, but the length of the exhaust manifold part is much shorter. In the Table 21 new opening and closing timing of the valves are shown. The range of the angle for which the valves are open is wider for both the intake valve and the exhaust valve. The exhaust valve opens earlier and closes later than in the original settings. The intake valve opens also earlier, but it closes a little bit earlier than in the original settings. This new setting of the valves causes an overlap for quite a long time, something about 53 °CA.

Table 20 Optimization number 3

	Initial value	Optimized value
Length of the exhaust manifold part [mm]	205	16.58
Length of the intake manifold part [mm]	17	16.21
Cam Timing Angle – intake [°CA]	0	-33.58
Angle Multiplier – intake [-]	1	1.14
Cam Timing Angle – exhaust [°CA]	0	19.28
Angle Multiplier – exhaust [-]	1	1.18

Table 21 Intake and exhaust valve settings of the third optimization

Exhaust valves	Initial	Optimized	Intake valves	Initial	Optimized
Open [°CA]	-204	-220.60	Open [°CA]	0	-33.59
Close [°CA]	0	19.28	Close [°CA]	204	198.37

The results and comparison of this optimization and the initial model are shown in the Figure 70. This optimization in the higher RPM range is quite promising, because the results with this new optimized data are better for every simulated engine speed. At 6000 RPM the increase of the brake torque is only by about 5 %, but at 6800 RPM the increase is the largest by about 18 %.

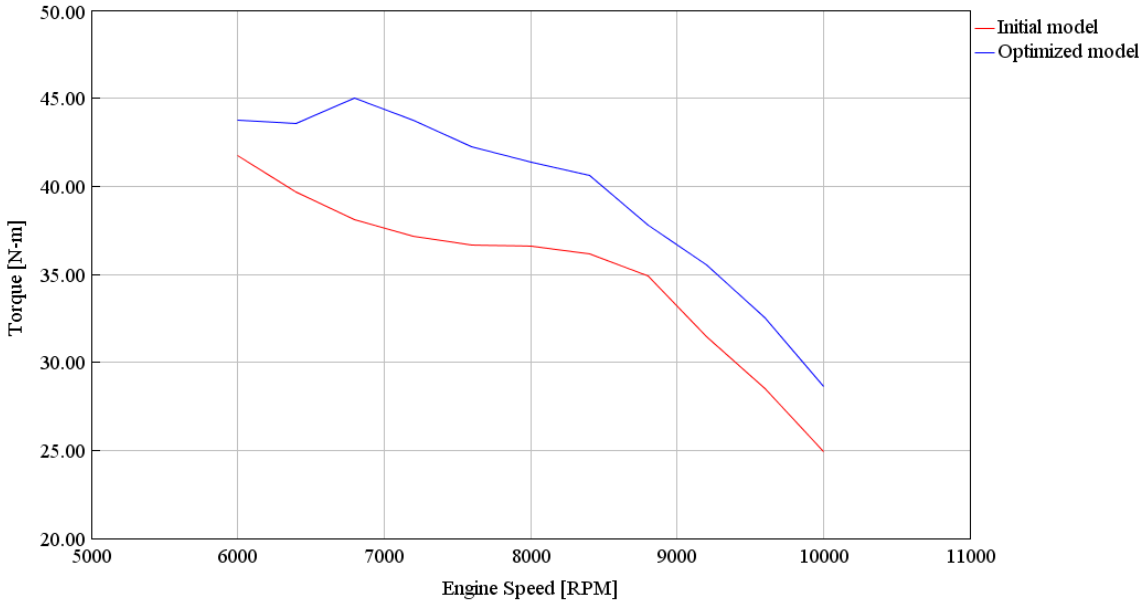

Figure 70 Comparison of brake torque of initial model and the third optimized model

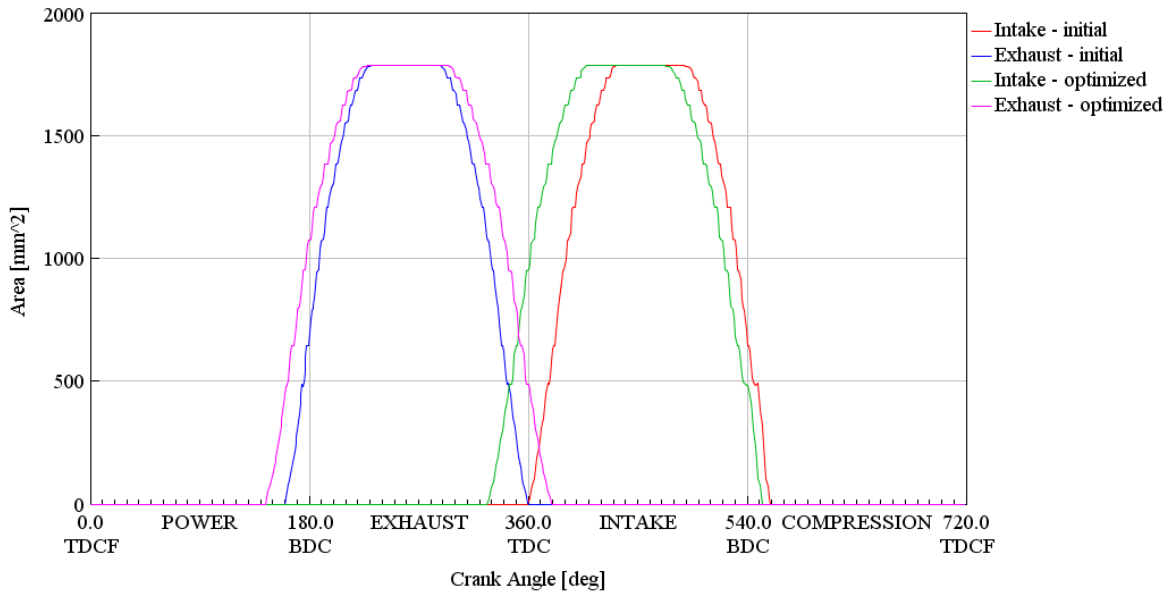

Figure 71 Comparison of intake and exhaust effective´s areas for optimization number 3

7.7. Optimization number 4

The fourth optimization has exactly the same settings as the third one. It is also using the brake torque as the RLT response and it is also maximizing it for the average case RLT. The RPM range is also the same. The only difference is that in this case the model of clearances is not used, therefore, as in the optimization number 2, this one is also made for the ideal model.

In the Table 22 are shown the new parameters after the optimization. The length of the intake manifold part is slightly shorter, and the length of the exhaust manifold part is also shorter than the initial value. The angle multiplier is greater than 1 for both valves, which means that the valves are open for a longer period. The Table 23 shows us the new timing of the valves. The exhaust valve opens earlier and closes later than the original one. The new setting of the intake valve is that it opens a little bit earlier and closes almost at the same time as the original valve. With these optimized values an overlap is made again for about 35 °CA.

Table 22 Optimization number 4

	Initial value	Optimized value
Length of the exhaust manifold part [mm]	205	85.08
Length of the intake manifold part [mm]	17	10.27
Cam Timing Angle – intake [°CA]	0	-4.39
Angle Multiplier – intake [-]	1	1.02
Cam Timing Angle – exhaust [°CA]	0	31.26
Angle Multiplier – exhaust [-]	1	1.21

Table 23 Intake and exhaust valve settings of the fourth optimization

Exhaust valves	Initial	Optimized	Intake valves	Initial	Optimized
Open [°CA]	-204	-216.82	Open [°CA]	0	-4.39
Close [°CA]	0	31.26	Close [°CA]	204	204.11

Figure 72 shows the results and the comparison of the initial and optimized model. The results are good because the brake torque is higher for all the chosen engine speeds. The lowest increase of about 6 % is at 7600 RPM and at 6800 RPM the increase is about 11 %.

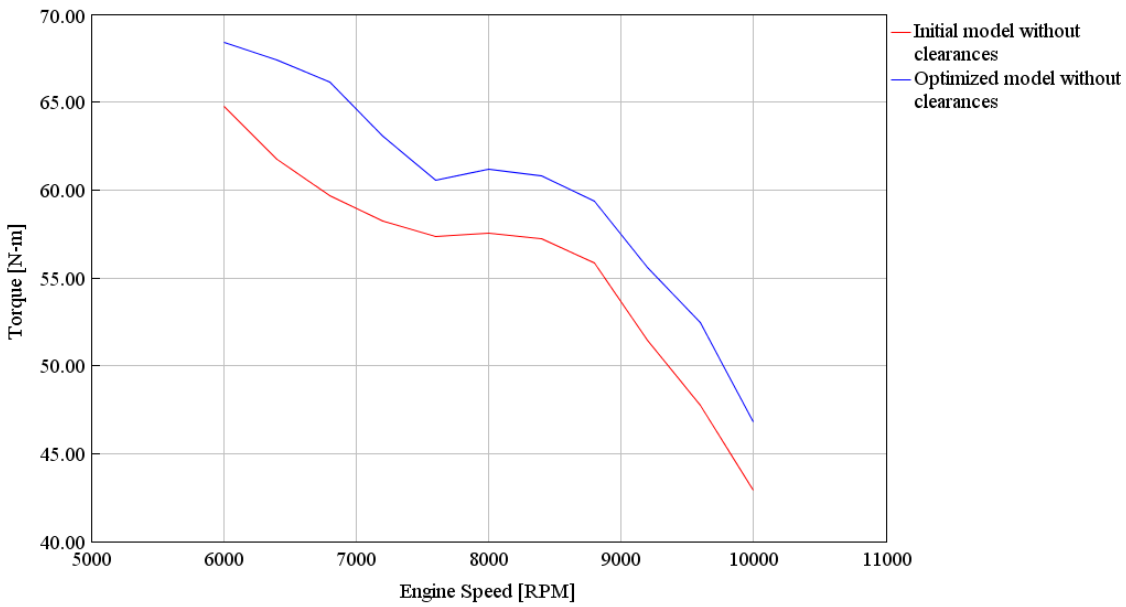

Figure 72 Comparison of brake torque of initial model and the fourth optimized model

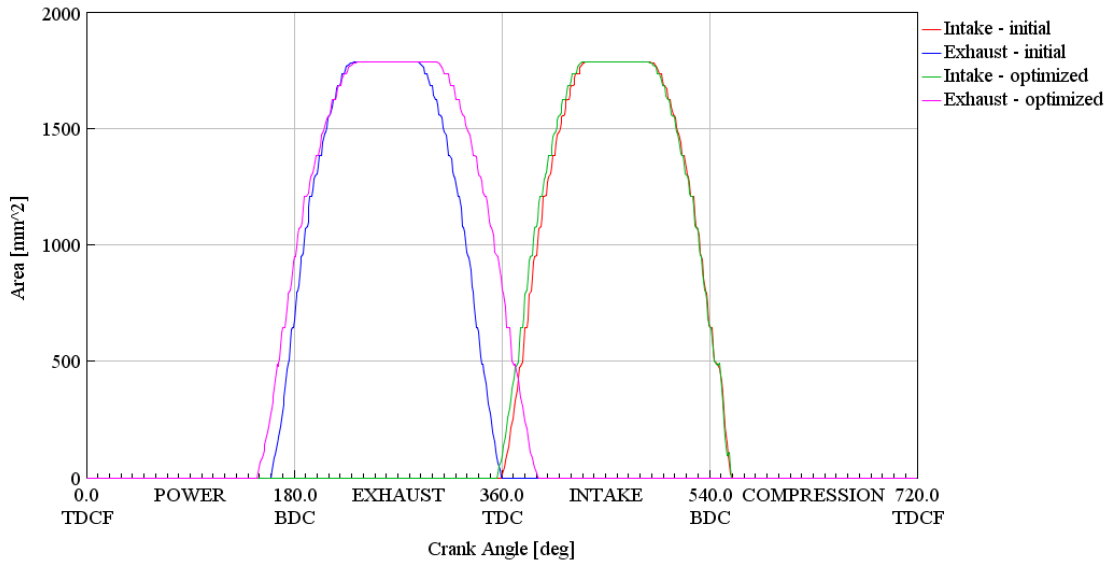

Figure 73 Comparison of intake and exhaust effective´s areas for optimization number 4

8. Conclusion

The main task of this thesis was to propose and build a sub-model of clearances between the stationary case, rotary cylinder block and their sealing. Before this could be done several other things had to be made first.

Firstly, the research about the rotary and birotary engines was made to get familiar with this topic. A small part of the review is also dedicated to the Knob engine, whose GT–Power model is used for all further simulations.

The first step of the practical part was to update the provided old GT–Power model. Since the model was created a lot of changes were made on the engine, which were not included in the model. The first change which had to be done was compression ratio, then it was blowby, which were not included at all in the original model. Then it was an update about the intake and exhaust manifolds, which as it is described in the chapter four, were originally created as straight pipes. The last update was about the timing of the intake and exhaust ports. Unfortunately, the flow coefficients of the ports could not be updated, because this required a new measurement, which could not be performed, due to the Covid-19 situation.

After performing a measurement of the engine, new data were collected, to make the GT–Power model even more accurate. With this new data the model was calibrated to get the same results from the simulation as from the measurement, or as close as possible. The calibration was mostly based on the blowby and creating of the simple model of clearances with a small leaking. The results of the maximum cylinder pressure from the simulation were quite close to the measured data, but not for the whole RPM range. Another important parameter which was calibrated was a friction object. The results of the friction calibration are shown in the Figure 39 and as it can be seen, the new data are now more accurate than before. The difference can be caused by estimating the coefficients for the Chen-Flynn model and by extracting IMEP from the model as it is described and not calculating it from the measurement.

When the model was updated and well calibrated a sub-model of clearances could be proposed and created in the GT–Power model. In the Figure 57 the GT–Power map of the sub-model can be seen and because it is quite complicated, several parameters in the map objects had to be created as dependencies, which are described in the chapter six. The new model had to be also calibrated by changing the discharge coefficient. This model shows that only about two thirds of the fuel burns, the rest is trapped in the clearances and the flame propagation cannot reach inside these clearances, because of the small entrances. That indicates that it should be desired to make all these spaces between the rotary cylinder block, stationary case, and their sealing as small as possible.

After performing all the optimization, it can be seen, that there are some better settings, which would improve the engine output. In the optimization number 3, the brake torque at 6800 RPM increases by 18 % and that is a significant improvement. This is the optimization, which is set for the higher RPM range, because the engine should ideally operate in this range.

9. References

[1] Rotary engine [online]. The Editors of Encyclopaedia Britannica. Encyclopædia Britannica, 2017 [cit. 2020-12-08]. Available from: https://www.britannica.com/technology/rotary-engine

[2] NAHUM, Andrew. The Rotary Aero Engine. Science Museum, 1987. ISBN 190074712X

[3] Rotary engine [online]. Autopedia, the free auto encyclopedia [cit. 2020-12-08]. Available from: https://automobile.fandom.com/wiki/Rotary_engine#cite_note-nahum-1

[4] MILLET, Félix-Théodore (1844 - 1929) [online]. Digital Mechanism and Gear Library [cit. 2020-12-08]. Available from: https://www.dmg-lib.org/dmglib/main/biogrViewer_content.jsp?id=24297004&skipSearchBar=1

[5] PIERARD, Amandine Romano. Millet, one of the world's first motorcycles. Retro mobile [online]. 2017 [cit. 2020-12-08]. Available from: https://www.retromobile.com/Visitors/News/Actu-2018/Millet-one-of-the-world-s-first-motorcycles

[6] RADIAL ROTARY ENGINE. Lawrence Hargrave Centre [online]. 2011 [cit. 2020-12-08]. Available from: http://lawrencehargravecentre.com/radialrotary.html

[7] Engine made by Geoffrey Hargrave, 1911. Museum of Applied Arts & Sciences [online]. [cit. 2020-12-08]. Available from: https://collection.maas.museum/object/214054

[8] Race to the Museum: Balzer automobile, 1894. American History [online]. National Museum of American History, 2010 [cit. 2020-12-08]. Available from: https://americanhistory.si.edu/fr/blog/2010/12/race-to-the-museum-balzer-automobile-1894.html

[9] The Balzer Cyclecar & The Balzer Motor Company. American Automobiles [online]. [cit. 2020-12-08]. Available from: http://www.american-automobiles.com/Cycle-Cars/222Balzer-Cyclecar.html

[10] Langley-Manly-Balzer Radial 5 Engine [online]. National Air and Space Museum [cit. 2020-12-08]. Available from: https://airandspace.si.edu/collection-objects/langley-manly-balzer-radial-5-engine/nasm_A19080003000

[11] Charles M. Manly: An Early American Innovator in Aircraft Engines [online]. SAE International in United States, 1995 [cit. 2020-12-08]. Available from: https://saemobilus.sae.org/content/950503

[12] 1894 Balzer. Free Library of Philadelphia [online]. [cit. 2020-12-08]. Available from: https://libwww.freelibrary.org/digital/item/29608

[13] Adams-Farwell Rotary 5 Engine [online]. National Air and Space Museum [cit. 2020-12-08]. Available from: https://airandspace.si.edu/collection-objects/adams-farwell-rotary-5-engine/nasm_A19130001000

[14] REISS, Jason. Video: One Of Three Existing Adams-Farwell Engines In The World. ENGINELABS [online]. 2015 [cit. 2020-12-08]. Available from: https://www.enginelabs.com/news/video-one-of-three-existing-adams-farwell-engines-in-the-world/

[15] ADOLPHUS, David Traver. A Fresh Spin on Engine Design. Hemmings [online]. 2009 [cit. 2020-12-08]. Available from: https://www.hemmings.com/stories/article/a-fresh-spin-on-engine-design

[16] GENCHI, Giuseppe a Francesco SORGE. The Rotary Aero Engine from 1908 to 1918. 2012, , 15. Available from: doi:10.1007/978-94-007-4132-4_24

[17] Gnome Type N Rotary Engine [online]. National Air and Space Museum [cit. 2020-12-08]. Available from: https://airandspace.si.edu/collection-objects/gnome-type-n-rotary-engine/nasm_A19660002000

[18] Gnome Rotary Engine. Animated Engines [online]. [cit. 2020-12-08]. Available from: http://animatedengines.com/gnome.html

[19] Gnome 9B-2 Engine History. The vintage aviator [online]. [cit. 2020-12-08]. Available from: https://thevintageaviator.co.nz/projects/engines/gnome-9b-2-engine/history

[20] Gnome N-9. National Museum of the United States Air Force [online]. 2015 [cit. 2020-12-08]. Available from: ttps://www.nationalmuseum.af.mil/Visit/Museum-Exhibits/Fact-Sheets/Display/Article/197466/gnome-n-9/

[21] Charles Benjamin Redrup. Grace's Guide [online]. [cit. 2020-12-08]. Available from: https://www.gracesguide.co.uk/Charles_Benjamin_Redrup

[22] FAIRNEY, Bill. The Knife and Fork Man, The Life and Work of Charles Benjamin Redrup. Speedreaders [online]. 2009 [cit. 2020-12-08]. Available from: http://speedreaders.info/11048-knife-fork-man-life-work-charles-benjamin-redrup/

[23] BENJIMAN, REDRUP CHARLES a RICHARDS WILLIAM ALBAN. Improvements in or relating to Gas, Oil, and like Engines. 1905. GB190413314A. Registration date: 1905-08-12.

[24] Rotary engine. Truck [online]. [cit. 2020-12-08]. Available from: https://tentangtruck.blogspot.com/2010/01/rotary-engine.html

[25] HEGE, John B. The Wankel Rotary Engine: A History [online]. 2001 [cit. 2020-12-08]. ISBN 13:978-0-7864-2905-9. Available from: https://books.google.cz/books?id=IB2lMFqTTl8C&printsec=frontcover&dq=wankel&hl=en&sa=X&ved=2ahUKEwi2u6eWuqzsAhUL8KQKHbgRDf4Q6AEwA3oECAQQAg#v=onepage&q&f=true

[26] Two-stroke cycle. Britannica [online]. [cit. 2020-12-08]. Available from: https://www.britannica.com/technology/gasoline-engine/Two-stroke-cycle#ref250532

[27] Rotary engine inventor Felix Wankel born. HISTORY [online]. A&E Television Networks, 2009 [cit. 2020-12-08]. Available from: https://www.history.com/this-day-in-history/rotary-engine-inventor-felix-wankel-born

[28] HISTORY OF ROTARY: Chapter I: Opening a New Frontier with the Rotary Engine. Mazda [online]. [cit. 2020-12-08]. Available from: https://www.mazda.com/en/innovation/stories/rotary/newfrontier/

[29] LINDSLEY, E. F. Unbelievable - but we´ve seen it all work. Popular Science. 1974. Available from: https://books.google.ca/books?id=uRAgliO29ZwC&pg=PA62&lpg=PA62&dq=frank+turner+rotary+vee+engine&source=bl&ots=ME6WT2Lkd0&sig=gnUji-fVYaVKx9e6Isi7V2uFuLQ&hl=en&ei=SqF2TvSlOunu0gHmhfC4DQ&sa=X&oi=book_result&ct=result#v=onepage&q&f=true

[30] CAVIN, Dick. Rotary Vee Engine. 1986, 5. Available from: http://acversailles.free.fr/documentation/08~Documentation_Generale_M_Suire/Moteur/Documentation/Rotary_Vee_engine.pdf

[31] Torque Meter: Winter 2007 Issue. Engine History [online]. [cit. 2020-12-08]. Available from: http://www.enginehistory.org/TM/htm/tmv6n1.shtml

[32] ROULSTON, Murray. Bi-rotary engine. WO1996035862A1. Registration date: 1996. Available from: https://patentimages.storage.googleapis.com/4c/27/f0/331a2d76822979/WO1996035862A1.pdf

[33] MEYER, Andre J. Birotary Engine. US23557138A. Registration date 1940. Available from: https://www.freepatentsonline.com/2207749.pdf

[34] The aircraft engine Siemens & Halske Sh.IIIa [online]. [cit. 2020-12-08]. Available from: https://artsandculture.google.com/story/the-aircraft-engine-siemens-halske-sh-iiia/vwJiOiCbWHH5Kw

[35] Siemens and Halske SH 111 German WWI aero engine, 1918. Museum of Applied Arts & Sciences [online]. [cit. 2020-12-08]. Available from: https://collection.maas.museum/object/213283

[36] Devaere Franky's Radial Bi Rotary Balanced Piston Combustion Engine. The Tech Journal [online]. 2012 [cit. 2020-12-08]. Available from: https://thetechjournal.com/tech-news/devaere-frankys-radial-bi-rotary-balanced-piston-combustion-engine.xhtml

[37] CROWE, Paul. Radial Bi Rotary Balanced Piston Combustion Engine. The Kneeslider [online]. 2012 [cit. 2020-12-08]. Available from: https://thekneeslider.com/radial-bi-rotary-balanced-piston-combustion-engine/

[38] RBR - Radial Bi Rotary by Devaere Franky. Ecomodder [online]. 2011 [cit. 2020-12-08]. Available from: https://ecomodder.com/forum/showthread.php/radial-bi-rotary-balanced-piston-combustion-engine-16217-2.html

[39] KNOB ENGINES S.R.O. BIROTARY ENGINE.

[40] DENISH, D. William. Exhaust Pipe Fundamentals - Exhausting Fundamentals. BAGGERS [online]. 2009 [cit. 2020-12-08]. Available from: https://www.baggersmag.com/exhaust-pipe-fundamentals-exhausting-fundamentals#page-2

[41] ANDERSON, TREVOR. Performance Exhaust System Design And Theory. ENGINELABS [online]. 2016 [cit. 2020-12-08]. Available from: https://www.enginelabs.com/engine-tech/exhaust/performance-exhaust-system-design-and-theory/

[42] Rodrigo Caetano COSTA, Se´rgio de Morais HANRIOT a Jose´ Ricardo SODRÉ. Influence of intake pipe length and diameter on the performance of a spark ignition engine. 2013, 7 Available from: doi:10.1007/s40430-013-0074-2

[43] SlaveFlowState - Simple Splitter/Combiner with No Geometry (Caution! See Help). Gamma Technologies, 2018.

[44] ZRALÝ, Martin. Exhaust manifolds - BE-Z300-70-030-A-00-N. KNOB ENGINES

[45] ZRALÝ, Martin. Intake manifolds - 1bm1-sani_asm_TOP. KNOB ENGINES.

[46] GT-SUITE: Engine Performance Application Manual. Gamma Technologies, 2018.

[47] PIETER, Václav. Skodne prostory. KNOB ENGINES.

10. List of abbreviations

TDC	Top dead center	
BDC	Bottom dead center	
BMEP	Break mean effective pressure	[Pa]
FMEP	Friction mean effective pressure	[Pa]
IMEP	Indicated mean effective pressure	[Pa]
W_e	Effective work	[J]
V_s	Displaced volume	[m^3]
P_e	Effective power	[W]
n	Engine speed	[1/s]
T_e	Effective torque	[Nm]
ω	Angular speed	[rad/s]
RLT	Average results	
$FMEP_{const}$	Constant part of FMEP	[bar]
A	Peak cylinder pressure factor	[-]
$P_{cyl,max}$	Maximum cylinder pressure	[bar]
B	Mean piston speed factor	[bar*s/m]
$C_{p,m}$	Mean piston speed	[m/s]
C	Mean piston speed squared factor	[bar*s^2/m^2]
°CA	Degree of a crank angle	

11. List of figures

12. List of tables